



UNIVERSITÀ DEGLI STUDI DI SASSARI

**SCUOLA DI DOTTORATO DI RICERCA
Scienze e Biotecnologie
dei Sistemi Agrari e Forestali
e delle Produzioni Alimentari**



Indirizzo Agrometeorologia ed Ecofisiologia dei Sistemi Agrari e Forestali

Ciclo XXVII

Olive tree system in Mediterranean basin:
a mid-term survey on C sequestration dynamics and modelling

dr. Lorenzo Brilli

Direttore della Scuola
Referente di Indirizzo
Docente Guida

prof. Alba Pusino
prof. Donatella Spano
prof. Marco Bindi

Anno accademico 2013- 2014

This report can be cited as:

Brilli, L. (2014). *Olive tree system in Mediterranean basin: a mid-term survey on C sequestration dynamics and modelling*. PhD Thesis. University of Sassari. Italy.

135 pages.

The research presented in this thesis was conducted at University of Sassari, Sassari, Italy.

*“The Appearance is always changing.
The Changing is just the Appearance”*

The Heart Sutra

“Reflection of fear make shadows of nothing”

Akeboshi - Wind

Preface

Since long time agricultural activities have promoted positive changes in crop yield and animal production, thus satisfying the continuous increase of food demand as well as the improvement of co-operation and trade exchanges. However, in order to reach these aims, modern agriculture has been more and more often characterized by the use of practices and methods that are widely considered harmful for environment. More in detail, the widely application of deep tillage, pesticide, fertilization and many other agricultural practices that are commonly used under intensive agriculture have contributed, among other, also at increasing the greenhouse gas concentration in atmosphere that is widely accepted to be the main cause of global warming.

Agricultural sector, however, can also reduce or absorb these emissions, thus contributing to reduce global warming and its associated impacts. Agriculture can play a very important role in greenhouse gas mitigation through the increase of C-sequestration in soil or plant compartment (e.g. within branches and roots). On these premises, the chapters within this thesis were focused at illustrating as one of the most important agricultural systems more suitable for this aim are fruit orchards.

In particular the work reported into the chapters of this thesis has been carried out with the aim to evaluate the role of the most spread Mediterranean orchard: olive orchard. Each of the three chapter helps bridge our current knowledge gaps about the climate change mitigation capacity provided by olive orchard, changes in C-dynamics depending on climate conditions and agricultural practices, and the current status of tools able to predict C-fluxes from this long term agro ecosystem.

This research was carried out with the aim to improve the know-how about the functional role of olive orchards in climate change mitigation. Despite our research provided proofs about the climate change mitigation capacity that this system can provide both currently and in the next decades, many challenges still lie ahead. Therefore, more detailed micrometeorological and GHG emissions analysis should be conducted over this ecosystem. I hope that results provided by this thesis can be a little step to develop or improve new ways and strategies to cope with climate change through the managing of these long-term agro ecosystems.

Abstract

The contribution that olive orchards can provide in climate mitigation should be more deeply analyzed given that these systems can stock large amount of C in woody compartments and soils. These systems could play a fundamental role especially over Mediterranean basin that is one of the most sensitive areas to climate change and where they are widely cultivated. However some issues are still open: what do we really know about the C-sequestration capacity provided by these systems? Can these really contribute to climate change mitigation both for current and future periods? In order to solve these questions, a mid-term study (3 years) was carried out at Follonica (Tuscany, central Italy), where an eddy covariance tower was installed over a typical rainfed olive orchard. Data from eddy covariance were then used for calibrating and validating two different models able at simulating C-exchange and biomass production from this system.

Our work firstly allowed to assess the C-fluxes dynamics from this system and their relation with the main meteorological parameters and agricultural practices, thus indicating the magnitude of C-sequestration capacity offered by a typical Mediterranean olive orchard; as second the implementation of new tools that can be used for assessing the efficiency of mitigation strategies or to predict changes in mitigation capacity that these systems will probably encounter over the next decades.

Table of Contents

Preface.....	3
Abstract	5
Chapter 1	11
General Background.....	11
1.1. <i>Climate change and Agriculture</i>	12
1.2. <i>European context: Instruments and Strategies</i>	13
1.3. <i>Long term agro-ecosystems: role in climate change mitigation</i>	14
Chapter 2	16
Materials and methods	16
2.1. <i>Olive tree</i>	17
2.1.1. <i>Taxonomic framework</i>	17
2.1.2. <i>Geographical range</i>	17
2.1.3. <i>Botanic description</i>	18
2.1.4. <i>Phenology</i>	18
2.1.5. <i>Ecophysiology</i>	20
2.1.6. <i>C-exchanges</i>	21
2.1.7. <i>Economy and statistics</i>	22
2.2. <i>Eddy Covariance Method</i>	25
2.2.1. <i>State of methodology</i>	25
2.2.2. <i>Physical and mathematical principles</i>	26
2.2.3. <i>Flux footprint</i>	30
2.2.4. <i>Processing eddy covariance</i>	33
2.2.5. <i>Gap-filling and flux-partitioning</i>	35
2.3. <i>Simulation models</i>	37
2.3.1. <i>C-Fix</i>	39
2.3.2. <i>Daycent</i>	41

Chapter 3	47
<i>Effects of inter annual and inter-seasonal variability in rainfall regimes on C-exchanges of a rainfed Olive orchard</i>	47
Chapter 4	63
<i>Simulation of olive grove Gross Primary Production by the combination of ground and multi-sensor satellite data</i>	63
Chapter 5	81
<i>Calibration and validation of biogeochemical model Daycent in a Mediterranean olive orchard: assessment of carbon sequestration capacity for current and future scenarios</i>	81
Chapter 6	99
General discussion and conclusions	99
6.1. Main theme and questions	100
6.1.1. Role of olive orchards in C-sequestration capacity and influence of climate conditions and management.	100
6.1.2. Current status, calibration, validation and application of the most suitable tool able at reproducing C-fluxes from a complex system such as olive orchard.	101
6.2. Conclusions	102
Chapter 7	104
References	104
Acknowledgments	132
Annexes	133

List of figures

- Figure 2.1: Simple graphical representation of turbulent flux in a forest ecosystem.
- Figure 2.2: Graphical representation of flux footprint.
- Figure 2.3: Simple scheme of energy balance.
- Figure 2.4: Conceptual diagram of the Daycent ecosystem model, Del Grosso et al. (2008).
- Figure 2.5: Conceptual diagram of the check of Daycent outputs.
- Figure 3.1: Rainfall variability range for the period 1981-2012.
- Figure 3.2: Correlation between SP NEE and SP Δ rainfall and between SMP NEE and SP Δ rainfall during the 3 years of study.
- Figure 4.1: MODIS NDVI image of June 2010 showing the position of the study area in Tuscany as well as its main features (enlarged box). NDVI window extends over 8-13° East Longitude, 42-45° North Latitude.
- Figure 4.2: Thermo-pluviometric diagram for study area. All monthly data derive from eddy covariance station.
- Figure 4.3: Scheme of the multi-step methodology used to estimate olive grove GPP.
- Figure 4.4: NDVI profiles of olive trees and ground vegetation during 2010 and 2011. Filled line = olive; dotted line = ground vegetation.
- Figure 4.5: Daily estimated GPP profiles of olive trees and ground vegetation during 2010 and 2011. Filled line = olive; dotted line = ground vegetation.
- Figure 4.6: Daily values of GPP estimated by C-Fix model (dotted line) and re-constructed from eddy covariance measurements (filled line). The two black bars on the x axis indicate the periods likely affected by the tillages (see text for details).
- Figure 4.7: Daily values of GPP estimated by C-Fix model (dotted line) and re-constructed from eddy covariance measurements (filled line). The GPP after the two tillages has been estimated by considering simulated ground vegetation NDVI values (see text for details).
- Figure 5.1: Model calibration reported at daily time step.
- Figure 5.2: Model validation reported at daily time step.
- Figure 5.3: Average daily NEE reported for the 4 different timeline under A1B scenario.
- Figure 5.4: Average monthly NEE reported for the 4 different timeline under A1B scenario.

List of tables

<u>Table 2.1</u>	List of the 7 Mediterranean countries with the highest worldwide production.
<u>Table 2.2</u>	List of irrigated or not irrigated areas over the main European olive oil makers data 2011*; data 2008 **
<u>Table 3.1</u>	Monthly meteorological data (i.e. cumulated rainfall, air mean temperature and mean global radiation) of the study area. Data were reported both as long-term average (LTA, 1981-2010) that specifically for the three years of measurements (2010, 2011 and 2012).
<u>Table 3.2</u>	Rainfall amount aggregated over 4-months period for the 3 years of study (i.e. 2010, 2011 and 2012) and for LTA. WIN=November, December, January, February; SPR= March, April, May, June; SUF= July, August, September, October.
<u>Table 3.3</u>	Monthly cumulated NEE, GPP and Reco during the three years of measurements.
<u>Table 3.4</u>	Correlation between NEE and meteorological variables (air temperature, rainfall and solar radiation) at monthly scale over the three years of study. Signif. codes: 0 ‘****’ 0.001 ‘***’ 0.01 ‘**’ 0.05 ‘.’ 0.1 ‘ ’ 1.
<u>Table 3.5</u>	Correlation between NEE and rainfall aggregated at seasonal scale over the three years of study. SMP=July, August, September, October. SP= March, April, May, June. WP=November, December, January, February. Signif. codes: 0 ‘****’ 0.001 ‘***’ 0.01 ‘**’ 0.05 ‘.’ 0.1 ‘ ’ 1.
<u>Table 4.1:</u>	Monthly mean temperature (°C), total rainfall (mm) and months with mean temperature < 0 °C in the study area for 30 years average (MARS JRC data set), 2010 and 2011.
<u>Table 4.2:</u>	Number of half-hourly data measured by eddy covariance station in 2010 and 2011. <i>Num. tot. val.</i> indicates all the measured data; <i>Num. orig. val.</i> indicates all the measured data used to obtain observed daily GPP data; <i>Num. gaps</i> indicates the measured data that cannot be directly used to obtain observed daily GPP data. For these half-hourly data GPP data were reconstructed using the gap-filling procedure. The quality classification scheme for gap-filled values is: A: best; B: acceptable; C: dubious.
<u>Table 4.3:</u>	Accuracy of GPP estimates obtained applying C-Fix model for different time intervals (see text for details on r, RMSE and MBE).
<u>Table 5.1:</u>	Soil characteristics of test site. Texture, pH and Bulk density were provided for 4 different soil layers.
<u>Table 5.2:</u>	Parameters changed in the file “crop.100” to adjust biomass production for grass layer (Mixed grass from crop default file with 50% warm and 50% cool, N fixation).
<u>Table 5.3:</u>	Parameters changed in the file “tree.100” to adjust biomass production for tree layer (Olive

tree from tree default file based on century data).

Table 5.4: Statistical analysis concerning model calibration and validation carried out at different time step.

Table 5.5: Total annual NEE simulated by Daycent model and observed from Eddy Covariance. Total annual NEE was reported considering the same days for observed and simulated.

Table 5.6: Monthly NEE simulated by Daycent model for the baseline and the 3 future timeline under A1B scenario.

Chapter 1

General Background

Abstract

This chapter gives a general overview about the relationship between agriculture and climate change. Here were indicated the observed and expected climate changes as well as the double role that agricultural systems play in climate change. Main policies and strategies adopted to reduce these changes were also briefly described. Finally, the role of long-term agro ecosystems in climate mitigation has been questioned, focusing the attention especially on the olive orchards.

Keywords: Climate change, agriculture, policies, mitigation, long-term agro-ecosystems

Chapter 1.

General Background

1.1. *Climate change and Agriculture*

In the last decades a greater and greater scientific consensus proved that climate change and global warming are a real threat and that they were mostly originated by human-activities. Proofs of changes in climate trends have been provided by several scientific authorities and particularly from IPCC, a scientific intergovernmental body of the United Nations that produces reports aimed at supporting the United Nations Framework Convention on Climate Change (UNFCCC). The latest observations of the atmosphere and surface provided by WGI of AR5-IPCC (IPCC, 2013) indicate that in the last century (1901-2012) almost the entire globe has experienced surface warming (IPCC, 2013). In particular, the global surface temperature (lands and oceans) calculated over the period 1880-2012 showed a warming of 0.85°C (IPCC, 2013). Moreover, it is virtually certain that since 1950 both maximum and minimum averages temperatures are increased. Concerning hydrological cycle and especially precipitation regimes, despite data quality cannot guarantee high levels of confidence, precipitation has been estimated to be increased over northern areas from the beginning of the century. IPCC 2013 also reported that the numbers of cold days and night is decreased while those of warm days and night is increased. Furthermore, heavy precipitation events are increased over several worldwide region, especially Europe and North America (high confidence). Even drought and dryness periods are probably increased since 1970 (low confidence).

Looking at future climate projections for the end of the 21st century with respect to a baseline period of 1986–2005, climate trends are expected to worsening significantly with a general strongest warming comprises between 0.3 and 4.8 °C depending on the concentration-driven RCPs applied (IPCC, 2013). Focusing on Europe, Kjellström et al. (2011) indicated that the strongest warming will be observed during summer especially over Southern Europe, whilst it will be expected in wintertime in Northern Europe. They also indicated a precipitation increase in Northern Europe and a strong decrease in Southern Europe. Concerning extremes, Lenderink and Van Meijgaard, (2008) indicated a very likely increase in heat waves, droughts and heavy precipitation events over the whole Europe. These changes in climate are expected to be particularly detrimental for agriculture. Agricultural sector, indeed, is characterized by a complex two-way relationship with climate. From one hand, crop growth is highly sensitive to change in temperature and precipitations since these factors can cause modification in phenology

that can bring a decrease of crop yield and increases in cultivation cost (Chmielewski et al., 2004; Seguin et al., 2007; Olesen et al., 2011; Brilli et al., 2014). By contrast, agriculture contributes to global warming through the emissions of greenhouse gases (GHGs) that are originated by the most common agricultural activities such as fertilization, mechanical harvesting, tillage, etc. (Paustian et al., 2004; Smith et al., 2007; IPCC, 2007; Fisher et al., 2012; Bennetzen et al., 2012). Currently, agriculture contributes to 14% of all anthropogenic GHG emissions and to 58% of the world's anthropogenic non-carbon dioxide (CO₂) GHG emissions (Denman et al., 2007; Beach et al., 2008).

1.2. *European context: Instruments and Strategies*

In the last years several policies and agricultural strategies have been developed with the aim to reduce crop yield losses or limiting the GHG emissions. Despite these measures should be quickly implemented and applied, just few countries have currently developed large-scale programmes to cope with climate change and its associated impacts on crop systems Europe, however, is currently the global area where these programmes were more widely developed and applied (e.g. European Climate Change Programme (ECCP), European Union Emissions Trading System (EU ETS), Renewable Energy Directive, the “20-20-20” Policy, among others).

These programmes in agree with the appointed organisms (e.g. IPCC) have indicated as the best way to cope with climate change those measures for "adaptation" and "mitigation". The first are strategies aimed at reducing economic losses due to crop yield decrease and the high costs of management inputs as fertilizer or irrigation (Smith and Olesen, 2010). These strategies, usually adopted by farmers, mainly consist of changes in cultivar types, sowing date, management, etc. (Bindi and Olesen, 2011). Differently the latter are strategies aimed at reducing GHG emissions from agriculture and, at the same time, at stabilizing the GHG already present in atmosphere, thus minimizing the vulnerability of physical and biophysical systems.

Mitigation strategies are referred both to forestry that agriculture and are mainly based on three aims: i) enhancing removals by increasing of reforestation and carbon sequestration from forest and agricultural soils; ii) reducing emissions by increasing efficiency energy and change in land management; iii) avoiding or displacing emissions through bioenergy production. These aims can be achieved through the application of several practices aimed at increasing C in soil or reducing N emissions (i.e. minimum or no tillage, fertilizer application reduction, energy consumption reduction, grass cover, etc.).

1.3. *Long term agro-ecosystems: role in climate change mitigation*

According to Dickie et al. (2014), mitigation potential estimated for agricultural sector can vary from 5.4 to 6.3 Gt CO₂eq. This magnitude is mainly due to a combination of three important factors: emissions reduction, sequestration of carbon in agricultural systems, and major shifts in consumption patterns. Estimates provided by Dickie et al. (2014) indicate that agricultural sector may result roughly GHG neutral. However, whilst the mitigative potential of several crop systems has been analysed, just few studies were focused at evaluating the role of long term agro-ecosystem. The contribution that these systems can provide in mitigation should not be neglected since they can stock large amount of C in woody compartments and soils. Moreover, the cultivation of these systems is widespread over the most sensitive areas to climate change such as Mediterranean basin. Despite according to IPCC, (2013) “tree cover and biomass in long term agro ecosystem (e.g. fruit orchard or savanna) has increased over the past century” (Angassa and Oba, 2008; Witt et al., 2009; Lunt et al., 2010; Rohde and Hoffman, 2012), thus enhancing carbon storage per hectare (Hughes et al., 2006; Liao et al., 2006; Throop and Archer, 2008; Boutton et al., 2009), there is still an open issue: how much do we really know about the mitigation capacity provided by these systems?

In order to solve this question, it is needed to know the prevailing ecological usage of the term "savanna". Savannas systems are complex ecosystems usually structured in two different layers (grass and trees) in which contrasting plant life forms co-dominate (Scholes and Archer, 1997). These systems are widely extensive especially over tropical and temperate regions where they result to be very economically important since involved in fruit production. They are usually assessed and categorized based on several parameters such as stature, canopy cover, and arrangement of woody elements (Sarmiento, 1984; Johnson and Tothill, 1985; Cole, 1986; Burgess, 1995). According to several studies (Archer et al., 1988; Menaut et al., 1990; Tongway and Ludwig, 1990; San Jose et al., 1991; Montania, 1992) these systems are classified within specific ecoregions: tropical and subtropical savannas; temperate savannas; Mediterranean savannas; flooded savannas and montane savannas.

Around Mediterranean basin, where climate change is expected to be detrimental for agriculture, the most typical tree species into Mediterranean savanna are oaks and olive trees. In particular these latter can be considered the most important fruit tree around the basin. This specie has high agronomic and economic value besides at providing a multitude of ecosystem services.

Based on these premises the main aim of this work was assessing the role that a typical Mediterranean olive orchard can play in climate change mitigation. This aim was reached through a mid-term study (3 years) carried out at Follonica (Tuscany, central Italy), in which eddy covariance measurements allowed the assessment of the C-sequestration capacity as well as the evaluation of C-fluxes dynamics in respect of the main meteorological variables or management practices.

Processed eddy covariance data were additionally used to calibrate and validate two different models which resulted to be able at simulating gross primary production (GPP) and the net ecosystem exchange (NEE) of our test site. Doing so, we implemented new tools able to predict changes in mitigation capacity that savanna systems such as olive orchard will encounter in the next decades, or at developing and evaluating new mitigation strategies based on the changed climatic conditions.

Chapter 2

Materials and methods

Abstract

Chapter 2 is divided into 3 sections: section 2.1 explores the fruit tree species (i.e. *Olea Europaea*, L.) that has been studied. This section discusses about taxonomic framework and the characteristics of the specie, phenology, eco-physiology and C-fluxes, as well as the economic importance both at local and worldwide. Section 2.2 describes the eddy covariance method. The major part of information presented in this section make reference to the book “Eddy Covariance Method for Scientific, Industrial, Agricultural and Regulatory Applications” by George Burba. This section is intended to provide the physical and mathematical principles, the major sources of errors and data processing of the eddy covariance method. Finally, section 2.3 explores mathematical models, especially more deeply analysing those remote sensing and biogeochemical models that were used in this thesis.

Keywords: Olive trees, mathematical models, C-fix model, Daycent.

Chapter 2.

Materials and methods

2.1. Olive tree

2.1.1. Taxonomic framework

The olive tree (*Olea europaea* L.) is a fruit tree belonged to Oleaceae family. Some authors insert Oleaceae family within the Scrophulariales order (12 families and more than 12000 species), while others authors insert it in an itself order, called Oleales. Although Oleaceae family have a regular tetramera corolla and only two stamens, these latter should be considered modifications occurred from the reduction of the typical flower (which has a pentamer corolla), therefore it would not have to be inserted in another taxon nor considered more archaic than the rest of the order. The Oleaceae family is composed of 24 genera, consisting of approximately 600 species. Among these, more than half belong to *Jasminum* genus, very important as it includes species of considerable economic importance such as *Olea europea*. The family consists of trees and shrubs, characterized by mostly opposite leaves , simple or compound (Grossoni, 1997). Flowers are usually complete, commonly grouped into inflorescences. Corolla consists of 4 petals. The form of fruit is variable, ranging from "Samara" (i.e. *Fraxinus* L.) to "capsule" (*Syringa* L.), or "berry" (*Ligustrum* L.), until most-known "drupe" (*Phillyrea* L. and *Olea* L.).

2.1.2. Geographical range

Olive tree is a typical Mediterranean specie which extends from the Iberian Peninsula to Anatolia, including coastal areas of Italy and North Africa. Although olive trees cultivation is currently widespread around the whole Mediterranean basin, the original area of this specie can be considered the Caucasus (Syria and Palestine), where the first farming communities began a systematic selection of different varieties. The olive trees cultivation was for long time exclusive of Mediterranean countries due to the favourable climate conditions. In the last years, however, olive tree cultivation has been spread in many other countries with similar climate conditions such as California, Australia, Argentina and South Africa. Olive trees systems are placed on the marginal land that are unsuitable for intensive cultivation due to soil type, topography, lack of water for irrigation, etc., therefore the major part of the traditional orchards are formed by widely spaced trees. The very old origin of this specie in conjunction with the longevity of individual trees and the continuative use of vegetative propagation, allowed the development of a wide numbers of cultivars. According to Connor et al. (2005), whilst in Spain, Greece, and Tunisia, a

small numbers of cultivars dominate intensive production areas, in Italy there is more variation between the several cultivation areas. In Italy, the cultivation area of olive tree correspond to *Lauretum*. The specie prefers temperate climates, ranging from areas characterized by warm and dry summers (evergreen sclerophyllous Mediterranean) to cooler areas until 500-600 m above sea level, while, on the contrary it avoids foggy areas with cold temperatures in winter. The best areas for growth is central and southern Italy, including islands and other areas where climate is tempered by the presence of large bodies of water such as lakes (i.e. Lombardy and Veneto).

2.1.3. Botanic description

Olive tree under free growth conditions can reach 10 meters in height, but it does not exceeds 4-5 meters. It is a long-lived plant that, under favourable conditions, can live more than thousand years. The canopy have a rounded shape (oval, enlarged, lax) but it can change based on pruning and variety. Trunk is irregular and twisted, with the presence of ribs or cords, tending to divide itself forming some cavity. The wood is hard and heavy. The bark is characterized by a grey-ash colour that does not change along the entire life. Olive tree can easily regenerate itself from the stump thanks to several globular structures (i.e. spheroblasts or ovules) that yearly provide many basal shoots. Leaves are simple, elliptical, leathery and shortly “petiolate” with the entire margin. They are green at the top of the page with the other side silvery-grey. This latter can vary depending on species and age. Flowers are hermaphrodite, with a small persistent calyx for 4 deciduous teeth and a tubular corolla with 4 lobes long white 1 cm. Flowers are usually inflorescences (10-15) that are produced from the axils of the leaves of the branches of the previous year. Flowering duration is different for individual trees (i.e. 10 days) and orchards (i.e. from 20 to 30 days). Pollen production lasts for about 5 days while individual stigmas remain receptive for about 2 days. Wind is the main driver of pollen production. This eco-physiological process is very delicate since it is hindered by strong or hot winds, intense rainfall and high temperatures. Orchards with an average pollen production are able to guarantee the reproductive success. By contrast, the reproductive success for individual trees is strictly connected to the number of flower and pollen produced.

2.1.4. Phenology

Olive tree is a day-neutral plant. Fruit production begins when the specie has 3/4 years, whilst the full production after 8 years. Complete maturity is reached after about 20 years. Production

of nodes, the expansion of leaves and the thickening of stems (i.e. vegetative growth) occur at any time during the year. Vegetative growth is constrained by specific meteorological parameters such as solar radiation, low temperature in winter, and water availability during summer. Typical Mediterranean orchards (i.e. rainfed orchards) show two different peaks of vegetative growth, in spring and autumn, respectively (Connor, 2005). The phenological cycle of olive tree consists of several stages characterized by different level of sensitive to climatic conditions. During winter, the vernalization process (or dormancy) happens when trees are exposed to cooler temperatures ($<7^{\circ}\text{C}$). This process leads to the second phase of the reproductive process (i.e. the initiation of induced buds). The length of this phase depends on meteorological conditions (i.e. length of cold time). Then, the vegetative growth starts in February/March, when the lateral and apical buds begin to grow and stretch, showing the issuance of new vegetation that is clearly recognizable by the colour of the new buds. During this period the vegetative growth is mainly driven by the increase of temperature. Vegetative growth is characterized by the growth of shoots and buds. This physiological phase ends around the middle of the Spring, when both shoots and buds reach their final dimensions. The growth of fruits and seeds can lead to the floral induction inhibition, thus contributing to the alternate bearing. This characteristic is particularly clear observing the pattern of biennial flowering and yield. More specifically, years with intense fruiting are usually followed by years with restricted flowering. Although this pattern is very common in almost all fruit trees, olive tree is the fruit tree mostly representative, however (Rallo, 1998). Floral induction occurs in mid-summer (7 to 8 weeks after full bloom) around the time of pit hardening (endocarp hardening). The bloom is characterized by a very high number of flowers. Flowers dropping is considerable and it takes the name of "colatura". The transition from flower to fruit is defined as Fruit Set and usually occurs at the end of June. At this stage corolla enlarges and dries out, persisting until the enlarged ovary causes the detachment. During this phase many factors such as the sudden lowering and remarkable of the temperature, water stress and warm winds can have a negative impact on the percentage of Fruit Set. During the next 4/5 months, olives develop and grown. This long period, which consists of 3 distinguishable sub-phases, ends around November when the fruit has reached the final dimensions. The first sub-step is characterized by the increase (until 20%) of the drupes. Then the hardening of the heart is observed in conjunction with a decrease of fruits growth. The drupes reach the 50% of their final dimensions while the core becomes hard. This sub-step lasts until the end of August. Finally, fruits growth vary based on the climate elapse. In rainfed orchards the olives growth and oil

content are mainly driven by summer rains, especially those between August and September. Drought conditions can lead to small fruit size and low oil yield. On the contrary, autumnal rainfalls increase the size of the olives, but do not influence the olive oil yield. The olives ripening takes place between October and December, depending to the variety and geographical location. Ripening phase is characterized by the change of colour of the olives. This change is gradual, from green to straw yellow, up to purplish red. It usually includes at least 50% of the surface of the drupe. This period takes the name of veraison and it is characterized by a strong scalar component both among different varieties and intra-variety. Olives range from 1 to 6 grams and their size, shape and colour vary based on the different varieties. During veraison the olive oil content increases while the pulp becomes more soft. Olives reach the complete maturity before the plant ends its growing cycle.

2.1.5. Ecophysiology

Crop growth and productivity are mostly determined by intrinsic characteristics of the specie and climatic conditions of the site. Crop growth, however, is also determined by soil characteristics (physical-chemical structure, morphology, texture, etc.) and management (tillages, fertilization, pruning, etc.). The interactions involving the relation plant-environment are very complex. These interactions affect the plants at physiological and biochemical level, causing different response in terms of development and productivity. Understanding these interactions in olive trees is complex due to physiological characteristics of this specie since it has characterized by a particular reproductive cycle and alternate bearing (Fiorino, 2001). Olive tree is a typically thermophile species with strong xerophil characters. The spontaneous subspecies of olive tree (wild olive tree) is found in degraded spots, scrublands and rocky vegetation, coastlines, etc. The specie is characterized by high grazing resistance, taking on a bushy habit with dense and thorny branching. Olive tree has a remarkable ability to re-grow vigorous suckers from the stump after fires, while is sensitive to low temperatures. The specie suffers shading. When it is found under shadow conditions produces few branches, little canopy and low flowering. The climatic factor determining for olive trees distribution is temperature. The first signs of suffering are clear at temperatures of 3-4 ° C, below these temperatures the tips of the shoots wither. The cold sensitivity increases from the stump to branches. Frosts can cause the death of the entire tree, but the most critical damages appear when temperatures are stable for longer time below -5/6 ° C. According to long term studies carried out in California by Hartmann's group (Denney and

McEachern, 1983) the optimum temperature regime for olive tree flowering is in a range from 2 to 4°C (minima) and from 15.5 to 19°C (maximum). Water stress is the main parameter affecting production, especially in warm environments such as many areas of Mediterranean. In particular flowering and fruit growth are the most critical periods during the whole vegetative cycle. In these stages water stress (both lower or stronger) reduces the percentage of fruit set, leading to a fruit drop and causing the ripening during summer with a consequent low percentage of olive oil production. Olive tree, however, even in dry areas can provide a minimal level of production. Harmful climatic factors are also strong wind, especially when associated with low temperature, excessive rainfall and elevated air humidity. This specie does not require specific soils, preferring however loose soil and medium texture, fresh and well drained. Optimal soil conditions for growth are also coarse soils or shallow with outcropping rocks. On the contrary, it suffers heavy soils and subject to stagnation. The dynamics of roots growth is still little known. Olive tree root systems can be extended until the edge of canopy projection. They are also superficial, with root length density (RLD, cm/cm³) that can be less than in herbaceous crops and some deciduous orchards (Feres and Goldhamer, 1990). Roots are mostly shallow and temporary. The 70% of roots is found in the first 50-60 cm. Palese et al. (2000) in a study aimed at evaluating the seasonal distribution of olive root growth in southern Italy, observed that they tend to be concentrated within the wetted volume. Maximum root length density is usually observed in winter-spring under rainfed conditions, and during summer under irrigation (Connor, 2005). Olive tree is also one of the fruit tree species that can better tolerate high level of salinity, thus resulting suitable for cultivation close to coastlines.

2.1.6. C-exchanges

Olive tree is a C₃ specie with high rate of photorespiration. The major photosynthesis limitations are high temperatures and light intensity as well as high level of CO₂ concentration. Concerning the plant compartments, leaves are the main element involved in gas exchanges. This is due to the abundance of persistent elements which regulate in- and out-fluxes from leaves. The net photosynthesis rate is not much high, reaching the maximum just for short periods and under specific physical-chemical conditions (i.e. high organic N content in leaves, optimal temperature, high soil water content, etc.). The photosynthetic rate, on average, usually varies with the changes of environmental and varietal conditions. The highest photosynthesis values are usually recorded during the morning, followed by a gradual decrease during the hottest hours

(afternoon). The photosynthetic activity can be observed also within fruits, especially in the early stages of development whilst it is reduced during veraison. The assimilation rate changes even according to temperature values. It decreases with temperatures higher than 35 °C and lower than 5-7 °C due to the considerable increase of plant respiration. On the contrary, the specie finds the highest assimilation rate in a range between 25 and 28 °C. Although this specie can tolerate high level of water stress, it is highly influenced by the levels of light. Therefore, olive tree is very vulnerable to photoinhibition when water deficit happens in conjunction with excess of light.

2.1.7. Economy and statistics

Although olive tree is a typical Mediterranean species and its cultivation has always been widespread around the whole basin, in the last 30 years its cultivation has also been extended in others countries such as California, Australia, Argentina and South Africa. The spreading of olive tree cultivation in these countries was due to the interaction between favourable climate conditions for the growth of the specie with new type of feeding required. Nowadays, the area involved in olive tree cultivation consists of about 9 million 200 thousand hectares around the world (FAO, 2009) with overwhelmingly development (over 98%) in countries bordering the Mediterranean basin. This is confirmed by data from FAOSTAT (FAOSTAT, 2013), which indicate that more than 85% of the area cultivated with olive trees and 52% of worldwide production comes from 7 Mediterranean countries (i.e. Greece, Italy, Spain, Tunisia, Morocco, Syria and Turkey) (Tab. 2.1).

Country	Area Harvested (Ha)	Production (tonnes)	% (Ha)	% (tonnes)
World	9661531.8	18294357.44	100.00	100.00
Greece	820304.8	1123772	8.49	6.14
Italy	1173406	1591104	12.15	8.7
Morocco	615362.6	641002.6	6.37	3.5
Spain	2412106	3146124	24.97	17.2
Syria	637039.4	616001.8	6.59	3.37
Tunisia	1853830	1673430	19.19	9.15
Turkey	766020	842231.4	7.93	4.6
Total	8278068.8	9633665.8	85.68	52.66

Table 2.1 - List of the 7 Mediterranean countries with the highest worldwide production.

Moreover, according to Vossen, (2007) this area consists of over 700 million olive trees thus representing the almost all of global areas where this specie is cultivated. Available data for 2010 indicate that the EU area involved in olive tree cultivation covers about 5 million hectares and the higher concentration is found in Spain (50%), Italy (26%) and Greece (22%). The higher production of fruits is mainly observed in southerly regions (Andalusia, Calabria, Apulia, Crete and the Peloponnese) due to the high drought tolerance of the specie. Infact the major part of olive orchards it's not irrigated (Tab. 2.2). For instance in Spain more than 80% of the production is concentrated in Andalusia, a region characterized by a predominance of non-irrigated olive trees, although there is an increase of irrigated areas. Its cultivation is usually placed in disadvantaged areas (i.e. mountain areas) covering until 88% of the total area of olive groves in Portugal, 71% in Greece, 60% in Spain and 51% in Italy. Latest data from FAO confirmed that the average production of olive oil in European Union was around 2.2 million tons, representing approximately 73% of world production. Spain , Italy and Greece accounted for roughly 97 % of the production of olive oil EU, of which 62% from Spain. From the point of view of quality, the production of the three types of olive oil (extra virgin, virgin, and lamp) showed differences in percentage between Spain and Italy. In particular Spain provided 35%, 32% and 33% of extra virgin, virgin oil, and lamp oil respectively, while in Italy the same categories have represented respectively 59% , 18% and 24 %. The percentages ranging from one year to another due to differences in meteorological conditions.

	Spain (Ha) *	Italy (Ha) **	Greece (Ha) **
Not irrigated	1800000	1069444	852204
Irrigated	700000	280556	307796
Total area	2500000	1350000	1160000

Table 2.2 - List of irrigated or not irrigated areas over the main European olive oil makers. data 2011*; data 2008 **

In 2009/10 the global consumption was about 2839000 tons, representing a situation of substantial stability among the major consumer areas (E.U and the United States) of which 65% (about 1856000 tons) in EU and 9% (about 260000 tons) in U.S. (AGEA and Italian olive oil consortium , 2010). Among the new consumers interesting data come from Australia (about 37000 tons) and Russia (about 18000 tons, while within the UE the greater demand come from Italy (38 %) Spain (30%) and Greece (12%) (AGEA, 2010). Concerning the international trade

Italy can be considered both as net importer than exporter of olive products . The foreign trade of olive oil is the greatest and it involves importation (over 500000 tons in the last four years) of which the main required products are extra virgin and virgin (73%). In 2009 were imported 517300 tons for a total value of 1.3 billion euro, while exportation involved 336210 tons and 1.2 billion euro (ISTAT 2010). The main foreign olive oil imported by Italy in the last four years was from Spain (52%), Greece (19%) and Tunisia (20 %). Exports is more or less constant , especially in terms of volume and especially thanks to the required of the U.S market . Improvements have occurred in Italian exports to France (+10%) and UK (+16%) (ISTAT 2010). Concerning Italy in the last forty years the agricultural area covered by olive orchards has increased more than 3 times compared to the previous years, especially considering that in 1967 was less of 3 million of hectares. In Italy the area covered by this cultivation is very wide (18 regions out of 20), and the only areas in which the specie is not commonly cultivated are mountains and Po valley due to winter low temperatures and the presence of fog and rime. According to the data released by the Italian Ministry of Agriculture (MIPAAF, 2010), about 18 million of olive trees are grown in Italy on 1350000 ha of land (about 165 trees/ha). Traditional plots are usually small, averaging less than one hectare at national level. Crop production average is around 3000 kg/ha or 16 kg/tree and is mainly concentrated in southern regions such as Apulia (32.25%), Calabria (30.31%) and Sicily (9.42%) (AGEA, 2010). Concerning Tuscany, olive trees occupy an area of 56000 hectares, corresponding to 15 % of the UAA . The major part of olive tree cultivation is found in hilly areas (68.3%), extending to the north (Lunigiana and Garfagnana) and in central and southern areas (Chianti, Val d'Orcia, Val d'Era, Val di Cecina). The remaining fraction (32%) involves mountainous areas (24%) and Maremma plains (8%). The world production for the year 2009 was 2.8 million tons (AGEA and Italian olive oil consortium, 2010).

2.2. Eddy Covariance Method

The information presented in this section make reference to the book “Eddy Covariance Method for Scientific, Industrial, Agricultural and Regulatory Applications” by George Burba (Burba, 2013). This section is intended to provide the physical and mathematical principles, the major sources of errors and data processing of the eddy covariance method.

2.2.1. State of methodology

In the last 70 years human activities have strongly contributed to rising atmospheric carbon dioxide concentration (CO₂). The effect of CO₂ increases on terrestrial ecosystems was widely studied since the beginning of the century, when Browne and Escombe (1902) performed the first plant growth experiments. Following, several instruments were developed and applied to understand the influence of CO₂ (ambient and elevated) on plant growth. However instruments such as Plant Growth Chambers, Leaf Chambers or Greenhouses open-top field Chambers did not provide very reliable results. This was due to two main issues: firstly, the alteration of the studied environment; secondly, the large number of replicas needed for having a statistically reliable measure. These issues were overcome through the development and application of the micrometeorological technique Eddy Covariance (E.C). In recent years this technique has established itself as an alternative method for the quantitative assessment of C exchanges at ecosystem scale (Baldocchi and Meyers, 1988; Baldocchi et al., 1996; Running et al., 1999; Canadell et al., 2000; Baldocchi, 2003; Valentini, 2003). It allows continuous measurements within the test site and it does not disturb the environment above the canopies. Moreover, it is relatively independent from morphology and meteorological conditions (Wesely, 1970). E.C allows to measure the turbulent fluxes exchanged between canopy and atmosphere (Stull, 1988). This technique takes in account movements of air particles (eddies) which are developed above the canopy, in conjunction with the mass of gases transported by the motion itself. The technique is based on a simple principles: the net sequestration of carbon dioxide provided by an ecosystem is calculated as the difference between the C entering and leaving from the system (Wesely, 1970). Fluxes can be counted at different time-scale (from half-hour to seasonal) (Stull, 1988). The measures obtained can also concern heat and water fluxes, methane and trace gases. The technique is also used for calibrating climate models on different spatial-scale (medium and global scale) as well as ecological models able to show dynamics of biogeochemical cycles. These measures are also used for validating data from remote sensing or aircraft (Stull, 1988).

Currently, different methods, approaches, and numerous network (i.e. Fluxnet, Ameriflux, CarboEurope, FluxNet Canada, Icos, etc.) provide information with high accuracy about fluxes exchanged between several ecosystems (i.e. forests, long-term agro-ecosystems, crop systems, etc.) and atmosphere. Mostly applications have been developed on vegetation, but aerial experiences on board modified aircraft (Sky Arrow) and boats (usually limited by rainfall and gyroscopic effects) are currently increasing. The two main elements needed for the E.C technique application are the three-dimensional ultrasonic anemometer and the infra-red gas analyser (IRGA). The first detects the wind speed in its three spatial components (x, y, z), while the second measures the concentration of carbon dioxide and water vapor in the atmosphere. They work at high frequency, usually comprised between 10 and 20 Hz. Simultaneously to fluxes measures, ancillary measurements should be collected. In particular these measures concern net and global radiation, the air and soil temperature, precipitation amount and humidity. These data are necessary for understanding the response of fluxes based on meteorological parameters but also for improving data elaboration (i.e. gap-filling and flux partitioning). Although the E.C. methodology is difficult to unify, in the last years many efforts have been done to consolidate the terminology and provide a general standardization of processing steps (Lee et al., 2004). However, since the experimental sites are usually focused on different purposes, different treatments are often required.

2.2.2. Physical and mathematical principles

The air flux can be imagined as an horizontal flow consisting of several rotating eddies having 3-D components and vertical movement. The eddies responsible for the transport of most of the flux depend on their proximity to the ground. Smaller eddies can be more probably observed close to the ground and they are characterized by fast rotation as well as by higher frequency movements of air. On the contrary larger eddies can be more easily observed away from the ground. They are slower and characterized by lower frequency movements of air the movements of eddies can take from few seconds (or less) until some hours. The Eddy Covariance technique is mainly based on the theory of fluid dynamics, which was applied to the atmosphere by Reynolds (Reynolds, 1886) for the first time. Reynolds has correlated the atmospheric turbulence theory with principles and laws of fluid dynamics, highlighting how the turbulent fluxes, in addition to the momentum (vector quantity which is able to measure the body's capacity to change the movement of other bodies in which it dynamically interacts), carries the heat and

other scalar quantities. The equation of conservation of a scalar is the theoretical basis of the Eddy Covariance's technique.

$$\frac{\partial \bar{C}}{\partial t} + \left[u \frac{-\partial \bar{C}}{\partial x} + v \frac{-\partial \bar{C}}{\partial y} + w \frac{-\partial \bar{C}}{\partial z} \right] = \left[\frac{\partial \overline{u'C'}}{\partial x} + \frac{\partial \overline{v'C'}}{\partial y} + \frac{\partial \overline{w'C'}}{\partial z} \right] + D + S_c$$

I
II
III
IV V

Eq 1. Equation of a scalar conservation. I: temporal variation of the concentration of a C scalar at a given point in space ; II: local advection ; III: average horizontal and vertical divergence (or convergence) of turbulent flux; IV: molecular diffusion ; V: processes of formation (or destruction) of the molecules related to the considered scalar.

This mathematical formula can be used for an infinitesimal air volume in which “C” is the mixing ratio of a generic scalar, whilst “u”, “v” and “w” correspond to the three components of the wind velocity. The term “D” represents the molecular diffusion process while “Sc” summarizes the processes of formation/destruction of scalar molecules. Vertical bar on the different variables indicates their average over time, while the peak on the variables in III denotes the instantaneous fluctuation of the value from the mean.

The average value obtained between the instantaneous fluctuations of two variables represents the statistics covariance. The covariance between the three wind speed components and the scalar concentration represents the turbulent flux along the three spatial directions (x , y and z). The technique is based on the principle that the vertical flux of an entity on a surface turbulence layer is directly proportional to the covariance of the vertical velocity and to the concentration of that entity. Therefore it allows to measure the sensitivity of the eco-systemic processes which regulate the absorption of carbon dioxide and water vapour at short (hourly based) and long-term (seasonal or annual) (Lee et al., 2004). In a more simple way, flux can be defined as an amount of a particle that passes through a closed surface (i.e. a Gaussian) per unit of time (Wyngaard, 1990). In very simple terms, flux describes how much of an entity moves through a unit area per unit time (Swinbank, 1951).

Flux is dependent on:

- 1) the number of particles which cross an area
- 2) the size of the crossed area
- 3) the time they take to cross this area.

As reported in the figure 2.1, flux can be imagined as a stream consisting of several eddies, each one consisting of three spatial components (x, y, z), including the air vertical movement (Kaimal and Finnigan, 1994).

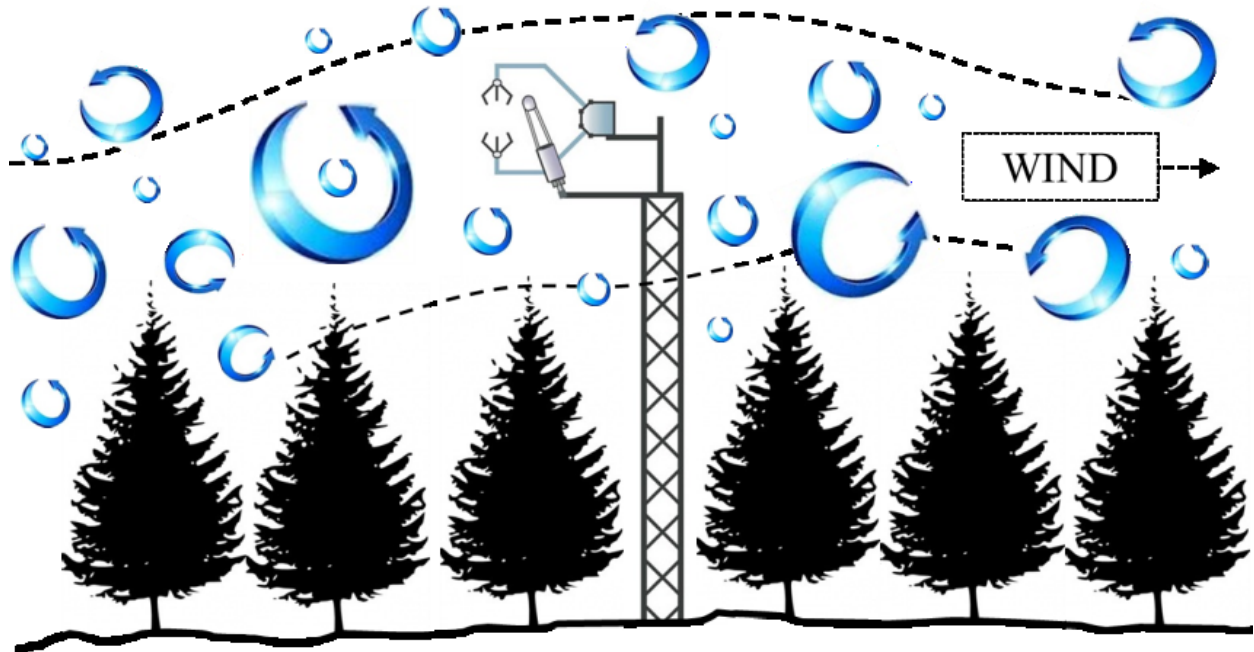


Figure 2.1. – Simple graphical representation of turbulent flux in a forest ecosystem.

For improving the understanding about how the vertical flux can be derived from the covariance between the vertical wind velocity and the concentration of the entity of interest, a simple example was reported: in a time "x", three molecules of CO_2 receive a boost upwards while in the next moment only two molecules of CO_2 go down, the net flux at that time correspond to one molecule of CO_2 directed upwards (Baldocchi, 2005). Therefore eddy covariance is based on assessment of the vertical wind flux by measuring the number of molecules in motion and how fast they continuously ascend and descend. Very sophisticated instruments are necessary to measure the turbulent flux, since the molecular fluctuations occur very quickly. Moreover the variations of molecular concentration, air density and temperature are very small, so needing of very quick and specify calculations.

In turbulent flow, vertical flux can be presented as:



Eq. 2. Vertical flux in turbulent flow. Flux is equal to a mean product of air density (ρ_a), vertical wind speed (W), and the dry mole fraction (S) of the gas of interest. The dry mole fraction is often called the mixing ratio.

Reynolds decomposition can be used to indicate means and deviations from the previous equation (Eq.2). Air density has represented as a sum of a mean over some time and an instantaneous deviation from this mean. A similar procedure can be reported also for vertical wind speed and dry mole fraction of the entity of interest.

$$F = \overline{(\bar{\rho}_a + \rho'_a)(\bar{w} + w')(\bar{s} + s')}$$

Eq. 3. Reynolds decomposition of the vertical flux in turbulent flow.

In the third step the flux equation is simplified as showed below:

$$F = (\bar{\rho}_a \bar{w} \bar{s} + \bar{\rho}_a \overline{w' s'} + \overline{w \rho'_a s'} + \overline{s \rho'_a w'} + \overline{\rho'_a w' s'})$$

Eq. 4. Simplified equation of Reynolds decomposition of the vertical flux in turbulent flow.

Two important assumptions have to be made in the conventional eddy covariance method (Lee et al., 2004). First, the air density fluctuations that in case of strong winds may be non-negligible in comparison with the gas flux, in the major part of the cases (i.e. over reasonably flat and vast spaces such as fields or plains) they can be assumed to be negligible. Secondly, the mean vertical flux is assumed to be negligible for horizontal homogeneous terrain, so that no flow diversions or conversions occur (Massman and Lee, 2002). By assuming to be negligible both flux diversion and conversions, the flux becomes equal to the product of the mean air density and the mean covariance between instantaneous deviations in vertical wind speed and mixing ratio, and the classical equation for eddy flux is:

$$F = \overline{\rho_a w' s'}$$

Eq. 5. Classical formula for the eddy flux of virtually any gas of interest, such as CO₂, CH₄, N₂O, O₃, etc..

Besides the turbulent flux, there are other fundamental formulas which allow to better understand the fluxes dynamics on ecosystems. In particular they concern: sensible heat, water vapour and latent heat (Eq. 6-7-8). Sensible heat flux is equal to the mean air density multiplied by the covariance between deviations in instantaneous vertical wind speed and temperature. Including the specific heat term within the equation, it is possible the conversion to energy units.

$$H = \overline{\rho_a C_p w' T'}$$

Eq. 6. Sensible heat flux

Depending on the units of fast water vapor content do exist several representation of water vapor equation. Water vapor is a fundamental parameter for the calculation of turbulent fluxes and it is often computed in energy units ($W m^{-2}$).

$$E = \frac{Mw/M\alpha}{P} \overline{\rho_a w' e'}$$

Equazione 7. Traditional water vapor flux.

Latent heat flux describes the energy used in the process of evaporation, transpiration, or evapotranspiration and therefore its values can be converted into other commonly used units such as $mm d^{-1}$, $inches ha^{-1}$, $kg m^{-2} h^{-1}$, etc..

$$LE \equiv \lambda E = \lambda \frac{Mw/M\alpha}{P} \overline{\rho_a w' e'}$$

Eq. 8. Latent heat flux

2.2.3. Flux footprint

Flux footprint is defined as the area mainly covered by the instrument on the tower. More in detail, it is referred to the area upwind from the tower where the major part of the fluxes generated are recorded by the instruments (Fig. 2.2). The concept of flux footprint is essential for proper planning and execution of an eddy covariance experiment. The mostly contribution does not come from extremes (i.e. underneath the tower or many kilometres away), but rather from

somewhere in between. The right distance to calculate the main area providing the most part of the contributions has to take in account the dependence of the flux footprint on

a) measurement height,

b) surface roughness,

c) thermal stability.

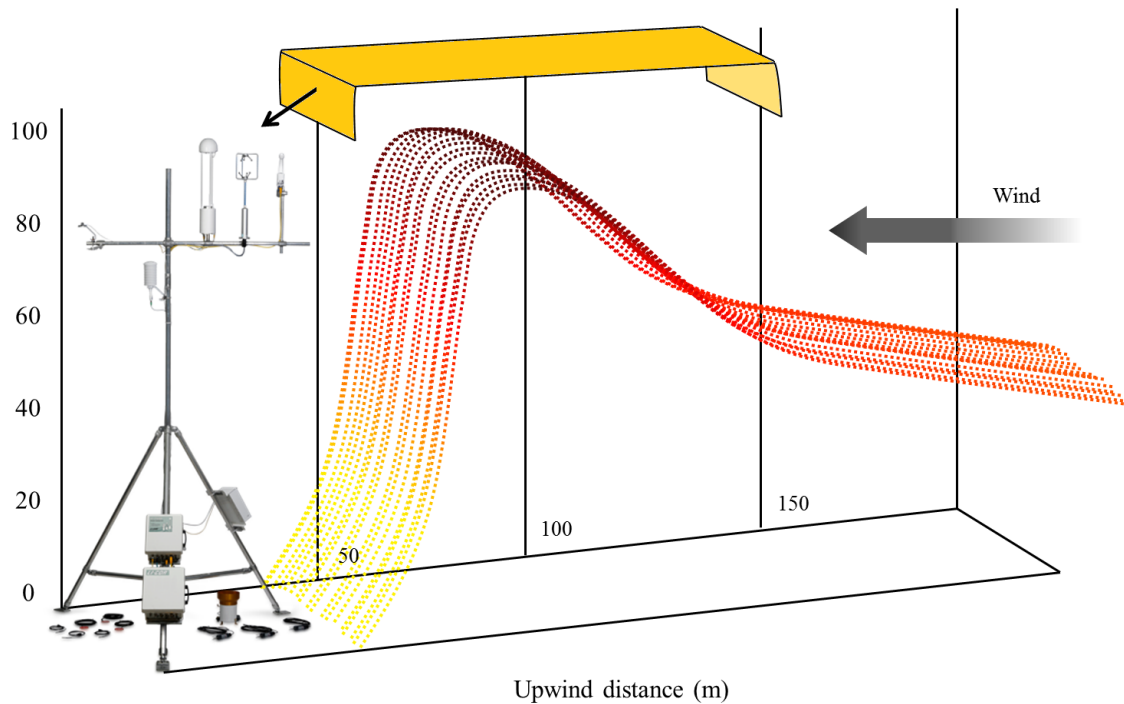


Figure 2.2. – Graphical representation of flux footprint. Modified from Burba et al. 2013.

Measurement height

Footprint strongly increases:

- at 1.5 m over 80% of the ET came from within 80 m upwind
- at 4.5 m over 80% of the ET came from within 450 m upwind

Footprint near the station may also be strongly affected:

- at 1.5 m, the area 5 m around the instrument did not affect ET
- at 4.5 m, the area 32 m around the instrument did not affect ET

Surface roughness

Footprint decreases with increased roughness:

- at a sensor height of 1.5 m:
- for rough surface over 80% of the ET came from within 80 m upwind
- for smooth surface 80% of ET came from about 250 m upwind

Footprint near the station is also affected by roughness:

- for rough surface, area 5 m around the instrument did not affect ET
- for smooth surface, area 10 m around the instrument did not affect ET

Thermal stability

Thermal stability can increase the footprint size several times:

- For a measurement height of 1.5 m and a canopy height of 0.6 m:
- in very unstable conditions, most of the footprint is within 50 m
- in neutral conditions, it is within 250 m
- in very stable conditions, footprint is within 500 m

Flux data under very stable conditions need to be corrected or discarded due to insufficient fetch.

Flux data at very unstable conditions may need to be corrected or discarded due to the fact that large portion of the flux may come from the disturbed area around the instrument tower.

a. Flux footprint depends on:

- Measurement height
- Surface roughness
- Thermal stability

b. Size of footprint increases with:

- Increased measurement height
- Decreased surface roughness
- Change in stability from unstable to stable

c. Area near instrument tower mostly contribute if:

- Measurement height is low
- Surface roughness is high
- Conditions are very unstable

Models able to calculate the flux footprint require specific parameters (i.e. type of instruments, height of the tower (m) of the canopy and eddy tower, wind speed, etc.). these parameters are needed for assessing the area where fluxes are originated and the contribution produced by this area compared to the total footprint. Under normal conditions the contribution of normalized cumulative flux is calculated in terms of percentage according to Eq. 9 (Swuepp et al., 1990).

$$\text{CNF}(X_2) = \frac{\int_0^{(X_2)} \frac{U(z-d)}{u^*kx^2} \cdot e^{-\frac{U(z-d)}{u^*kx^2}} \cdot dx}{\int_0^{\infty} \frac{U(z-d)}{u^*kx^2} \cdot e^{-\frac{U(z-d)}{u^*kx^2}} \cdot dx} = e^{-\frac{U(z-d)}{u^*kx^2}}$$

Eq. 9. Normalized cumulative flux

2.2.4. Processing eddy covariance

Processing of eddy covariance data can change depending on the methodology adopted by researchers. Methodology can change according to the site-specific design as well the sampling conditions. The major steps include the conversion of the signals from voltages to physical units, despiking, the application of calibration coefficients if needed, rotation of coordinates, correction for time delay, de-trending (if needed), average of fast data over 0.5 to 4 hour periods, the application of frequency response, sonic and density corrections, the quality control, filling of missing periods and integration of long-term flux data. Below are reported three main methods to assess the quality of dataset:

- Raw data assessment
- Stationary test
- Test on turbulence and its characteristics

Concerning the validation of eddy data, one of the main methods to evaluate their reliability is building of site-study energy balance. In Fig. 2.3 a simple scheme of energy balance has been reported.

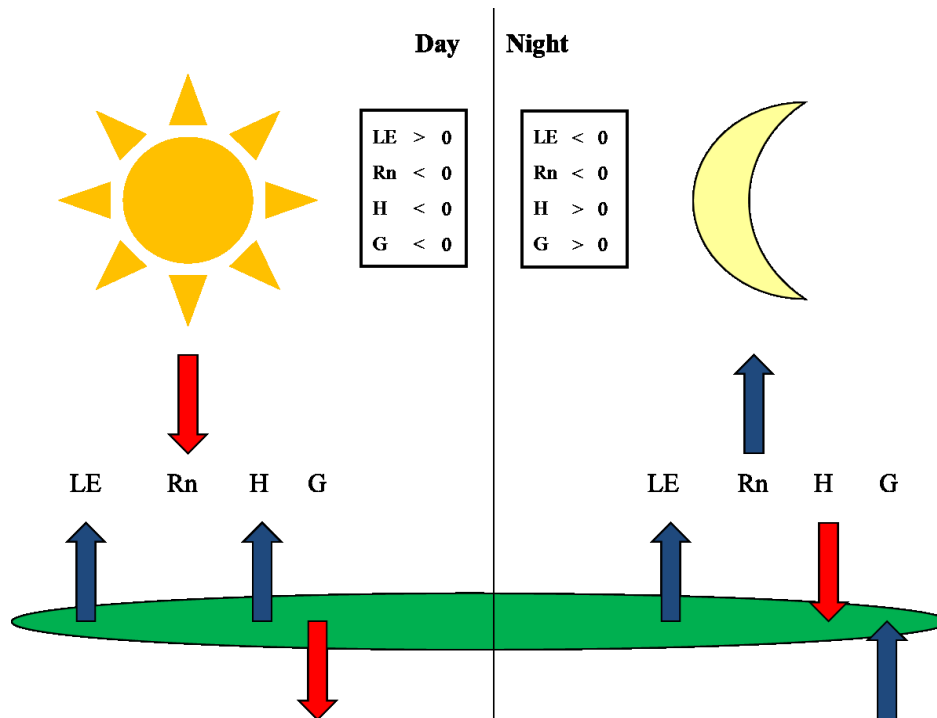


Figure 2.3 – Simple scheme of energy balance

The energy balance is represented by the follow equation:

$$Rn + H + LE + G = 0$$

Rn: net radiation; *L*: latent heat; *H*: sensible heat; *G*: ground heat or the storage of energy.

Validation using study-site energy balance is simple but functional. Sum of all these components must be equal to 0 to have a perfect closure of the balance. If this happens, all energy transfers have been correctly measured (Rosset et al.,1997). Although a good measure of latent heat doesn't mean a correct measure of CO₂ fluxes, correct values observed in latent heat can be taken as a positive-check about the probably good quality of C fluxes. However, by using eddy covariance the closure of energy balance may be incomplete due to the presence of secondary fluxes which can't be measured with this technique. The optimal closure of the energy balance is represented by the following equation:

$$Rn + G = - (H + LE)$$

Eddy covariance instruments measure fluxes over the canopy. During periods without atmospheric turbulence (e.g. night-time) these fluxes accumulate under canopies, reducing data reliability. The total contribution of these measures is fundamental to improve the evaluation of NEE in a certain ecosystem.

2.2.5. Gap-filling and flux-partitioning

A better understanding of ecosystem dynamics can be reached by separating the net ecosystem exchange (NEE) as the gross primary production (GPP) and ecosystem respiration (Reco) through an algorithm to partition the flow (flux partitioning). This method allows to improve the knowledge on the assimilators or breathings processes that are often poorly represented (Falge et al., 2002a; Reichstein et al., 2002b). Flux partitioning also improve the understanding of inter-annual variability of NEE and its dependence by climate or other parameters (Valentini et al., 2000). Before the application of the flux partitioning algorithm, a previous step is necessary. This step, called gap-filling, consists of filling the data gaps that occur in adverse weather conditions or in the event of failure to tools to estimate the long-term budgets.

These processes were following briefly described.

a. Gap-filling

The gap-filling method is built on the co-variation of the fluxes with meteorological variables (air temperature, radiation and vapour of pressure deficit, VPD) and the temporal auto-correlation of the fluxes. On the basis of the gap type (i.e. length of the period, available meteorological parameters, etc.), missing data are substituted by values obtained on the basis of data measured in similar meteorological conditions within a time window of $\pm 7-14$ days. Otherwise, missing data can be exchanged with values obtained on the basis of data measured in the same time of the day.

b. Flux partitioning

Flux partitioning algorithm allows to estimate Reco and Gross Primary Productivity (GPP) from NEE according to the definition equation:

$$\text{NEE} = \text{Reco} - \text{GPP}$$

Eq. 9. Net ecosystem exchange

Different methods to separate the net ecosystem exchange (NEE) into its major components (i.e. GPP and Reco) have been developed. The algorithms can use (filtered) night-time data for the estimation of ecosystem respiration, daytime data or both day- and night-time data, using light-response curves.

The most applied algorithm has been described by Reichstein et al. 2005 and consist of a regression model. Flux-partitioning uses raw data (not gap-filled) to derive Reco from the relation between temperature and nocturnal NEE, which represents the solely the respiratory process. The method proposed by Reichstein et al. (2005) refers to that developed by Lloyd and Taylor, (1994) (Eq. 11):

$$R_{eco}(T) = R_{eco,ref} \cdot e^{E_0 \left(\frac{1}{T_{ref}-T_0} - \frac{1}{T-T_0} \right)}$$

Eq. 11. Ecosystem respiration equation from the method proposed by Lloyd and Taylor, (1994); T: air temperature; T₀: is a constant 46.02; E₀: the activation energy (it determines the temperature sensitivity and is a free parameter); T_{ref}: set to 10°C.

Since Reco is a parameter that temporally varies in an ecosystem, Reichstein et al. (2005) used the nonlinear regression model by Lloyd and Taylor (1994) fixing all parameters with the only exception of 'Reco,ref'. They estimated this parameter just once using the long-term temperature sensitivity and another by the short-term temperature sensitivity. Thus, the 'Reco,ref' estimates were assigned to that point in time. Finally the 'Reco,ref' parameters were estimated for each period and linearly interpolated between the estimates, resulting as a dense time series of parameters. Consequently, for each point in time, Reichstein et al. (2005) provided Reco estimates according to the following equation:

$$R_{eco}(T) = R_{eco,ref}(T) \cdot e^{E_0 \left(\frac{1}{T_{ref}-T_0} - \frac{1}{T_{soil(t)}-T_0} \right)}$$

Eq. 12. Ecosystem respiration equation from the method proposed by Reichstein et al. (2005); T: air temperature; T₀: is kept constant at 46.02 as in Lloyd & Taylor (1994); E₀: the activation energy (it determines the temperature sensitivity and is a free parameter); T_{ref}: is set to 10°C as in the original model; (T): time-dependent parameters and variables.

2.3. Simulation models

Simulation is defined as the process able to imitate instantaneous or long-term processes of a system. Simulation can provide useful information concerning the assessment of the system's characteristics, the main elements that can affect it, and elements needed for its development. The ability to reproduce a certain system or process allows comparisons with similar systems, resulting in benefits such as an optimal parameterization, critical issues and possibility to predict future performances. Simulations can provide advantages such as possibility to test things or strategies before to apply them, time reduction, understanding of systems dynamics, exploration of new policies and managements, diagnostic, etc.. However simulations have two main problems: the first one is due to the cost for building or implementing the tools, the second is the difficulty to understand and interpret results obtained. In the last 30 years, crop simulation models are became fundamental tools for scientific research and planning of agro-systems. The spreading of these tools is due to their easy application in several environment and under different conditions (i.e. management, climate, variety) compared to those in which they have been developed. In addition, while ground based measurements are limited at small spatial and temporal scales (e.g. gas concentration) due to snapshots of state variables, the models can offer full spatial and temporal coverage (Del Grosso et al., 2008). In this work were used two different kind of models. The first one is a remote sensing model called C-fix that was described and applied in paper 2. The second is a biogeochemical model called Daycent, described and applied in paper 3.

a. Remote sensing models:

Remote sensing is a technology that involves specific electromagnetic sensors usually installed over satellite or aircraft to measure and monitor changes in the earth's surface and atmosphere (Showengerdt, 2006). In recent years remote sensing models have been widely applied to assess crop growth and yield estimation, thus resulting as the best source of data for large scale applications and study. This methodology is mainly based on satellite images which give a series of numbers resulting as the amount of the energy reflected from the earth's surface in different wavelength bands. Among the different bands, the major part of information concerning vegetation growth and physiological conditions can be found into the infrared bands, that are not visible to the human eye. Infact the majority of approaches using remote sensing for monitoring and managing both natural and crop systems involves dissimilarity in reflectance properties

between visible and NIR wavelengths (Knippling, 1970; Bauer, 1975). Green leaves show lower values for reflectance and transmittance within visible regions of the spectrum (i.e., 400 to 700 nm) but higher in the near-infrared regions (NIR, 700 to 1300 nm) (Bouman, 1992). One of the main advantages using satellite images is the possibility to observe many times changes in surface conditions. For instance, given that a satellite regularly passes over the same land, it become possible to continuously catch new data about land use as well as monitoring physiological conditions over the year. Remotely-sensed images are also usually combined with ground observations to obtain a complete picture of changes. For instance one of the most simple method for extracting the green plant quantity signal is the vegetation indices (VGT). This indices are computed as differences, ratios, or linear combinations of reflected light in visible and NIR wavebands (Tucker, 1979; Jackson, 1983). Vegetation indices such as the ratio vegetation index (RVI = NIR/Red) and normalized difference vegetation index NDVI = (NIR - Red)/(NIR + Red) are optimal for investigating biomass measures through the season since they are well correlated with green biomass and leaf area index of crop canopies (Pinter et al., 2003).

b. Biogeochemical models:

Biogeochemical or biogeochemistry (BGC) models are able to reproduce several ecosystemic processes concerning both plant physiology that entity exchanges. These models therefore can explain vegetation phases such as growth, competition, senescence and mortality but also processes related to natural energy and matter exchanges (i.e. H₂O, C, N) between vegetation, soil and the atmosphere. The major part of these models is mainly based on climate conditions, soil characteristics, nutrient and water supply. Although these tools can represent whole systems and their interaction with other components (i.e. biosphere, atmosphere, hydrosphere), they can be divided according to specific characteristics to deal with soil processes, agricultural crops or forestry only. They can be used also to simulate external effects such as the impact of current and future climate change on crop growth, the effect of different management on soil carbon and water balances, and many others. These tools can represent the behaviour of plant growth functions and exchange processes through mathematical equations. The main physiological processes (e.g. crop growth) are usually correlated with the most important meteorological parameters such as temperature, radiation and rainfall (water and nutrient supply). BGC models can vary also depending on their scale of investigation. For instance some models can be applied to a single plant or vegetation type while other can be used over large areas if representative of

specific plant types. In the second case, biogeochemical models tend to classify certain functional types as homogeneous (grass, trees, savanna, shrub, crop, etc.). Each of these types is calibrated according to empirical conditions. In the last years BGC models have been used by many researchers to assess the impact of climate change on crop systems as well as the effect of mitigation and adaptation strategies with the aim to reach the goal of Kyoto protocol. Starting with global studies carried out by entity such as IPCC until smaller examples of regional studies of climate change on vegetation, hydrology, agricultural production, and economic development, these models are currently widely used and applied. The main elements of strength in BGC models are the reliable representation of vegetation with relative processes, the high flexibility in temporal scale and coverage, ranging from days to millennia, the flexibility in spatial coverage (from single plants to global) and the ability to explain links between biophysical conditions and human activities, especially crops and forestry (Hermann Lotze–Campen, 2008, 2010). On the other hand, these models also show weakness due to their high complexity, limitation of data availability and request of many inputs , numerous empirical formulations, difficulty for uncertain analysis and the limited coverage of anthropogenic processes (Hermann Lotze–Campen, 2008, 2010).

2.3.1. C-Fix

C-Fix is a generally applicable model, conceptually easy and able to use inputs averaged over different time periods (most commonly ten-day to monthly). It is a Monteith type parametric model driven by temperature, radiation and fraction of Absorbed Photosynthetically Active Radiation (fAPAR). A first description of the model was given by Veroustraete et al. (1994, 1996). The model is quantified through its generalized relationship with NOAA/AVHRR data processed as well as vegetation (VGT) index. The most common index used for a long time in remote sensing is the vegetation index called Normalised Difference Vegetation Index (NDVI). This index is defined as the ratio between the difference and the sum of the reflectance in the red and infrared-wavelength bands (Maselli et al., 2009) (Eq. 13).

$$NDVI = (\rho_{nir} - \rho_{red}) / (\rho_{nir} + \rho_{red})$$

Eq. 13. Normalised Difference Vegetation Index (NDVI)

The NDVI is a dimensionless index, with a value ranging between -1 and 1 . The index is mainly influenced by the reflective characteristics of the vegetation such as pigmentation of the leaves, LAI, gap fraction and the BRDF or bi-directional reflectance distribution function, while is insensitive for variations in short-wave radiation (Veroustraete et al., 2002). NDVI values can be converted into fAPAR values by the generalized equation of Myneni and Williams (1994). The equation described by Myneni and Williams has indicated a linear relationship for a large set of different vegetation-soil-atmosphere observation conditions (Eq. 14).

$$fAPAR = \alpha \cdot NDVI + \beta$$

Eq. 14. fAPAR values by the generalized equation of Myneni and Williams (1994).

Where α and β are empirical constants equal to 0.8642 and -0.0814 according to Myneni and Williams (1994). This relationship is independent of the vegetation cover heterogeneity of the pixel and background effects, but it can vary according to the ‘greenness’ represented by the NDVI canopy, however. The fAPAR obtained by remote sensing is combined with field based estimates of incoming solar radiation and air temperature. Successively, all these elements are jointly used to simulate total photosynthesis and, in turn, the net carbon accumulation. This latter is calculated by subtracting respiratory fluxes from autotrophic and heterotrophic (Maselli et al., 2009). This methodology allowed estimates of specific ecosystemic parameters such as GPP, NPP and NEP. In particular for forest ecosystems, the GPP has usually been computed over monthly scale as $gC\ m^{-2}$ according to the following equation (Eq. 15):

$$GPP_i = \epsilon \cdot Tcor_i \cdot fAPAR_i \cdot Rad_i$$

Eq. 15. Gross primary production. ϵ : radiation use efficiency ($g\ C\ MJ^{-1}(APAR)$); $Tcor_i$: temperature correction factor of the month (different for plain and mountain forests); $fAPAR_i$: fraction of the photosynthetic active radiation absorbed by the forest during the month, derived from NDVI; Rad_i : incoming photosynthetically active radiation of the month ($MJ\ m^{-2}$); i : referred to day i .

With specific regard to Mediterranean ecosystems, Maselli et al. (2009) have modified the C-Fix model by integrating an additional water stress index called 'Cws', that limits photosynthesis in

case of short-term water stress. This index can vary between 0.5 and 1, depending on if short-term water shortage reduces photosynthesis to half of its potential value or there is no water shortage and photosynthesis reduction (Maselli et al., 2009). In addition, the new C-Fix version has also concerned the use of new temperature correction factors for MODIS (remote sensing) which have substituted the original factors proposed by Veroustraete et al. (2002).

The new equation representing the computation of GPP was reported below:

$$GPP_i = \varepsilon \cdot Tcor_i Cws_i fAPAR_i Rad_i$$

Eq. 16. Equation representing the computation of GPP; ε : is the maximum radiation use efficiency (from 1.4 to 1.2 g C/MJ APAR since the MODIS temperature correction factors are about 15% higher than the corresponding C-Fix factors) (Chiesi et al., 2011); $Tcor_i$: is the MODIS temperature correction factor for evergreen broadleaves; Cws_i is the water stress factor for Mediterranean trees $fAPAR_i$ is the fraction of absorbed PAR, and Rad_i is the solar incident PAR, referred to day; i : all referred to day i

2.3.2. Daycent

Daycent (Parton et al., 1998; Kelly et al., 2000; Del Grosso et al., 2001) is a biogeochemical model used to simulate C and nutrients fluxes in crop field, grassland, forest, and savanna ecosystems. Daycent was built from the monthly version of Century and it works at daily time step. It can simulate fluxes of carbon, nutrients, and trace gases among the atmosphere, soil, and plants as well as specific events (i.e. fires, grazing) and management practices (i.e. fertilization, tillage, pruning, etc.). It was worldwide applied to simulate the impacts of climate and land use change on several ecosystems such as crop systems, grassland, and forestry.

It is also currently used by USDA (United States Department of Agriculture) to estimate soil N₂O emissions from agricultural lands for the annual GHGs inventory. The ability of that model to work at daily time step allows a greater accuracy in the most important plant-soil processes, resulting in higher care to fluxes. The complexity of the model strictly depend on data availability, purpose and scale of application, and many other considerations. Although Daycent represents most of the main processes responsible of C and N fluxes, not everyone are mechanistically represented. For instance the model does not simulate N gas diffusion from soil nor O₂ diffusion into soil, which are both fundamental parameters to drive nitrification and denitrification rates. The model does account for the impacts of gas diffusion by calculating a relative gas diffusion index which, in turn, influences emissions of the different N gas species

(NO_x, N₂O, N₂). Concerning plant growth rates, nutrient availability has considered by the model as the main control. Photosynthesis process is not simulated but it considers the impacts of radiation based on day length calculated as function of latitude and day, and cloud cover, that is inferred by comparing diurnal maximum and minimum temperatures. Daycent requires some specific inputs such as soil texture, current and historical land use, daily maximum/minimum temperature and precipitation data, which have to be provided to run the model. Daycent includes specific sub-models (Fig. 2.4):

- plant productivity (green),
- decomposition of dead plant material and SOM (yellow),
- soil water and temperature dynamics (red),
- nitrogen (N) gas fluxes (blue).

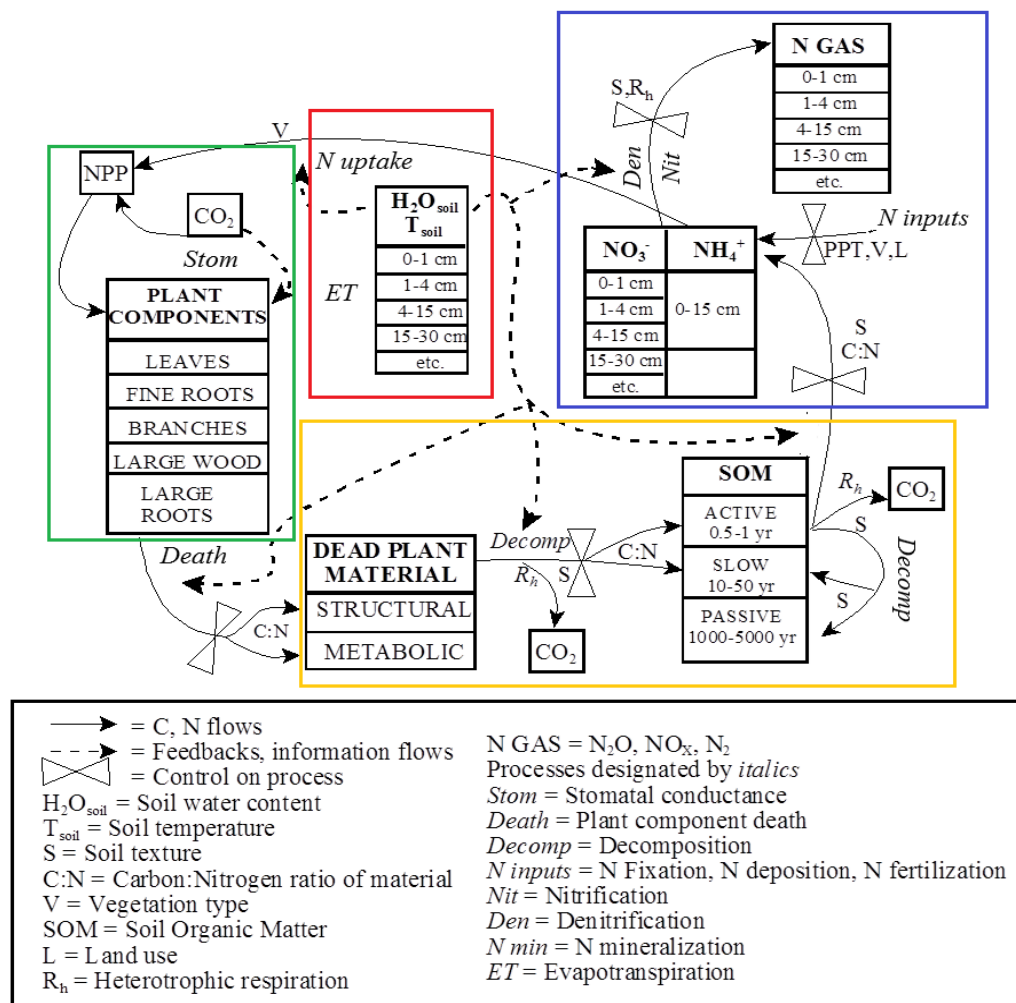


Figure 2.4. – Conceptual diagram of the Daycent ecosystem model, Del Grosso et al. (2008).

At the beginning of simulation process it should be needed model's spin up in order to generate stable values of soil carbon. Since initial values for C and nutrient are usually unknown for each single pool (i.e. active, passive, stable), spin up allows to reach an equilibrium in soil C and N dynamics. More specifically, Daycent model needs at least 2000 years of simulation. Model outputs could be improved if historical land use (base simulation) for model spin up is applied.

Daycent model inputs can be divided into 4 categories:

Weather Information (.WTH): Daycent can run using a simple weather file consisting in max/min temperature (°C) and precipitation (cm) or by adding 3 extra drivers such as solar radiation (langleys d⁻¹) wind speed (mph) and relative humidity (%). When model runs at site scale the weather data should be provided by a weather station close to the study area, on the contrary when it runs at regional or larger scales, data sets such as DAYMET (Thornton et al. 1997, 2000; Thornton and Running, 1999; <http://www.daymet.org>) can be used.

Site Information (.IN): Soil properties are fundamental when model runs at site level data since they influence plant growth, water, nutrient flows, and decomposition processes. In particular soil layer thickness and number of layers to bedrock or water table. Required soil properties for each layer include texture, bulk density, wilting point, field capacity, the extent to which water content can drop below the wilting point, root fraction, organic matter fraction, saturated hydraulic conductivity (Ksat), and pH. Soil texture, depth to bedrock, and pH are typically available for experimental plots and can also be derived from soil map units. Field capacity and wilting point, as well as Ksat, can be derived based on soil texture. The site latitude is used in the plant growth submodel to calculate solar radiation, and how many elements, in addition to C, are simulated. The N cycle, N and P, or N, P, and S, can be chosen as output data. Changes in some environmental conditions can be simulated through time especially concerning the increase or decrease of ambient CO₂ levels, daily temperature and precipitation values, soil pH, and soil temperature by specified amounts over a specified time period. The model can also simulate 14C or 13C labelling, incubation experiments, and microcosms (e.g. buried litter bag experiments).

Crop Information (.100): Daycent has been parameterized for the major U.S crops (corn, soybean, wheat, hay, sorghum, cotton) as well as other important crops (barley, potato, millet,

tomato, sweet corn, etc.). The model also includes parameterizations to represent grassland, forest, and savanna biomes (e.g., tallgrass, shortgrass, boreal forest, arid shrubland, tropical savanna, etc.). In case of crop or mix vegetation that are not represented in the crop library, a modification of an already existing parameterization that most closely resembles the new crop of interest can be done. In this case it is suggested to collect data needed for the new crop parameterization such as: portions of carbon allocated, death rates, lignin portions of plant components, maximum growth rate, growth response to temperature, harvest index, soil temperature and degree days. Crops need of some phenological parameters such as knowing if the crop is perennial or an annual or if the beginning and end of the growing season are specified or generated by the model, the begins of growth for perennials or germination for annuals , and the day when harvest or senescence occurs at the end of the growing season. Alternatively, the beginning of the growing season can be made a function of soil temperature and the end of the growing season a function of accumulated growing degree days. For instance, the amount of degree days and harvesting time can be used for flowering (beginning of anthesis).

Management Information (.100): Daycent provides several common management options (tillage, irrigation, fertilization, planting, harvesting, burning, grazing, etc.) besides the availability of automatic fertilization and irrigation options. The model affords to indicate the calendar day on which the management or disturbance event occurs which usually influence the controlling soil parameters , vegetation, litter pools, and the magnitude of impact on the different pools (SOM, SOC).

Generally, a simulation model can be well applied across different eco-systems without changing many parameters with the only exception of those relating to weather, soils, vegetation, and land management. However, a tuning can contribute to improve the representation of a specific eco-system under particular conditions, avoiding poor performances of the model especially for some site/treatment combinations. A good calibration consists in a change of parameters to improve model fitting, specifying how much and how model performances have been improved. This can be done by the identification of the most sensitive parameters, which can be found through a sort of sensitive analysis or basing on the already provided information for the site. These analysis are necessary to understand how a value of a specific parameter should change across sites.

The improvement of a model make sense just if parameters changed take a biological sense. Daycent consists of more than 1000 parameters but just a small subset of these is necessary for calibration. After the first run of the model an assessment of model outputs should be needed. More specifically it should be done by following a specific order: soil water content, crop yields and plant growth rates, soil organic carbon levels, and N loss vectors (Fig. 2.5).

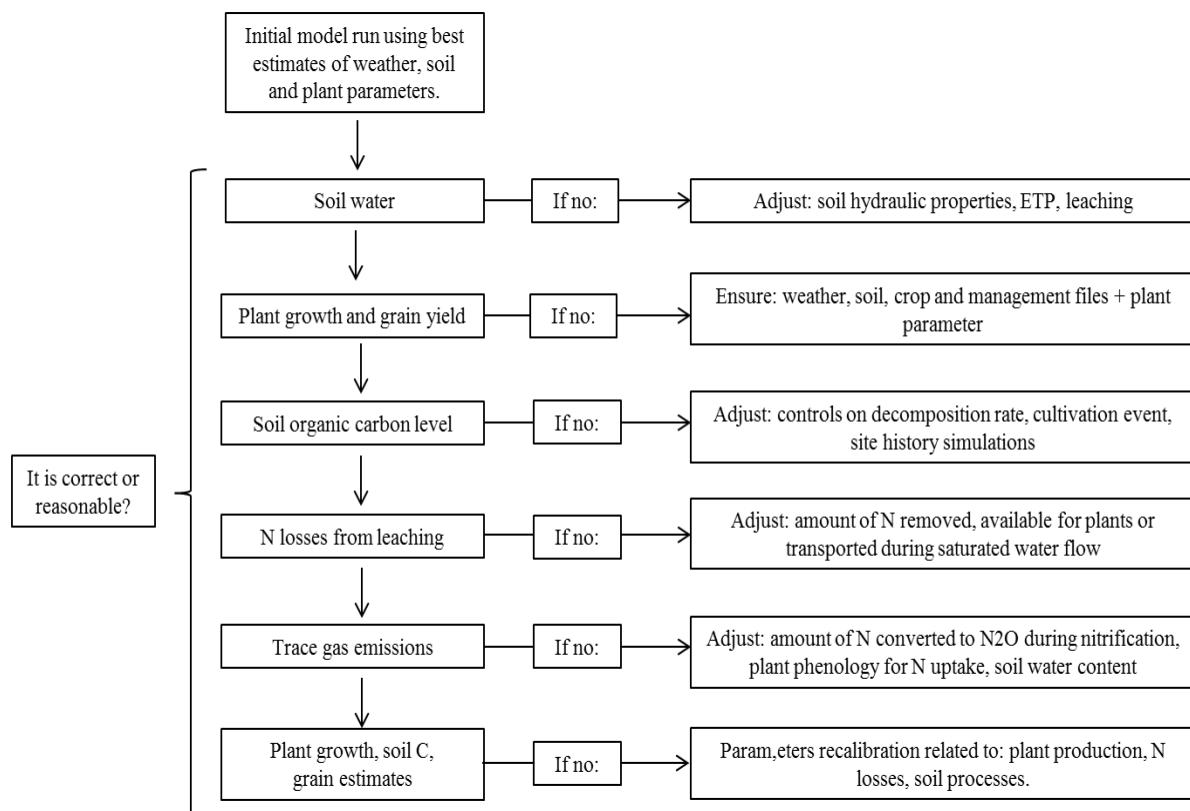


Figure 2.5. – Conceptual diagram of the check of Daycent outputs.

Del Grosso et al. (2008) suggest that the previous indicated check should be done because the soil water content is the primary control on most of the key processes represented in the model. By contrast plant growth rates and crop yields can be successively verified because yield data can be affected also by other variables of interest. In the same way a check of SOC levels appears fundamental since SOC integrates within the model many processes (e.g. NPP, decomposition) that are sensitive to environmental conditions and management. Lastly, N flows should be verified. Different uses of statistics methods such as R^2 , RMSE, MBE, mean error, etc.

must be considered as necessary for evaluating model performances. First analysis about the reliability of the model can be done following two ways: i) comparison between model outputs with field data; ii) comparison between the same outputs from different models. Generally speaking, model assessment strictly depends on the variable of interest, the scale of measured data, and the intended model application. For instance, according to Del Grosso et al. (2008), differences in SOM correctly simulated under different treatments are more important than finding absolute SOC values.

Daycent has been widely tested on several crop systems, grasslands and forests around the world (Morgan et al., 2004; Pepper et al., 2005; Conant et al., 2005). Beginning in 2005, the model was used at county scale to estimate N₂O emissions from cropped and grazed systems for the Inventory of U.S. Greenhouse Gas Emissions and Sinks compiled annually by the EPA (Del Grosso et al., 2006, 2010; EPA, 2010). Model's application was also focused to estimate soil greenhouse gas mitigation from cereals cultivation. In particular several studies at the global scale on corn, soybean, and wheat have been carried out (Del Grosso et al., 2009). Several researchers have also used the model to calculate crop yields and soil greenhouse gas emissions for different biofuel cropping systems (Adler et al., 2007; Davis et al., 2010, Robertson et al., 2010, 2011). To our knowledge, no one study has been carried out over savanna ecosystems.

Chapter 3

Effects of inter annual and inter-seasonal variability in rainfall regimes on C-exchanges of a rainfed Olive orchard

Abstract

Olive tree is a fundamental cultivation in the Mediterranean basin, where expected changes in temperature and rainfall regimes may affect biomass growth and carbon sequestration capacity. Using eddy covariance flux measurements made over a typical Mediterranean rainfed olive orchard in Italy, the relationships between Net Ecosystem Exchange (NEE) and the main climate variables (rainfall, temperature and solar radiation) recorded over three contrasting and extreme years spanning over 90% of the long-term rainfall variability, have been investigated. Across those years, the olive orchard resulted overall a net carbon sink ($3.6 \text{ tC ha}^{-1} \text{ year}^{-1}$), and annual and seasonal NEE was found to be mostly driven by rainfall regimes and their intra-seasonal variability. More specifically, spring-like rainfall was the main driver of both spring and summer NEE ($r=-0.941$; $p\text{-value}=0.00519$). On the contrary, monthly scale NEE was not correlated with rainfall ($r=-0.286$; $p\text{-value}=0.0908$), whilst good correlations were observed with air temperature ($r=0.473$; $p\text{-value}=0.00355$) and solar radiation ($r=0.541$; $p\text{-value}=0.00065$). These results indicated that rainfall amounts and timing represent the most important driver of carbon storage of rainfed olive trees in Mediterranean environment. Therefore, future expected changes in rainfall pattern (i.e. reduction in total annual rainfall, changes in seasonal distribution, etc.) may cause losses in the climate mitigation capacity of these ecosystems.

Keywords: Olive orchard, climate variability, NEE, eddy covariance.

Chapter based on:

Brilli, L., Gioli, B., Toscano, P., Moriondo, M., Zaldei, A., Cantini, C., Bindi, M. 2014. *Effects of inter annual and inter-seasonal variability in rainfall regimes on C-exchanges of a rainfed Olive orchard*. Biogeosciences (submitted).

3.1. Introduction

Olive (*Olea europaea* L.) is among the most ancient cultivated fruit trees in the Mediterranean Basin (Connor, 2005). Although its cultivation has been successfully introduced in other countries such as California, Australia, Argentina and South Africa (De Graaff and Eppink, 1999), Mediterranean basin is still the most relevant olive trees cultivated region. This area consists of more than 700 million olive trees cultivated on over 9 Mha, representing a large fraction of worldwide production (Vossen, 2007). More than 85% of cultivated area and 52% of worldwide production come from 7 Mediterranean countries (i.e. Greece, Italy, Morocco, Syria, Spain, Tunisia and Turkey) (FAOSTAT, 2013).

The primary role of olive orchards within Mediterranean basin concerns agriculture and, more in detail, the production of olives and olive oil. However, this cropping system can also indirectly contribute to increase local economies by providing ecosystem services such as soil preservation, environment conservation and climate mitigation (Lomou and Giourga, 2003; Sofo et al., 2005) but also through the increase of tourism due to the attraction of typical rural landscapes (e.g. Tuscany in Italy, Andalusia in Spain). Currently, the majority of studies carried out on olive trees have been focused on agronomic aspects (Castro et al., 2008; Gómez et al., 2009) or economic analysis (Iraldo et al., 2013; Palese et al., 2013), whilst just few studies have investigated their functional role for ecosystem services (e.g. Lomou and Giourga, 2003; Fleskens et al., 2008). Among these ecosystem services, the role that olive orchards can play in climate mitigation has often been neglected.

The lack of knowledge about the C-sequestration capacity provided by this system is mainly due to the fact that the majority of the studies was focused on forest ecosystems, that are characterized by extended areas with continuous canopy that allow a more straight forward C-fluxes assessment both from the ground (i.e. eddy covariance, FACE, respiration chambers, etc.) and from satellite (i.e. remote sensing). By contrast, orchards have an intrinsic structural complexity (different eco-physiological characteristics and agricultural practices) that makes measurements more challenging and expensive to obtain.

However, this system can play a fundamental role in climate mitigation due to their recognized long-term carbon storage capacity in soil and woody compartments (Nieto et al., 2010; Brilli et al., 2013). This aspect, in conjunction with their widespread cultivation in one of the areas mostly exposed to the risk of climate change (IPPC, 2013), may open new ways to achieve the

goals fixed by international regulations on greenhouse gas control (e.g. “20-20-20” Policy”; Directive 2009/29/EU).

Despite eco-physiological characteristics and agricultural practices can highly affect C-sequestration capacity, it is well known that climate conditions are the main driver affecting carbon fluxes dynamics and biomass growth. In particular, C-fluxes dynamics are influenced by changes in mean climate and climate variability which are noticeable especially over Mediterranean area, as confirmed by several studies (Vautard et al., 2007; Haylock et al., 2008; Durão et al., 2010; Rodda et al., 2010; Del Rio et al., 2011; IPCC, 2013).

Looking at future climate projections, predicted changes in temperature and rainfall trends are expected to lead more extreme climatic conditions compared to present (Jacob and Podzun, 2010; Lenderink and Van Meijgaard, 2008; Kjellström et al., 2011; IPCC, 2013). A joint occurrence of higher temperatures and drought period is expected to amplify the impacts on semi-arid ecosystems. In Mediterranean basin, while temperature and radiation are not usually considered as limiting factors for crop growth and development, water availability is widely recognized to be the key variable controlling mass exchange and growth (Noy-Meir, 1973; Chaves et al., 2002; Kwon et al., 2008; Jia et al., 2014, Medrano et al., 2009). Therefore, changes in rainfall patterns may lead to different response in terms of carbon fluxes and stocks.

Understanding how rainfall can affect C-stocks in Mediterranean olive orchards is crucial since the majority of studies was carried out on irrigated fruit systems (Dichio et al., 2005; Testi et al., 2008; Villalobos et al., 2012; Nardino et al., 2013). This agronomic practice, however, is unusual for Mediterranean environment and specifically for olive trees. According to the data provided by the 6th General Census of Agriculture (ISTAT, 2010), in Italy only 8.7% of olive trees farms are managed with irrigation systems, while the remaining forms of olive orchards (i.e. tiny land plots or abandoned systems) do not usually make use of this practice. Therefore, irrigated olive orchards may provide C-fluxes that do not reflect the actual contribution offered by the large majority of these ecosystems, nor are capable of assessing the ecosystem response to climate extremes.

In this study, we investigated the relation between GPP (Gross Primary Production), NEE (Net Ecosystem Exchange) and climate variables in a typical Mediterranean rainfed olive orchard. Although the study spans a relatively short period of 3 years (2010-2012), those were very contrasting and representative of the long term 30 years climate variability at the study area, allowing the investigation of ecosystem response to mean and extreme rainfall patterns

characterized by both positive and negative anomalies. Annual, seasonal and monthly rainfall interaction with C-balance dynamics was investigated to finally assess the capacity of Mediterranean olive orchard to front increasing occurrence of climate extremes and drought.

3.2. Materials and methods

3.2.1. Study Area

The study area is located in central Italy (Follonica, 42°56' N, 10°46' E). According to Thornthwaite's classification (Thornthwaite, 1948) the area has a mesothermic climate, with high temperatures and prolonged drought periods in summer and mild winters. The coldest month is January with a monthly mean temperature of 7.5°C, while the warmest is August (30.9°C). The long-term total annual rainfall average (RAIN-LTA) extrapolated by MARS JRC (JRC/MARS-Meteorological Data Base–EC-JRC: <http://mars.jrc.ec.europa.eu/>) data set for the period 1981-2009 is 626 mm, with rainfall events mainly concentrated in fall and early spring.

The natural vegetation of the area is typical of the Mediterranean basin. In particular the most common herbaceous species are *C. dactylon*, *Trifolium campestre*, *Medicago polymorfa*, *Picris hieracioides*, and *Bromus sp.*, while the major tree species are sclerophyllus holm-oak (*Quercus ilex* L.), cork oak (*Quercus suber* L.) and olive trees (*Olea europaea* L.). The study site is an adult olive orchard placed at 41 m a.s.l.. The orchard has irregular shape and covers about 6 ha. Olive trees have all the same age (20) and plant density (7x5m). Morphology is regular with slight slope from north to south. The orchard contains more than 1500 plants of 4-5 meters in height, while canopy cover is about 25% (Maselli et al., 2012).

Soil chemical analysis showed that the orchard consists of clay-loam textural class (40% silt and 38% clay) with an average pH of 7. In addition, according to the Harmonized World Soil Database (HWSD) (FAO/IIASA/ISRIC/ISS-CAS/JRC, 2009), the available water capacity of the area ranges from 60 to 90 mm/m.

Agricultural practices consist of inter-row superficial tillage, fertilization about one time per year (usually in late winter or early spring) while irrigation is not applied. During the whole study period (i.e.3 years from 2010 to 2012), the orchard was ploughed three times at 10 centimetres deep using disk-harrowing: the first time in early May 2010, the second in February 2011 and the last in late May 2012. Fertilizer was applied at the surface once per year, at the end of February (2011) or in May (2010 and 2012). Mechanical harvesting was applied in 2010 and 2012 in November, while in 2011 fruits were left on the trees due to the extremely low production.

Weeds beneath the trees, litter and residues due to mechanical harvesting (e.g. leaves, small branches, fruits) were incorporated into the soil during tillage.

3.2.2. Eddy covariance data and processing

The eddy covariance (EC) micrometeorological technique was used to measure fluxes of carbon dioxide (CO₂), water vapor (H₂O), sensible heat (H) and latent heat (LE) between the ecosystem and the atmosphere (Baldocchi et al., 1996). The EC tower was installed in March 2010 and placed in the central part of the olive orchard.

The tower was composed of a mobile carriage equipped with a 7 m mast, hosting a Metek USA 1 triaxial sonic anemometer and a Licor 7500 open path infra-red CO₂-H₂O analyser. Instruments were installed at 7 m above ground and 2 to 3 m above canopy top. A battery power supply was used, charged by 3 solar panels with 90 A/h capacity placed 30 m south from the tower to maximize solar radiation efficiency. This setup caused some power outages during wintertime. Ancillary data included soil temperature profiles from 5 to 20 cm (thermocouples J and T types), global and net radiation (CMP3 and NR LITE Kipp & Zonen), air temperature and humidity (HMP45 Vaisala), and rainfall (rain gauge Davis 7852), and were stored on half-hourly basis on a data logger (Campbell CR10X). Fast eddy covariance sensors (i.e. sonic anemometer and CO₂/H₂O IRGA) were acquired at high frequency (20 Hz) and stored on a handheld low consumption computer (Matese et al., 2009).

Eddy covariance raw data were then analysed and processed. First of all, in order to assess the extent of the area surrounding the tower from where the observed fluxes originated, a footprint analysis was made using an analytical model (Hsieh et al., 2000), that computed footprint distances as a function of wind speed and direction, atmospheric stability, measurement height and surface roughness. The area containing 90% of the observed flux, was computed at an average of 108 ± 16 m around the observation point, that is almost entirely contained within the olive orchard limits, extending 152 ± 26 m in the various directions. Then, the binary files and meteorological data collected by E.C. tower were processed using Eddy Pro® Software in Express Mode. Processing consisted of several steps such as spectral corrections for flux losses (Moncrieff et al., 1997), despiking procedure for detecting and eliminating short-term outranged values in the time series and control tests according to Foken et al. (2004).

The output of Eddy Pro® consisted, among others, of NEE data at half-hour resolution that were then used as input for the gap-filling and flux partitioning procedure developed by Reichstein et

al. (2005). During the 3 years of experiment some technical issues caused data loss concentrated in early 2010 and at the end of 2012. Because of that we did not report those months in which the high concentration of missing data did not allow a reliable assessment and gap filling of fluxes.

3.2.3. Statistical Analysis

The correlation between NEE and the climatological variables (air temperature, rainfall and solar radiation) was first examined at monthly scale. Then, the influence of rainfall on NEE was assessed at seasonal scale.

More specifically, both NEE and rainfall were aggregated over a four-months period based on the physiological activity of the vegetation:

- I. winter period with low physiological activity of vegetation (i.e. November, December, January and February; indicated as WIN);
- II. spring period with high physiological activity of vegetation (i.e. March, April, May and June; indicated as SPR);
- III. summer-fall period with high physiological stress and subsequent vegetation recovery (i.e. July, August, September and October; indicated as SUF).

Rainfall was accounted as Δ rainfall (i.e. the difference between the long-term total annual rainfall average (1981-2009) and the actual rainfall recorded during the study period, over the same sub-period). All inter-relations were assessed using correlation coefficient (r) and p-value to assess the goodness of fit metric and its significance.

3.3. Results

3.3.1. Climate trend

The rainfall pattern in the study area was obtained for the period 1981-2012 (Fig 3.1). During this period rainfall trends showed a wide inter-annual variability (mean= 626 mm; standard deviation (δ) = 128.4). In particular, the 3 study years can be considered as highly representative of average and extreme rainfall annual pattern. While 2012 is perfectly consistent with the RAIN-LTA (anomaly= -0.3%), 2010 and 2011 well represent both the extremes, with a positive anomaly of +27.4% and a negative one of -41.3%, respectively (Fig 3.1).

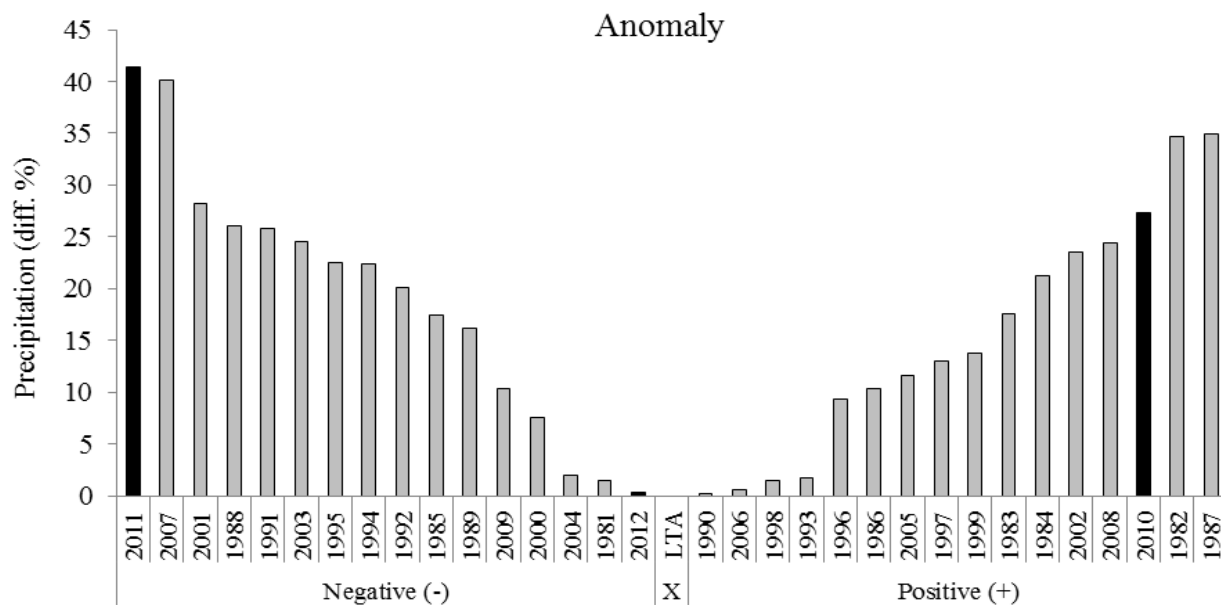


Figure 3.1. - Rainfall variability range for the period 1981-2012.

The first year (2010) was markedly wetter than the others with a total annual rainfall of 797.2 mm. The seasonal distribution reflected the typical Mediterranean climate, with maximum peaks in springtime (May, 96.4 mm) and autumn (November, 189.4 mm) (Tab 3.1). Annual mean temperature was only 0.3°C higher than the 30 years average (14.8°C).

The second year (2011) was the driest of the past 30 years record, with a total annual rainfall of only 367.2 mm. Springtime (March, April and May) was dry (95.4 mm), with low rainfall both compared to the 30 years average (133.6 mm) and with respect to the previous year (207.2 mm). Despite a general scarcity of rainfall over the year, July was characterized by a high and unusual amount of rain (51 mm) (Tab 3.1). Annual mean temperature was consistent with 2010 and 0.4 C° higher than the long-term average.

The third year (2012) was perfectly consistent with the RAIN-LTA (624 mm). It showed a typical Mediterranean seasonal distribution, with highest rainfall in spring (April, 65.8 mm) and autumn (November, 174.2 mm). However, whilst spring was consistent with the long-term average, summer was extremely dry. In particular, June and July were characterized by total absence of rainfalls, while in August a very low amount was observed (3.2 mm). Annual mean temperature was about 0.7 °C higher compared to long-term average (Tab 3.1).

Month	Rainfall (mm)				T.air (°C)				Rd (Wm ²)			
	LTA	2010	2011	2012	LTA	2010	2011	2012	LTA	2010	2011	2012
Jan	45.4	86	23.8	20.2	7.3	7.1	8.2	7	76.5	69.7	66	83.7
Feb	43.6	79.6	35.2	41.4	8.1	9.6	7.9	5.5	114.2	92.9	112.4	125.6
Mar	49.8	67.2	60.4	17.2	9.8	10.2	9.5	11.6	161.5	134.9	152.5	197.6
Apr	44.2	43.6	19.8	65.8	12.3	13.1	13.7	13.2	208.3	217.6	216.1	199.2
May	39.6	96.4	15.2	61	16.2	15.9	17.3	16.6	260.8	214.7	289	253.2
Jun	28.3	27.8	6	0	20.1	21.3	21.2	22.4	293.1	266	295.2	299.6
Jul	17.6	9.2	51.6	0	23.3	25.4	22.2	24.9	300.6	290.2	276	290.1
Aug	28.4	29.2	0.2	3.2	23.4	23.8	22.9	25.7	258.1	248.7	269.6	264.5
Sep	82.6	10.2	17.8	79.4	20.6	19.5	21.5	20.9	192.1	193.9	203.6	163.6
Oct	80.5	67.6	34.6	82.4	16.4	15.6	15.8	17.3	127.2	113.6	151.8	124.8
Nov	95.5	189.8	56.6	174.2	11.5	12.1	12.5	13.6	81.5	63.8	90	73.3
Dec	70.4	90.6	46	79.2	8.1	8.1	9.9	7.8	63.8	49.8	70.8	61.5
SUBTOT (Mar-Oct)	371	351.2	205.6	309	17.8	18.1	18	19.1	225.2	210	231.7	224.1
TOT	626	797.2	367.2	624	14.8	15.1	15.2	15.5	178.1	162.1	182.8	178.1

Table. 3.1 – Monthly meteorological data (i.e. cumulated rainfall, air mean temperature and mean global radiation) of the study area. Data were reported both as long-term average (LTA, 1981-2010) that specifically for the three years of measurements (2010, 2011 and 2012).

Based on the 4-months sub periods classification, rainfall showed great variability both among the 3 years of study and with respect to the RAIN-LTA (Tab 3.2). In 2010 both winter (WIN) and spring (SPR) rainfall showed an increase of about 45% compared to the RAIN-LTA, and conversely a strong decrease (-44%) during summer-fall (SUF).

In 2011, winter rainfall showed also a considerable increase (+33%) compared to RAIN-LTA, while a strong decrease was observed during spring and summer-fall (-37.4% and -50%, respectively). Finally, in 2012 a decrease for all 3 periods (WIN, SPR and SUF) was observed, of -35.6%, -11% and -21% compared to RAIN-LTA.

	Rainfall (mm)			Diff. %		
	WIN	SPR	SUF	WIN	SPR	SUF
LTA	255	161.9	209.1	0.0	0.0	0.0
2010	372.8	235	116.2	46.2	45.1	-44.4
2011	339.4	101.4	104.2	33.1	-37.4	-50.2
2012	164.2	144	165	-35.6	-11.1	-21.1

Table 3.2 – Rainfall amount aggregated over 4-months period for the 3 years of study and LTA. WIN=November, December, January, February; SPR= March, April, May, June; SUF= July, August, September, October.

3.3.2. C-fluxes dynamics

In order to provide a better understanding of assimilatory and respiratory processes observed within olive orchard, information about the strength of such processes and the length of the vegetative season, the three major ecosystemic components (i.e. NEE, GPP and Reco) were cumulated at monthly scale and summarized in Tab.3.3.

Year	NEE			GPP			Reco		
	2010	2011	2012	2010	2011	2012	2010	2011	2012
Jan	-----	-----	-----	-----	-----	-----	-----	-----	-----
Feb	-----	-23.55	-29.91	-----	55.72	34.01	-----	32.17	4.10
Mar	-32.61	-34.90	-62.28	114.63	80.58	88.75	98.02	45.68	26.47
Apr	-131.54	-16.22	-63.52	144.98	76.43	144.08	13.45	60.21	80.55
May	-111.88	-8.96	-38.26	113.39	118.23	118.05	1.51	109.27	79.78
Jun	-57.11	-36.09	-15.57	154.47	126.89	101.09	97.36	90.80	84.01
Jul	-77.70	3.21	-23.97	187.20	105.94	71.89	109.50	109.15	47.91
Aug	-85.30	-21.51	-1.53	142.36	77.79	48.21	57.06	56.28	46.60
Sept	-97.52	-13.15	-0.60	97.52	55.16	32.35	0.00	42.01	31.75
Oct	-30.32	-2.26	-53.5	95.83	56.27	57.30	62.22	54.01	3.80
Nov	-29.48	9.62	-----	65.06	50.05	-----	35.58	59.67	-----
Dec	-13.34	7.11	-----	63.54	72.70	-----	49.21	79.81	-----
SUBTOT (Mar-Oct)	-624	-129.9	-259.2	1050.4	697.3	661.7	439.1	567.4	400.9
TOT	-666.8	-136.7	-289.1	1179	875.8	695.7	523.9	739.1	405

Table 3.3. – Monthly cumulated NEE, GPP and Reco during the three years of measurements.

Here, we described the cumulative monthly trend of GPP, NEE and Reco thus showing the total gross primary production, the carbon sequestration capacity and respiration provided by olive orchard during the period 2010-2012. In these years the maximum GPP was observed at different times (Tab.3.3).

In 2010 spring was characterized by high gross primary production (124.3 gC/m^2 on average), with the highest value in April (144.98 gC/m^2). However, the highest growth was provided by summer months that contributed for a total of 484.3 gC/m^2 (161.34 gC/m^2 on average). In particular, July showed the highest GPP (187.20 gC/m^2). In 2011 the highest GPP was found in June (126.89 gC/m^2). In particular, the period between late spring and early summer (i.e. May, June and July) contributed for 351.06 gC/m^2 which was about 40% of the total GPP of 2011 (875.77 gC/m^2). On the contrary, in 2012 the monthly maximum growth was observed in advance compared to the previous years. The highest GPP was found in April (144.08 gC/m^2). April, May and June contributed for 363.22 gC/m^2 , more than 50% of the annual olive grove GPP (694.14 gC/m^2).

Similarly to GPP, during the three study years also the monthly Reco showed the maximum values at different times. In 2010 summer was characterized by the highest respiration (88 gC/m^2 on average), with the highest value in July (109.5 gC/m^2). Moreover, summer respiration was on average more than twice greater as compared to spring respiration (37.7 gC/m^2). Also in 2011 summer months were characterized by high respiration (85 gC/m^2 on average) while spring respiration was twice as much as that of the previous year (71.7 gC/m^2 on average). In 2011 the highest values of Reco were found in May (109.27 gC/m^2) and July (109.15 gC/m^2). On the contrary, in 2012 spring was characterized by the highest respiration (62.3 gC/m^2 on average), while summer months showed a considerable decrease (59.5 gC/m^2) compared to the summer months of 2010 and 2011 (-32.4% and -30.3%, respectively). The highest values of Reco was found in June (84 gC/m^2).

The monthly NEE showed the typical trend of the Mediterranean woody vegetation, with the maximum physiological activity mainly concentrated in spring and a partial autumnal recovery (Tab.3.3). April was the month characterized by the highest NEE in 2010 (-131.54 gC/m^2) and 2012 (-63.52 gC/m^2), while in 2011 it was recorded in March (-34.9 gC/m^2). (Tab.3.3). Summer months were characterized by high C-uptake in 2010 (-73.37 gC/m^2 on average), while lower values were recorded in the following years (-18.13 gC/m^2 and -13.79 gC/m^2 for 2011 and 2012, respectively). In particular, among the three vegetative seasons analyzed (March-September)

only in July 2011 there was a positive value of NEE (3.21 gC/m²). The autumnal physiological recovery was clear in September 2010 (-97.52 gC/m²), while it was less evident in 2011 (-13.15 gC/m²) and almost absent in 2012 (-0.60).

3.3.3. Relationships among NEE and climate conditions

The monthly correlation between NEE and meteorological variables over 3 years was reported in Tab.3.4. In 2010 and 2011 the correlations between NEE and air temperature and between NEE and solar radiation were clear but relatively low (Tab.3.4), while NEE and rainfall were almost uncorrelated with rainfall. Conversely, in 2012 monthly NEE was significantly correlated with some climatological variables. More in detail statistical analysis showed that the correlation between NEE and air temperature and between NEE and solar radiation were significant ($r=0.551$; $p\text{-value}=0.06313$) and highly significant ($r=0.751$; $p\text{-value}=0.00483$), respectively (Tab.3.4). Conversely, the correlation between NEE and rainfall was negative, relatively low ($r=-0.479$) and not statistically significant ($p\text{-value}=0.11552$). Then, based on the entire study period of 3 years, statistically significant correlations were observed between monthly NEE and air temperature ($r=0.473$; $p\text{-value}=0.00355$) and NEE and solar radiation ($r=0.541$; $p\text{-value}=0.00065$). On the contrary, the correlation between NEE and rainfall was very low ($r=-0.286$) and only slightly statistically significant ($p\text{-value}=0.0908$) (Tab.3.4).

Stat.	Label	Year			
		2010	2011	2012	2010-11-12
r	Air Temp.	0.483	0.383	0.551.	0.473**
	Rainfall	-0.109	0.129	-0.479	-0.286.
	Rad	0.443	0.404	0.751**	0.541***
p-value	Air Temp.	0.11153	0.21941	0.06313.	0.00355**
	Rainfall	0.73534	0.68884	0.11552	0.0908.
	Rad	0.149029	0.19259	0.00483**	0.00065***

Table 3.4. – Correlation between NEE and meteorological variables (air temperature, rainfall and solar radiation) at monthly scale over the three years of study. Signif. codes: 0 '***' 0.001 '**' 0.01 '*' 0.05 '.' 0.1 ' ' 1.

Furthermore, the relation between NEE and rainfall at seasonal scale was assessed by aggregating both parameters over a four-months period (Tab.3.5). It has been observed that when

seasonal NEE (spring + summer-fall) were compared with the rainfall of the same four month period (spring + summer-fall) or with the previous four month period (winter+spring), the correlations were rather higher, even if these were not statistically significant ($r=0.617$; p -value= 0.19229 and $r=0.645$; p -value= 0.16688 , respectively).

		2010-2011-2012	
	Label	r	p-value
NEE	NEE (SMP+SP) vs Rainfall (SMP+SP)	-0.617	0.19229
	NEE (SMP+SP) vs Rainfall (SP+WP)	-0.645	0.16688
	NEE (SMP+SP) vs Rainfall (SP)	-0.941**	0.00519**

Table 3.5. – Correlation between NEE and rainfall aggregated at seasonal scale over the three years of study. SMP=July, August, September, October. SP= March, April, May, June. WP=November, December, January, February. Signif. codes: 0 ‘***’ 0.001 ‘**’ 0.01 ‘*’ 0.05 ‘.’ 0.1 ‘ ’ 1.

Conversely, the seasonal NEE (spring + summer-fall) was found highly significantly correlated with the only spring (SPR) rainfall ($r=-0.941$; p -value= 0.00519) (Fig.3.2).

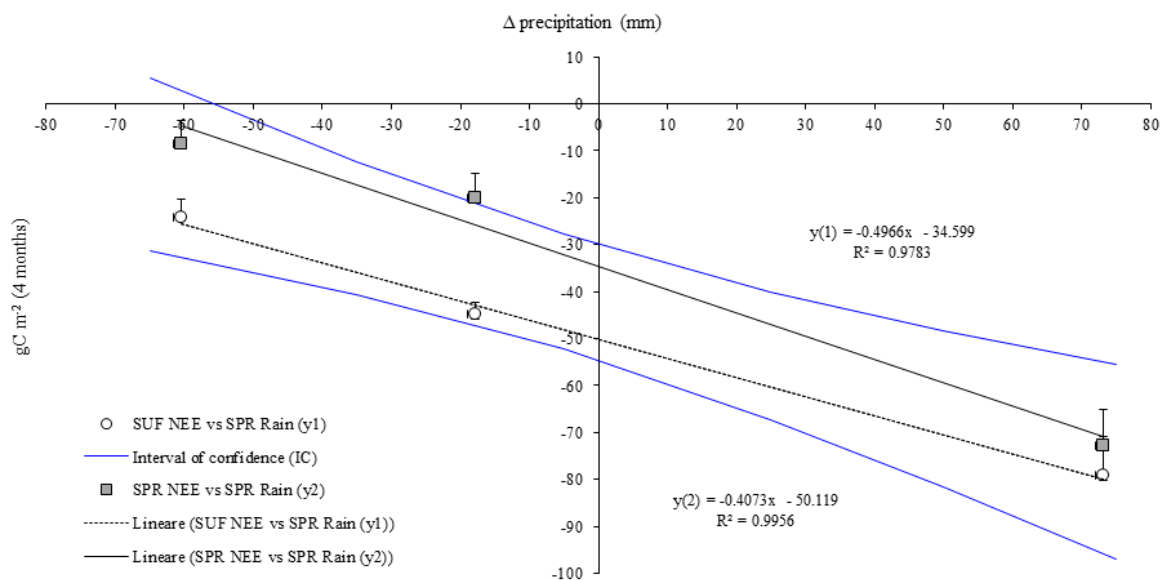


Figure 3.2 - Correlation between NEE and total amount of rainfall during the growing season (March-October) over the 3 years of study.

Finally, based on the whole period of growing season (from March to October), the NEE was found correlated with rainfall regimes ($r=0.87$, data not shown).

3.4. Discussion

The 3 years study period can be considered highly representative of the rainfall variability of the study area (Fig.3.1). While 2012 was perfectly consistent with the RAIN-LTA (anomaly= -0.3%), 2010 and 2011 do well represent extremes (anomaly= -41.3% and +27.4%, respectively). This peculiar climatic pattern poses great value to the collected dataset, allowing to derive relations between NEE and rainfall that can likely well represent the long-term C dynamics in an adult Mediterranean olive orchard.

Across the whole period of study the olive orchard resulted overall a net carbon sink. More specifically the NEE measured over three years was on average (i.e. $3.6 \text{ tC ha}^{-1} \text{ year}^{-1}$, see Tab.3) comparable to several Italian forestry systems. For instance Valentini et al. (2000) observed that at Mediterranean latitude the forest carbon accumulation is less than $6 \text{ tC ha}^{-1} \text{ year}^{-1}$, whilst Matteucci et al. (2007), reported that the Italian forestry capacity to sequester C is about $4 \text{ tC ha}^{-1} \text{ year}^{-1}$. Maselli et al. (2008), reported that during the period 1997-2003 the mean annual NEE values from eight Italian forest sites belonging to the FLUXNET network ranged on average from 2 to $6.5 \text{ tC ha}^{-1} \text{ year}^{-1}$. Similarly, Chiesi et al. (2011), showed that the annual NEE totals measured by eddy covariance in two Italian forest sites (i.e. a pine wood and an Holm oak forest) were 4.4 and $2.4 \text{ tC ha}^{-1} \text{ year}^{-1}$, respectively.

These results confirm the findings by Zanutelli et al. (2013), suggesting that C-fluxes from long term agro-ecosystem can be compared to natural forest ecosystems growing in the same biome rank. This similarity may be due to the characteristics of orchards that, according to Zanutelli et al. (2013), usually reflect those observable in forest but appear smaller in size and density. The observed annual NEE was also comparable with other deciduous and evergreen orchards. More specifically, some studies (e.g. Liguori et al., 2009; Zanutelli et al., 2013; Nardino et al., 2013) observed that NEE can range in these ecosystems from 2 to $12 \text{ t(C) ha}^{-1} \text{ year}^{-1}$. Such extremely large variability reflects the susceptibility of these ecosystems to climatic conditions, among other factors such as management, soil structure, and biome characteristics.

Although NEE was on average comparable to other forestry systems, considerable differences were found among the 3 study years. These differences were found strictly correlated with the rainfall regimes of the sub-period considered (March-October) ($r=0.87$, data not shown). More

specifically, a higher NEE was found over years characterized by higher amount of rainfall. This was consistent with Xu and Baldocchi (2004) that indicated a strong correlation between total photosynthesis and total annual rainfall. Similarly, Luo et al. (2007) confirmed that does exist a positive relationship between yearly rainfall and NEE.

According to our results, with the only exclusion of solar radiation in 2012, the NEE measured at monthly scale did not show any significant correlation with the selected climate variables including rainfall. This absence of correlation at monthly scale between NEE and rainfall is explained by the fact that the response of photosynthesis to water availability in a dry tolerant specie as olive tree can be longer, depending on water stress level (Pavel and Fereres, 1998). Therefore statistical analysis carried out at monthly scale might not be suitable for evaluating the influence of rainfall on NEE. On these basis, seasonal dynamics offered a more complete overview about the control of rainfall on NEE. Accordingly, seasonal NEEs over three periods of 4-months based on the physiological activity of the vegetation indicated that spring NEE + summer-fall NEE (SPR+SUF) was highly correlated with spring rainfall ($r=-0.941$; $p\text{-value}=0.00519$) (Tab.3.5).

During Spring, NEE was highly negatively correlated with spring rainfall ($r=0.95$) (Fig.3.2), while it was not with the previous season rainfall (i.e. WIN) ($r=0.28$) (Data not shown). The very high correlation found over spring months is consistent with the photosynthetic process that is highly sensitive to temperature, light and water availability. Indeed, in this period of the year where temperature and light tend to increase, photosynthetic activity is mainly limited by water availability. When soil water is found close to the optimum of field capacity the photosynthetic activity is high, while it strongly decreases approaching the wilting point. Therefore, a decline in rainfall may actually behave as the most limiting condition for plants activity (Schroter et al., 2005; Resco et al., 2007). Conversely, wintertime rainfall were not correlated with spring NEE. This may be explained by the soil characteristics of the study area: while sandy soils quickly deplete the available water for plants when evapotranspiration rates are high, the textural class of our soil (i.e. clay-loam) may have allowed a considerable water soil recharge through spring rainfall. These soil characteristics may have reduced the importance of winter rainfall on water soil content and, in turn, their influence on the photosynthetic capacity of vegetation during springtime.

By contrast, statistical analysis showed that during summer-fall, NEE was highly and negatively correlated with spring rainfall ($r=0.95$) (Fig.3.2), while it was not with the same season rainfall

(i.e. SUF) ($r=0.044$) (Data not shown). This result may be due to the combined effect of spring rainfall and olive tree physiology. The spring rainfall through the increase of soil water at the beginning of the growing season had a large impact on rainfed agro-ecosystems in semi-arid regions since it may have contributed to extend the soil water availability also over dry months. This is consistent with Scott et al (2012), that indicated as in Mediterranean areas water tends to accumulate in soil until energy inputs (radiation and temperature) rise up. Then, the effect of spring rainfall on soil water content was reinforced by the particular physiology of olive tree that, as indicated by Connor (2005), relies on conservative water use in Spring with the aim of reducing the extent and intensity of the summer drought. These results were consistent with literature. In a study carried out in a Mediterranean climate (California), Ma et al. (2007) observed that spring-time rainfall was the predominant factor driving inter-annual differences in NEE over an oak/grass savanna site. Similarly, Kwon et al. (2008) by analyzing a semi-arid climate ecosystem observed different responses of NEE across two growing season characterized by dissimilar spring rainfall. Moreover, they also suggested that the intra-seasonal variability in rainfall can cause clear differences in the patterns and total amount of NEE at different time scale. Conversely, the absence of correlation against summer-fall rainfall is probably due to the prolonged dry and hot periods that usually characterize the Mediterranean summers. Although olive tree can tolerate prolonged dry periods because of typical adjustments that allow higher resistance to gas diffusion in the leaf such as the reduction of intercellular volume spaces within tissues (Bongi et al., 1987; Gucci, 1998), the combined impacts of these climatic conditions are expected to lead water stress. When water stress is particularly severe, it leads to photosynthesis and metabolic activity reduction with possible prolonged and permanent damages that, in turn, can cause NEE decrease. This condition was clearly observed in September 2012 (Tab.3.3), where rainfall events after a very prolonged dry period did not positively contribute to the recovery of photosynthesis. This evidence is consistent with Sorrentino, (2001) that found how a strong water stress can modify the photosynthesis's biochemistry and reduce the maximum photosynthetic capacity, which can be completely re-instated only after the complete rebuilding of photosynthetic metabolism. This behaviour was also confirmed by Fereres et al. (1996) that in a 22 years old olive orchard observed a stomatal conductance recovery after several weeks from the re-hydration of the water potential. According to Pavel and Fereres (1998), this effect is usual for olive trees in Mediterranean environments especially during the hotter season, where photosynthesis during highest irradiance period is limited by water shortage. The behaviour of

olive tree previously reported was consistent with our results, where NEE was observed to be very low during the hottest period of 2011 and 2012 and close to zero after prolonged drought (e.g. 2012). Moreover, the summer-fall rainfall was also characterized by sporadic and high intensity episodes. For instance in July 2011 were recorded two events characterized by rainfall higher than 20 mm representing about 40% of the total summer-fall rainfall in that year. Similarly in September 2012 were recorded two events characterized by rainfall higher than 25 mm representing about 65% of the total summer-fall rainfall. The contribution of these extreme episodes at recharging the soil water capacity cannot be compared to regular rainfall events. Soil infiltration capacity is usually limited, therefore large rainfall events can more easily lead to an increase in surface run-off and evaporation from soil, rather than contributing to recharge the water table (Nitsch et al., 2008).

3.5. Conclusions

Understanding the impacts of inter-year and intra-seasonal variability in climate conditions on the magnitude and pattern of NEE and GPP provides fundamental information about the contribution that olive orchards can give to reach the goals fixed by international regulations on greenhouse gas control (e.g. “20-20-20” Policy).

In this perspective, our study provides evidence that a typical managed olive orchards was a carbon sink almost comparable with other Italian forestry ecosystems along the three years of study. The magnitude of yearly NEE has been found highly correlated with annual rainfall regimes. Moreover, whilst winter rainfall was not correlated with the spring NEE, the spring rainfall resulted to be the main driver for spring and summer NEE.

Finally, our results assess the efficiency in climate mitigation offered by olive orchards through direct measurements, also suggesting that these systems might encounter consistent loss in C-sequestration capacity in the next decades, where a strong decrease in rainfall is expected over Mediterranean basin. In particular, applying the relationships between rainfall and NEE found in this work on the projected future changes for this region under the SRES scenario A1B (Nakicenovic and Swart, 2000; Artale et al., 2010), the expected decrease in rainfall over the olive tree growth period (March-October) of 4.5% for the period 2031-2050 may lead to a 12% reduction of C-sequestration capacity of olive rainfed ecosystems compared to the current period.

Chapter 4

Simulation of olive grove Gross Primary Production by the combination of ground and multi-sensor satellite data

Abstract

We developed and tested a methodology to estimate olive (*Olea europaea* L.) Gross Primary Production (GPP) combining ground and multi-sensor satellite data. An eddy-covariance station placed in an olive grove in central Italy provided carbon and water fluxes over two years (2010-2011), which were used as reference to evaluate the performance of a GPP estimation methodology based on a Monteith type model (C-Fix) and driven by meteorological and satellite (NDVI) data. The main issues arising in this study were: i) how to consider the two main olive grove components, i.e. olive trees and inter-tree ground vegetation: this was addressed by the separate simulation of carbon fluxes within the two ecosystem layers, followed by their final recombination; ii) how to include management practices, which greatly alter carbon exchange on short time scales, in the modelling framework: this was addressed by superimposing synthetic NDVI values to take tillage effects into account. In this way, the estimation methodology was capable of reproducing daily olive grove GPP with a good overall accuracy ($r=0.662$ and $RMSE=1.31 \text{ g C m}^{-2} \text{ day}^{-1}$) during the study years.

Keywords: Olive orchard, climate variability, NEE, eddy covariance.

Chapter based on:

Brilli, L., Chiesi, M., Maselli, F., Moriondo, M., Gioli, B., Toscano, P., Zaldei, A., Bindi, M. 2013. *Simulation of olive grove Gross Primary Production by the combination of ground and multi-sensor satellite data*. International Journal of Applied Earth Observation and Geoinformation 23 (2013) 29–36.

4.1. Introduction

Olive (*Olea europaea* L.) is one of the most ancient cultivated fruit trees in the Mediterranean basin (Zohary and Spiegel-Roy, 1975; Moriondo et al., 2008; Villalobos et al., 2012) where it plays a fundamental role by integrating agriculture, environment and landscape into a complex system. Although in recent years olive trees have been cultivated successfully in countries such as California, Australia, Argentina and South Africa (De Graaff and Eppink, 1999), olive is the basic tree cultivation in the Mediterranean basin and dominates its rural landscape (Loumou and Giourga, 2003). This region includes about 700 million olive trees over 9 Mha, representing about 96% of areas cultivated worldwide (Vossen, 2007).

In addition to the agronomic and economic value, olive cultivation systems (agro-forestry stands, traditional groves and new intensive orchards) provide additional ecosystem services by improving soil conservation and allowing high carbon sequestration (Sofu et al., 2005; Loumou and Giourga, 2003). This major economic and ecological importance, in one of the areas most exposed to the risk of climate change (IPCC, 2007), requires the development of adequate monitoring strategies, such as techniques able to monitor olive carbon sequestration. In particular, the gross primary production (GPP), defined as the overall carbon fixation rate through the process of photosynthesis, is an important variable related to the global carbon cycle and climate change research, because approximately half of this amount is incorporated into new plant tissues such as leaves, roots and wood, and the other half is released back into the atmosphere through autotrophic respiration (Kotchenova et al., 2004).

To estimate the productivity of ecosystems, one of the most often used techniques is Eddy Covariance, which, through the measurement of net ecosystem CO₂ exchange, can be used for GPP calculation at ecosystem scale. However, eddy covariance systems provide integrated CO₂ flux measurements over limited footprint areas, with sizes and shapes that vary with tower height, canopy physical characteristics and wind speed, and therefore do not allow observations over large areas (Osmond et al., 2004).

The lack of spatially extensive flux tower observations over large areas can be overcome through the combination of ground and remotely sensed data. Remote sensing provides information on photosynthetic processes of plants on several spatial and temporal scales (Veroustraete et al., 2002; Prince, 1990; Kumar and Monteith, 1981). In the last years the use of remote sensing allowed systematic observations to be made of vegetation and relevant ecosystem parameters, becoming a fundamental instrument for the characterization of vegetation structure and for

estimating GPP on large scale (Keenan et al., 2012; Xiao et al., 2010; Yang et al., 2007; Behrenfeld et al., 2001; Running et al., 2000). In particular, many studies have shown that tree production can be simulated, with Monteith's approach, through the combination of estimates of the fraction of absorbed photosynthetically active radiation (fAPAR) from remote sensing with standard meteorological data (Maselli et al., 2009; Veroustraete et al., 2004). This approach has obtained great benefit from the recent availability of MODIS images, which represent the best descriptor of vegetation properties with moderate spatial resolution (250 m) and high temporal frequency (8-16 days) (Maselli et al., 2013).

Nonetheless, the application of Monteith's approach to estimate olive grove GPP involves particular complications due to the multi-layer nature of this ecosystem type. Olive groves are composed of trees and inter-tree ground vegetation which, showing different eco-physiological constraints to the photosynthetic process, must be treated separately in the simulation of ecosystem GPP. This paper has built on these premises adopting a multi-step methodology to estimate the GPP of olive groves. In particular, a modified version of the parametric, Normalized Difference Vegetation Index (NDVI) - driven model C-Fix was applied considering the contributions of the two vegetation types (i.e. olive trees and ground vegetation). The modeling performances were validated against GPP data derived from eddy covariance measurements taken in an olive grove in South Tuscany (Follonica, Central Italy) during the period 2010-2011.

4.2. Materials and Methods

4.2.1. Study area

The study was conducted on an olive grove situated in an agricultural area near Follonica (Gr), Tuscany (Central Italy, 42°56' N , 10°46' E). In Tuscany olive trees cover an area of 96,828 ha with a total production of 117482 t (<http://www.istat.it/it/>). Around 49,300 grow olives, representing 62% of Tuscan farms. Olive trees have a strong effect on the Tuscan landscape and land use, occupying about 11% of the regional utilized agricultural area (UAA). Olive tree cultivation contributes about 95 M€ to the value of regional agricultural production, which is approximately 4% of the total value of agricultural gross domestic product (GDP) (IRPET, 2011). Olive groves are mostly situated on the plain and in hilly areas. However, given the heterogeneity of climatic and soil conditions in Tuscany, the distribution of olive groves varies in each administrative province.

The experimental site at Follonica (Fig. 4.1) covers an area of about 6 ha, with a southerly exposure and lies about 41 meters above sea level.

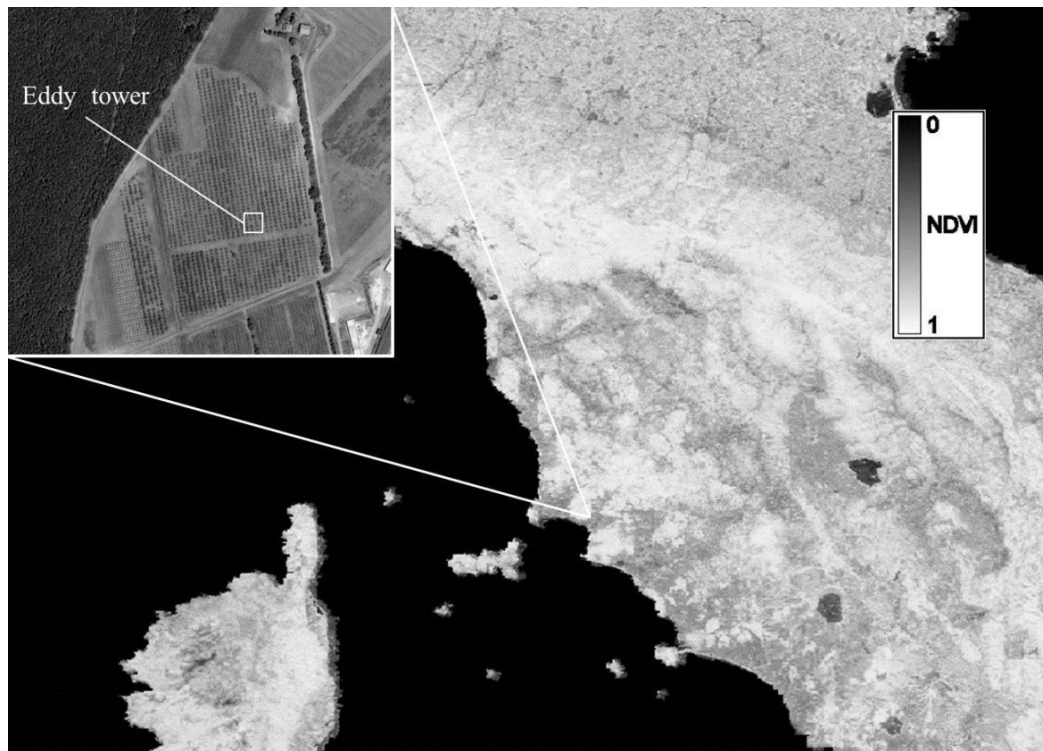


Figure 4.1. – MODIS NDVI image of June 2010 showing the position of the study area in Tuscany as well as its main features (enlarged box). NDVI window extends over 8-13° East Longitude, 42-45° North Latitude.

It is characterized by a regular morphology and a slight slope from north to south. The olive grove dates back to 1993 and contains around 1500 trees of about 4 meters in height. Olive canopy cover is about 25%, and inter-tree areas are covered by several herbaceous native species (*C. dactylon*, *Trifolium campestre*, *Medicago polymorfa*, *Picris hieracioides*, *Geranium* sp., *Convolvus arvensis*, *Anagallis arvensis*, *Calendula arvensis*, *Rumex acetosella*, *Eruca sativa*, *Linula viscosa*, *Ordeum murino*, *Daucus carota*, *Bromus* sp.). Cropping management follows the typical tradition of the area, with no irrigation and superficial plowing (disc harrowing). During the study period, the site was plowed twice: the first time in late April 2010, the second in February 2011. The site was treated with inorganic fertilizer in spring 2010 and February 2011. Olive production in 2010 and 2011 was 3.1 t ha⁻¹ and 4.1 t ha⁻¹, respectively. The soil belongs to the clay-loam textural class, with 40% silt and 38% clay. Soil texture and depth were obtained from the soil map produced by the Tuscany Region (<http://sit.lamma.rete.toscana.it/websuoli/>).

According to the classification of Thornthwaite (1948), the climate of the area can be described as meso-thermic, between dry sub-humid and semiarid, with the high summer temperatures and mild winters that are typical of the Mediterranean climate (Tab. 4.1).

	Monthly mean temperature (°C)	Rainfall (mm)	Months with mean temperature < 0 °C
30 years average (1980 – 2010)	15.2	626	---
2010	16	797	---
2011	16.8	367	---

Table 4.1 – Monthly mean temperature (°C), total rainfall (mm) and months with mean temperature < 0 °C in the study area for 30 years average (MARS JRC data set), 2010 and 2011.

Meteorological conditions differed in the two study years as shown in Fig. 4.2. The first year (2010) was markedly wetter than the second (2011), with intense rainfall events concentrated in spring (i.e. May) and late autumn (i.e. November), as is typical of the Mediterranean climate.

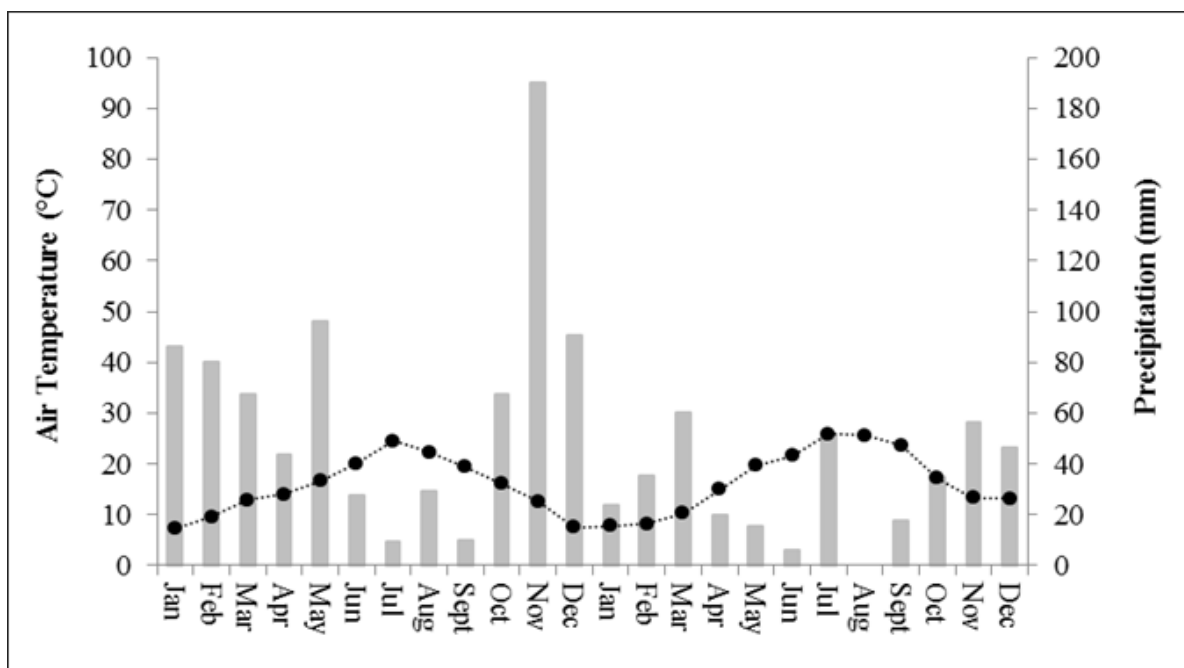


Figure 4.2 – Thermo-pluviometric diagram for study area. All monthly data derive from eddy covariance station.

The second year was much drier, especially in spring (42.8 mm against 170 mm in spring, 2010). Moreover, the dry period during the first year continued for about 4 months, whilst in 2011 it lasted from April to September with only a short break in July.

4.2.2. Satellite data

The olive tree canopy cover was estimated through processing of pan-sharpened color IKONOS images with high spatial resolution, downloaded from Google Earth. To predict the fraction of coverage in the olive grove, a Landsat ETM+ image collected on July 12th 2002 was also used. This image was selected because it was completely free of atmospheric disturbances such as clouds or fog. In addition, the image acquisition time coincided with maximum solar illumination, so minimizing the shadows produced by the trees, and increasing maximum spectral contrast between tree crowns and understory. MODIS NDVI data with a spatial resolution of 250 m were downloaded from USGS (<http://earthexplorer.usgs.gov/>). The NDVI dataset used is composited over 16-day periods. The images covering Central Italy were downloaded for the years 2010-2011.

4.2.3. Eddy covariance data

Eddy covariance measurements at the study site were recorded for almost two years, from February 2010 to December 2011. The tower mast was placed 3m above the canopy, in the center of the olive grove, and was equipped with a Metek USA 1 triaxial sonic anemometer in conjunction with an open path infra-red CO₂-H₂O analyzer (Licor 7500) (high frequency sensors). Ancillary slow sensors included: 2 soil temperature profiles from 5 to 20 cm (thermocouples J and T types), global and net radiation (NR LITE Kipp & Zonen CMP3), air temperature and humidity (HMP45 Vaisala), rain gauge (Davis 7852). High frequency (20Hz) data were stored on a PC, while slow frequency data were stored on a data-logger (CR10, Campbell Scientific). Fluxes of sensible heat, latent heat, momentum and CO₂ (Net Ecosystem Exchange, NEE) were derived at half-hourly time resolution (Aubinet et al., 2000). Density corrections were applied according to Webb et al. (1980). Data quality was assessed and quality flags created using the methods of Foken and Wichura (1996). Filtering for low turbulence conditions was applied by investigating the dependence of friction velocity (u^*) with night time CO₂ flux, and a threshold of 0.17 ms⁻¹ was derived. Data were then gap-filled and flux-partitioned using the methodology of Reichstein et al. (2005), whose final products are

continuous datasets of NEE, GPP and ecosystem respiration (R_{eco}). This type of flux partitioning procedure is based on using night time turbulent flux data to constrain the temperature dependence of ecosystem respiration, and then applying such dependence on the whole dataset. GPP was then calculated as the difference between NEE and daytime R_{eco} .

4.2.4. Development and validation of olive grove GPP estimation methodology

As previously mentioned, the olive grove soil was covered, in addition to olive trees, by a significant proportion of inter-tree ground vegetation, which contributed to total olive grove GPP. Since the two components showed different eco-physiological features, the prediction of GPP by a Monteith model was performed separately. More specifically, two versions of C-Fix were concurrently applied for olive trees and ground vegetation, which were fed by respective fAPAR estimates. MODIS spatial resolution (250m) was not capable of resolving the individual trees and directly separating the two components, therefore the image processing required the use of a multi-step methodology. The fraction of olive tree canopy above each olive grove in fact varied depending on local management practices and the size of the trees. The olive tree NDVI was therefore predicted by applying a statistical method based on the extraction of spatially variable endmembers (Maselli, 2001). This method required accurate estimates of olive tree canopy cover for relatively large areas, which were obtained by the processing of higher spatial resolution images. In summary, a map of olive tree cover fraction was produced for the area around Follonica by applying the procedure described in Maselli et al. (2012A) to the available Landsat ETM+ image. The tree canopy cover estimated automatically for the studied olive grove was 24%, in agreement with that obtained by visual interpretation of Ikonos images downloaded from Google Earth. This map was then used to obtain olive tree NDVI endmembers from MODIS images, which were converted into fAPAR values by the generalized equation of Myneni and Williams (1994). The NDVI values of inter-tree ground vegetation were linearly extrapolated using the extracted endmembers and the original values of the olive grove, and were converted into fAPAR by the same equation. The two fAPAR series were used to drive two versions of C-Fix. For olive trees, GPP was predicted by modified C-Fix as (Maselli et al., 2012A):

$$GPP_i = \varepsilon \cdot Tcor_i Cws_i fAPAR_i Rad_i$$

where ε is the maximum radiation use efficiency (1.2 g C/MJ APAR) (Maselli et al., 2012), $Tcor_i$ is the MODIS temperature correction factor for evergreen broadleaves, Cws_i is the water stress

factor for Mediterranean trees, $fAPAR_i$ is the fraction of absorbed PAR, and Rad_i is the solar incident PAR, all referred to day i . All meteorological driving variables (i.e. daily temperatures, rainfall and solar radiation) were estimated through the sequential application of the DAYMET and MT-Clim procedures, as fully described in Chiesi et al. (2011). For inter-tree ground vegetation, GPP was predicted by applying a similar equation but considering different factors (Maselli et al., 2012). In particular, ϵ was set to 1.65 g C/MJ APAR, $Tcor_i$ was the MODIS temperature correction factor for C3 grasses and Cws_i was derived from a water balance computed over one month instead of the original two months (Maselli et al., 2013). As fully explained in Maselli et al. (2013), these modifications take into account the generally lower green biomass of ground vegetation with respect to trees, as well as their different capacity to respond to thermal and water limitations. The daily GPP estimates of olive trees and inter-tree ground vegetation were finally combined to produce relevant photosynthesis estimates for the entire olive grove examined (Fig. 4.3). These estimates were validated by comparison with the GPP measurements of the tower using the correlation coefficient (R), the mean bias error (MBE) and the root mean square error (RMSE) as accuracy statistics.

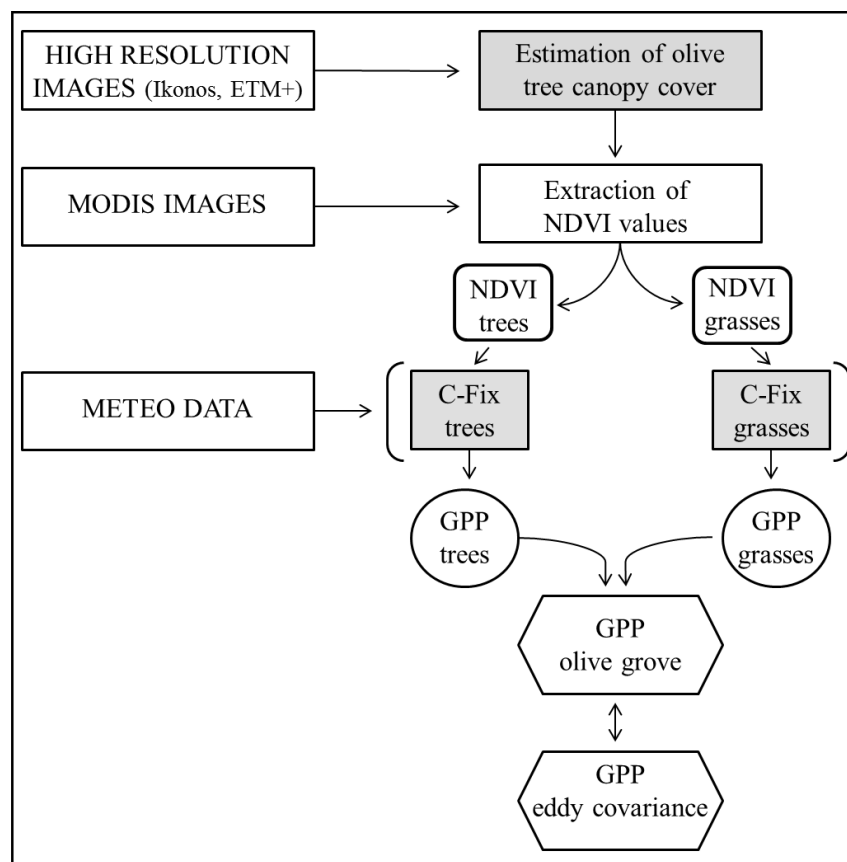


Figure 4.3. - Scheme of the multi-step methodology used to estimate olive grove GPP.

4.3. Results

4.3.1. Estimation of NDVI profiles

During the two study years the NDVI profile of olive trees and ground vegetation showed notable inter- and intra-year variations (Fig. 4.4).

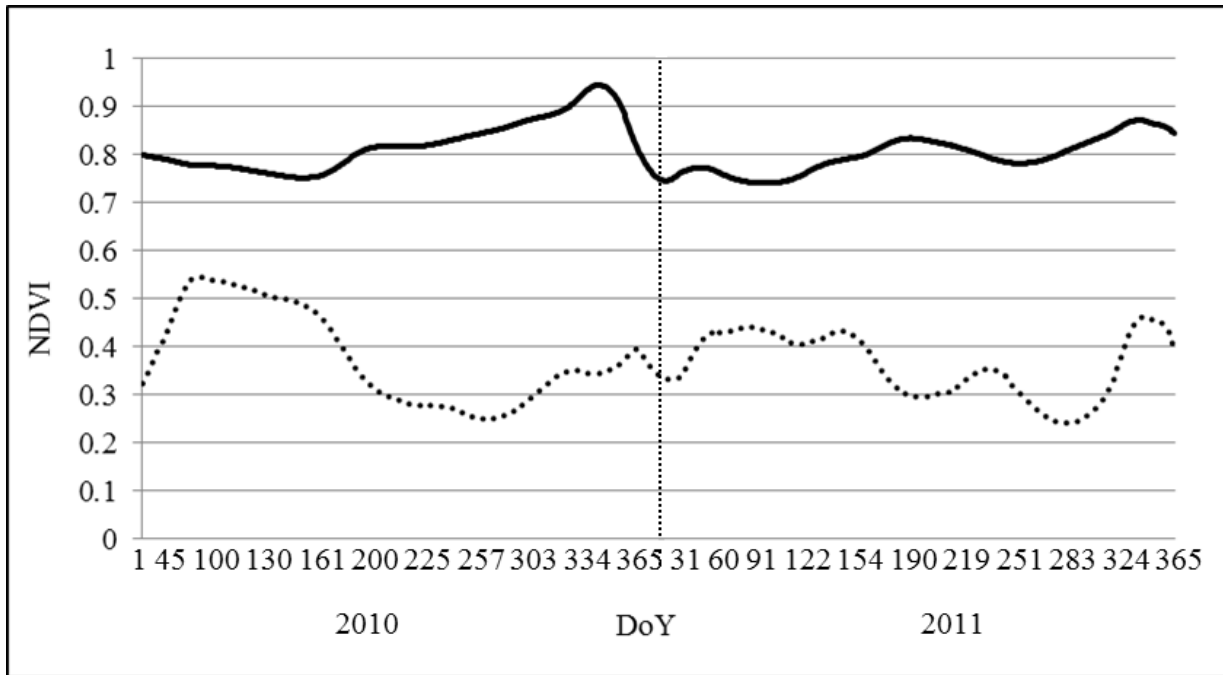


Figure 4.4. - NDVI profiles of olive trees and ground vegetation during 2010 and 2011. Filled line = olive; dotted line = ground vegetation.

The NDVI profile of olive trees was uniformly high, around a value of 0.8. In the first year it showed a unique minimum (0.75) in mid-spring and a unique maximum (0.94) in winter, with a steady increase that indicated the absence of a long summer dry period or decrease in water soil content. In the second year, the NDVI olive profile showed more xerophic features, with a primary peak in early summer, a secondary peak in fall, and two minima in winter and summer. The NDVI profile of ground vegetation was markedly lower than that of olive trees. In the first year the maximum value (0.54) was found in winter, while the minimum value (0.25) was in summer. In the second year, the profile showed many intra-year variations, with two minima in spring and late summer typical of arid conditions. Generally, NDVI was maximum in late winter and minimum in summer. The greatest differences were in late winter and early spring, when the index was markedly lower in 2011.

4.3.2. Analysis of simulated GPP profiles

The simulated GPP profiles of olive trees and ground vegetation are reported in Fig. 4.5. The olive simulated profile was typical of Mediterranean woody vegetation. The active growing phase started in March and reached its peak in late spring/early summer, then it decreased progressively, at first due to water stress (i.e. summer months) and then to leaf senescence and low temperature (i.e. fall and winter months). The main differences in GPP profiles between the two years were recorded during late spring/early summer (14-13 g C m⁻² d⁻¹ in 2010 vs. 8-9 g C m⁻² d⁻¹ in 2011).

The simulated GPP profiles of ground vegetation followed that of olive trees, but with significantly lower GPP values (i.e. maximum GPP: 7-8 g C m⁻² d⁻¹ in 2010 vs. 4-5 g C m⁻² d⁻¹ in 2011). Also for ground vegetation the main differences in simulated GPP between the two years were recorded in late spring/early summer. The more extreme meteorological conditions recorded in 2011 determined a reduction in annual GPP, which was markedly lower in 2011 (976.8 gC m⁻² d⁻¹) than in 2010 (1227.33 gC m⁻² d⁻¹).

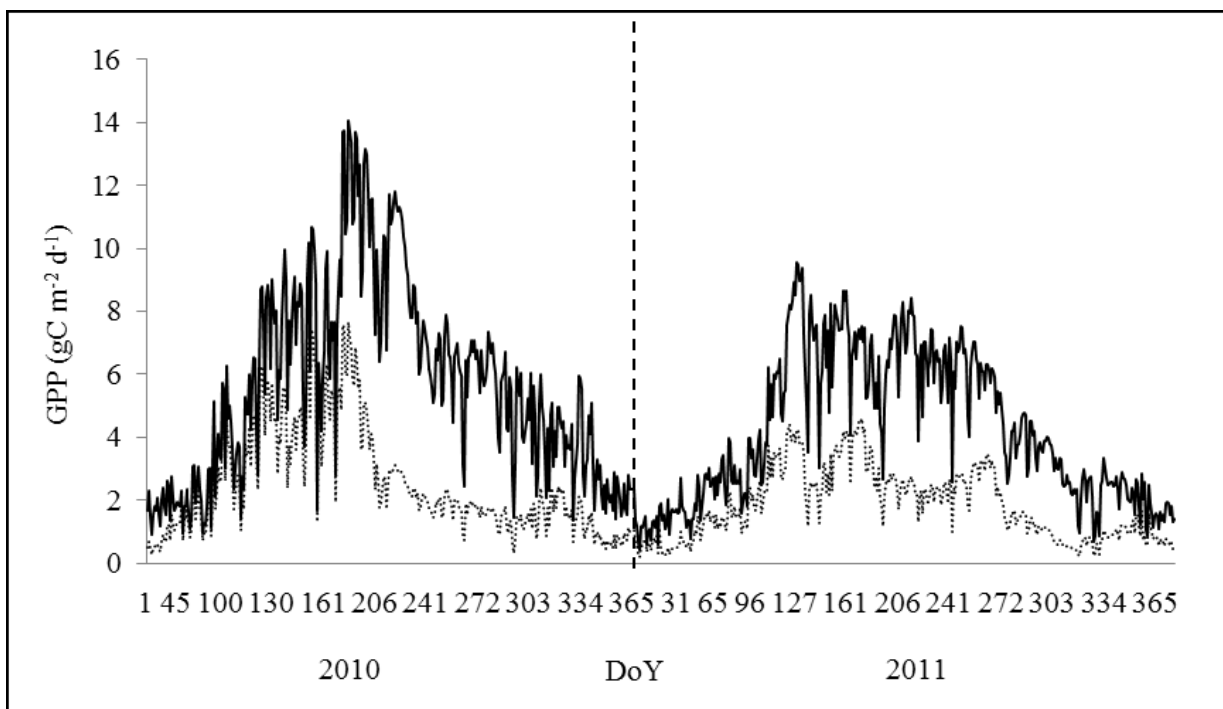


Figure 4.5 – Daily estimated GPP profiles of olive trees and ground vegetation during 2010 and 2011. Filled line = olive; dotted line = ground vegetation.

4.3.3. Comparison of observed and simulated olive grove GPP

During the two study years some problems due to experimental planning and eddy covariance instruments did not allow a complete reconstruction of daily GPP data. In particular, the 134 missing daily GPP data (i.e. 18.35%) were mainly concentrated in early 2010 (10.4%). On the remaining days, the eddy covariance tower collected a total of 28624 values of CO₂ fluxes (i.e. NEE) at half-hourly time resolution.

Among these 6147 (21.43%) were considered usable for the reconstruction of observed GPP. The gap-filling procedure was applied to the low quality dataset, and considered both the co-variation of fluxes with meteorological variables and the temporal auto-correlation of the fluxes (Reichstein et al., 2005). Filled data were conventionally classified into three categories (A, B, C) corresponding to best, acceptable and dubious, respectively. According to this quality classification for gap-filled values, the majority of these data were classified as best (14.61%) (Tab. 4.2).

	2010		2011		2010-2011	
		%		%		%
Num. tot. val.	13936	(100)	14688	(100)	28624	(100)
Num. orig. val.	11191	(80.3)	11286	(78.84)	22477	(78.57)
Num. gaps	2745	(19.7)	3402	(23.16)	6147	(21.43)
Category: A	2532	(18.17)	1623	(11.05)	4155	(14.61)
Category: B	201	(1.44)	679	(4.62)	880	(3.03)
Category: C	12	(0.09)	1100	(7.49)	1112	(3.79)

Table 4.2 – Number of half-hourly data measured by eddy covariance station in 2010 and 2011. Num. tot. val. indicates all the measured data; Num. orig. val. indicates all the measured data used to obtain observed daily GPP data; Num. gaps indicates the measured data that cannot be directly used to obtain observed daily GPP data. For these half-hourly data GPP data were reconstructed using the gap-filling procedure. The quality classification scheme for gap-filled values is: A: best; B: acceptable; C: dubious.

The agreement between the observed and estimated GPP data series was rather good, with the exception of two periods in spring 2010 and late-winter early-spring 2011 (Fig. 4.6).

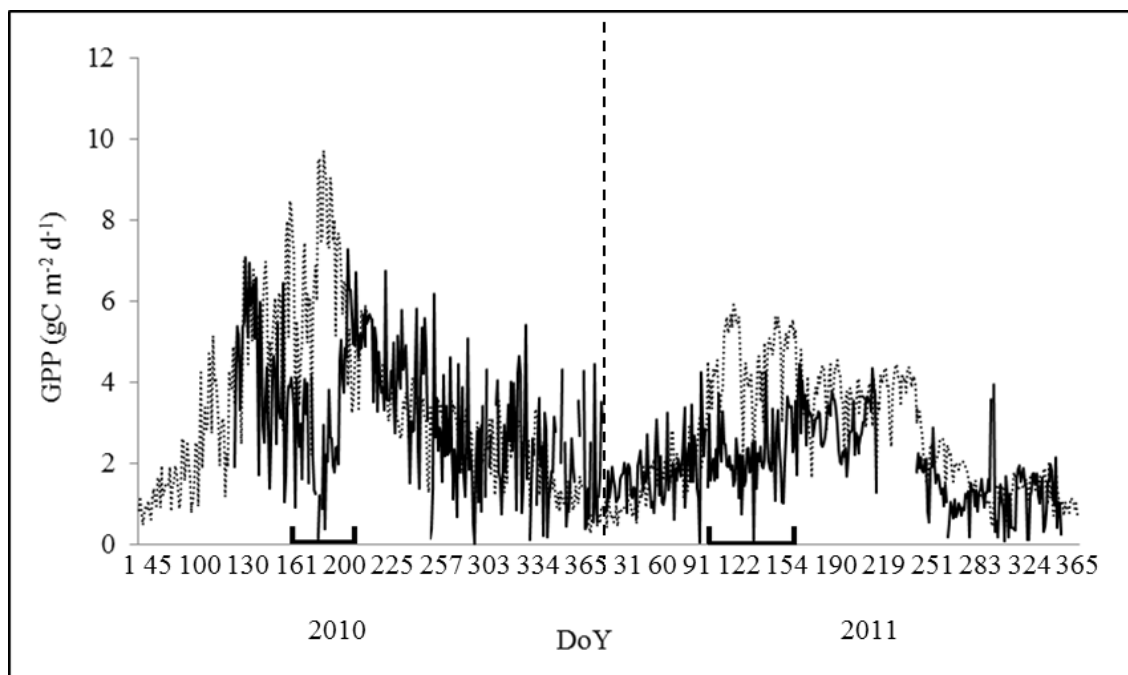


Figure 4.6 - Daily values of GPP estimated by C-Fix model (dotted line) and re-constructed from eddy covariance measurements (filled line). The two black bars on the x axis indicate the periods likely affected by the tillages.

These periods coincided with those subsequent to tillages. The presence of these periods significantly reduced the correlation between measured and estimated GPP ($r = 0.462$ and $RMSE = 1.88 \text{ g C m}^{-2} \text{ day}^{-1}$) (Tab. 4.3).

GPP	Time Interval	R	RMSE	MBE
			(g C m ⁻² day ⁻¹)	(g C m ⁻² day ⁻¹)
All data	Daily	0.462	1.88	0.66
	10-days	0.604	1.51	0.63
	Monthly	0.657	0.66	0.61
Post-tillage removed	Daily	0.662	1.31	0.16
	10-days	0.844	0.83	0.16
	Monthly	0.815	0.81	0.17
Post-tillage simulated	Daily	0.581	1.45	0.36
	10-days	0.771	0.98	0.34
	Monthly	0.817	0.82	0.33

Table 4.3 – Accuracy of GPP estimates obtained applying C-Fix model for different time intervals (see text for details on r , $RMSE$ and MBE).

This was confirmed by the comparison of observed and estimated GPP after the removal of data subsequent to tillages, i.e. in 2010 32 days from May 6th to June 5th; in 2011 69 days from March 19th to May 26th. The different number of daily data removed in the two years was due to the season when tillage occurred and the different meteorological conditions recorded in these periods (see discussion). After removing these periods the accordance between the two data series (observed and estimated) was substantially higher ($r = 0.662$ and $RMSE = 1.31 \text{ g C m}^{-2} \text{ day}^{-1}$). The two tillages were expected to affect almost exclusively the GPP of the ground vegetation layer; in particular, they caused an abrupt reduction of fAPAR consequent to ground vegetation removal, followed by a slow recovery during subsequent weeks.

In an attempt to simulate this effect, the NDVI values of ground vegetation used to drive C-Fix were replaced by synthetic values. More precisely, synthetic NDVI drops to 0.15 just after the tillage, remains unvaried for about half of the above-mentioned periods and then linearly recovers to the original values (Fig. 4.7). This reconstruction significantly improved the correlation between observed and estimated GPP ($r = 0.582$ and $RMSE = 1.45 \text{ g C m}^{-2} \text{ day}^{-1}$, Tab. 4.3).

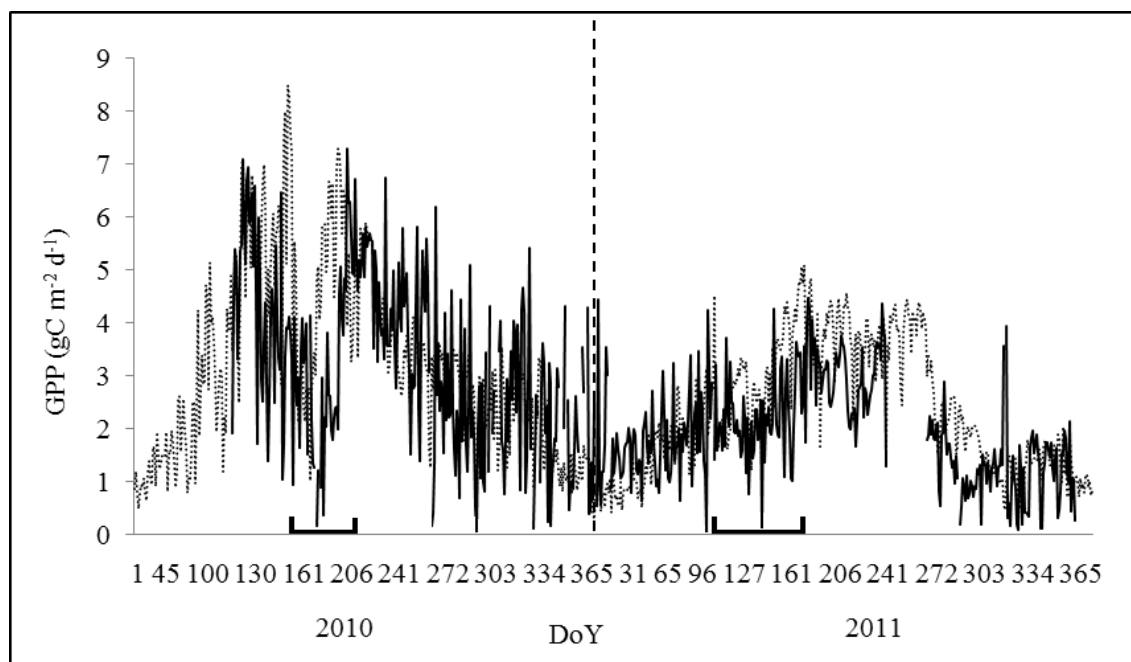


Figure 4.7 – Daily values of GPP estimated by C-Fix model (dotted line) and re-constructed from eddy covariance measurements (filled line). The GPP after the two tillages has been estimated by considering simulated ground vegetation NDVI values (see text for details).

4.4. Discussion

4.4.1. Flux tower data

The GPP of the studied olive grove was determined by the seasonal growth of olive trees and inter-tree ground vegetation. In particular the intensity of ground vegetation growth varies during the growing season. Several studies have indicated a spring peak production mainly caused by the behavior of the herbaceous species, where their reproductive phase of growth is much faster than the vegetative stage (Cavallero and Ciotti, 1991; Parsons, 1988). The best growing season for the majority of herbaceous species in the Mediterranean environment is during spring, while they can suffer from water shortage in summer months (De Marco et al., 2008; Xu et al., 2004). Both patterns, and particularly the latter, may be influenced by agricultural practices. In the current case two main tillages were done in spring 2010 and 2011. Tillage can affect the GPP estimates by removing ground vegetation cover, causing reduction in GPP and consequently changes in its daily trend. In the first study year (2010) tillage was done in spring (May 5th), which is usually the period of maximum vegetative activity and greater biomass amount. As a consequence, tillage may have caused a removal of herbaceous biomass and consequently a strong reduction in ecosystem GPP. On the other hand, tillage was done in a period with high temperatures and intense rainfall, which may have ensured an increase in soil water content. In the semi-arid climates that characterize most of the Mediterranean basin successful germination and subsequent plant establishment is mostly determined by rainfall amount and soil moisture availability (Veenendal et al., 1996), while temperature mainly influences the rate at which leaves expand and the frequency at which they appear (Peacock, 1976). After these tillages the soil was almost bare, but some herbaceous species within the olive grove are characterized by fast growth and development. Indeed, direct visual observations showed that two weeks after tillage, some plants (especially dicotyledons) started to re-grow from those parts of roots that had been pulled out above the soil level, as confirmed by Janicka (2005). In 2011 tillage was done in late winter-early spring (March 19th) in a period with sparse herbaceous cover and low biomass amount. As a consequence, tillage may have removed less herbaceous biomass than in the previous year, and consequently a lower reduction in the GPP ecosystem. Visual observations showed that the re-growth of the herbaceous cover after tillage was slower in 2011, with a longer period of bare soil (about four weeks), probably due to lower temperatures. This condition, added to the dryness of the 2011 growing season, may have caused a reduction in soil water content and consequently water stress. Several studies have indicated that individual plants are

often water-limited during the growing season in regions with dry summers, and water competition is frequent between species (Vignolio et al., 2002; Dyer & Rice, 1999). Globally, this situation may have slowed down ground vegetation development in the second study year. The eddy covariance flux partitioning procedure was likely affected by tillage practices. In fact, the procedure is based on both a seasonal long-term window, and a short-term running temporal window of 15 days, which is considered representative of the characteristic temporal length scale of an ecosystem dynamic (Reichstein et al., 2005). In the case of tillage, as well as other management or natural actions that act as a temporal discontinuity by instantaneously changing some of the system properties, it is likely that the flux partition procedure may be biased in the first period after the discontinuity, while it recovers to proper values after the transient period is stabilized. Tillages can affect GPP by removing the vegetation from the soil and, in turn, can also result in a reduced carbon sequestration (Baker and Griffis, 2005). In addition, tillage in different climatic conditions can influence soil respiration: in periods with high temperatures and high water soil content tillage can induce large carbon loss due to increased bacterial growth in the short-term (Reicosky, 1997). The higher bacterial activity increases oxidation of soil organic matter causing a loss of soil carbon and consequently a higher ecosystem respiration (USDA-NRCS, 2004). On the other hand, when tillages are done in periods with low temperature, their influence on ecosystem respiration and maximum microbial activity is reduced. In our study, tillage events in the warm season may have suddenly removed biomass and increased ecosystem respiration, resulting in increased NEE, and this likely induced an under-estimation of flux tower GPP until new higher respiration rates were observed over a multiple day time scale.

4.4.2. C-Fix GPP estimated data

The current application of C-Fix had to overcome particular problems linked to the peculiar composition of olive grove ecosystems. These ecosystems, in fact, are composed of a variable mixture of olive trees and inter-tree ground vegetation, which obviously show different ecophysiological properties that must be taken into account in the modeling operation. This issue was addressed by the separate application of C-Fix for the tree and herbaceous components, which was made possible by the preliminary estimation of olive tree canopy cover based on the use of very high spatial resolution satellite data. Two versions of C-Fix were then applied, tuned in previous research conducted in the Tuscany region (Maselli et al., 2012A; Maselli et al., 2013; Maselli et al., 2009). The whole approach relies on the correct definition of the olive grove

fractions covered by tree canopies and inter-tree ground vegetation. This is a non-trivial issue, due to the difficulty in obtaining correct area estimates of different cover types from satellite imagery (Conese and Maselli, 1992). In the current case, the use of very high spatial resolution Ikonos imagery to obtain point cover fraction estimates is complicated by the effects of tree shadows, of varying canopy and ground vegetation densities. These problems are exacerbated by the use of lower spatial resolution ETM+ images to extend the estimates over larger areas. These issues have been addressed by the sequential application of a semi-automatic procedure to Ikonos imagery and of locally calibrated regressions to ETM+ images, which should guarantee a substantial reduction in bias of the final estimates (Maselli et al., 2012A). This is confirmed by the accuracy assessment performed over the studied olive grove, which shows a substantial agreement between the olive tree cover fraction estimated automatically and that defined visually. The correct estimation of olive tree and ground vegetation cover fractions has allowed the prediction of the different temporal NDVI profiles that are necessary to drive relevant C-Fix versions. In this regard, the use of the current MODIS NDVI data posed some theoretical and practical problems concerning the spatial and temporal resolutions of the investigation. In fact, the spatial resolution of these data (250 m) is not sufficient to detect subtle changes in vegetation cover due to the application of management practices over small areas (2-3 ha) (Sing, 2011; Lamb, 1998; Fitzpatrick et al., 1990). In particular, it is not sufficient to distinguish the different NDVI values of inter-tree ground vegetation subsequent to the tillage, especially in 2011, when the ground vegetation cover was sparse and low before plowing. As a consequence, this limitation could lead to an overestimate of the ground vegetation biomass, increasing the ecosystem GPP. Considering all these possible error sources, the C-Fix GPP estimates are in reasonable agreement with the GPP data derived from the eddy covariance tower. The results obtained indicate that C-Fix can reproduce the observed GPP values fairly well, with the exception of the periods following tillage. During the days following plowing in 2010 observed GPP significantly goes down, while the estimated GPP increases. Maximum disagreement is reached at the end of May, where the model shows the maximum peak of production. The GPP data series again shows good agreement at the end of spring, when the observed GPP increases, probably due to the reduction of tillage effects. There is a similar trend in 2011, where observed GPP decreases during the days following plowing, which was done in late winter. The accuracy of the daily GPP values predicted by the model was confirmed by a simulation that considered the NDVI values after the tillages (for 15 and 30 days in 2010 and 2011, respectively) to be

equal to 0.15, followed by a slow recovery. In this way the observed and simulated GPP daily values for the two study years are quite well correlated ($R=0.581$ and $RMSE=1.455$), and have more similar bi-annual totals ($1865.06 \text{ gC m}^{-2} \text{ year}$ and $1479.63 \text{ gC m}^{-2} \text{ year}$). In this regard it should be kept in mind that in the post-tillage transient period the model GPP overestimation could be partly due to the previously mentioned problems in the correct application of the eddy covariance partitioning methods.

4.5. Conclusions

Carbon exchange data taken in agro-ecosystems provide the fundamental basis for developing and validating simulation models to monitor gross/net primary production over wide areas and lengthy time periods (i.e. Joseph et al., 2012; Suyker et al., 2005; Xiao et al., 2004; Gitelson et al., 2003; Ruimy et al., 1994). Such models may have a different level of complexity and simulate processes such as whole-plant photosynthesis and heterotrophic/autotrophic respiration. In this work, we presented a modified version of a simple parametric model, C-Fix, to estimate daily GPP of an olive grove by separating the contribution of the autotrophic components dominating this ecosystem, i.e. olive trees and ground vegetation. The daily GPP values estimated by C-Fix were compared against GPP daily data obtained from eddy covariance flux measurements taken for two years in an olive grove located in South Tuscany, Italy. A major issue that was found is related to the discrepancies between estimated and observed flux tower daily GPP data for post-tillage periods (i.e. the model overestimates photosynthesis of olive trees). Considering the effects of tillage practices on soil and its vegetation, most of these discrepancies were accounted for by super-imposing ground vegetation NDVI variations during the post-tillage periods. The length of post-tillage periods and the consequent model GPP overestimation were strongly linked to weather conditions, which determined the re-growth of the herbaceous component. Some of the limitations we encountered, related to the low resolution of satellite data that are not capable of separately resolving tree canopies and soil, might be overcome with a future availability of high spatial resolution spectral satellite data at low cost. Our results confirm that the Monteith type parametric model C-Fix, properly tuned for the two components, can be used to simulate total olive grove GPP based on the main driving factors of solar radiation, thermal and water stresses and fAPAR. Given the impact that crop management (i.e. tillage) may have on the C-cycle and the scarce knowledge on C fluxes dynamics in agro-ecosystems such as olive groves, studies should be conducted to assess the possibility of further

improving the model performances. Since management practices may significantly affect the carbon balance of olive groves, a management parameterization should be included in any ecosystem modeling framework. In particular, studies should be conducted in olive groves characterized by the same climatic conditions but different agronomic practices (i.e. tillage types and times or no tillage), with the aim of assessing the accuracy of the method under different management practices.

Chapter 5

Calibration and validation of biogeochemical model Daycent in a Mediterranean olive orchard: assessment of carbon sequestration capacity for current and future scenarios

Abstract

In this work we calibrated and validated the biogeochemical model Daycent with the aim to estimate the C-sequestration capacity of a typical Mediterranean olive orchard. An eddy-covariance station placed into the orchard provided the net ecosystem exchange (NEE) data over three years (2010-2012). NEE data from the first year of study were used to calibrate the model whilst the two remaining years were used for model validation. Daycent resulted to be able at reproducing daily olive orchard NEE with a good accuracy ($r=0.5$ and $RMSE=1.93$ and $r=0.41$ and $RMSE=0.62$ g C m⁻² day⁻¹, for calibration and validation respectively) during the whole period of study. Once model was calibrated and validated, a stochastic weather generator LARS-WG was used to generate 100 years of synthetic weather data under the SRES emission scenario A1B for 4 time slices (1981-2010; 2010-2030; 2045-2064; 2080-2099). Model prediction indicated that the C-sequestration capacity of the olive orchard is expected to be reduced of 14.8, 26.6 and 36.3% for 2011-2030, 2046-2065 and 2080-2099 compared to the baseline scenario (1981-2010).

Keywords: Olive orchard, Daycent model, NEE, C-sequestration.

Chapter based on:

Brilli, L., Lugato, E., Gioli, B., Toscano, P., Moriondo, M., Zaldei, A., Cantini, C., Ferrise, R., Bindi, M. 2015. *Calibration and validation of biogeochemical model Daycent in a Mediterranean olive orchard: assessment of carbon sequestration capacity for current and future scenarios.* (Forthcoming).

5.1. Introduction

The role of long term agro ecosystems in C-sequestration should be more deeply investigated since it may open new options for greenhouse gas emission reduction and, in turn, climate mitigation. These systems, also called savanna systems, are usually characterized by the presence of two different vegetation layers, trees and ground vegetation, which interact each other creating a biome that is neither grassland nor forest (Scholes and Archer, 2013). Although the term savanna indicates a wide range of these systems, the most important savanna systems can be considered the fruit orchards. At worldwide scale indeed, these systems are involved in agricultural production and they can also provide ecosystemic services such as landscape protection, environment conservation and climate mitigation, thus resulting very important from an economic point of view (Lomou and Giourga, 2003; Sofo et al., 2005, Brilli et al., forthcoming). This kind of cultivation assumes high relevance especially over the Mediterranean area, widely recognized as the most traditional fruit-growing area due to historical, environmental and evolutionary reasons (Connor, 2005). In this geographical area the most representative Mediterranean savanna system can be considered the olive trees system. The widespread cultivation of this system indeed characterizes the rural landscape in many countries such as Italy, Spain, Greece, etc. (Lomou and Giourga, 2003; Vossen et al. 2007). Despite the olive tree cultivation has always been aimed at olives and olive oil production, in the last years some studies have argued the importance of these systems also in respect of international regulations about greenhouse gas control and the mitigation of climate change. For instance Nardino et al. (2013) and Brilli et al. (forthcoming) indicated that, regardless on management and climate conditions, the C- sink capacity of olive orchards is on average comparable to Italian forestry systems. Furthermore, the magnitude of C-sequestration capacity reported in these studies has been clearly associated with water availability. In particular, according to Brilli et al. (forthcoming), the C-sequestration capacity of a rainfed olive orchard is strictly connected with pattern and timing of precipitation. Looking at the future climate projections, according to recent WGI contribution to the AR5-IPCC (IPCC, 2013), Mediterranean area will probably experience a general warming that will be associated with a strong reductions in precipitation, with a decrease from 25% to 30% by the end of the 21st (Giorgi and Lionello, 2008). On these premises, the precipitation decrease in conjunction with the expected changes in frequency and pattern of precipitation may reduce the mitigative capacity provided by olive orchards or even turning these systems into carbon source. In this context, whilst the contribute that this system

play in climate change mitigation is not well studied, the contribute that this system will play in the next decades is completely unknown. In particular, the complex structure of this system does not allows a simple straight forward C-fluxes assessment from the ground (i.e. eddy covariance, FACE, respiration chambers, etc.) nor from satellite (i.e. remote sensing). This condition joint with the high costs needed to obtain these measurements has often brought to a lack of knowledge about the efficiency offered by this system for greenhouse gas emissions control. On these basis, it would be therefore fundamental the implementation or development of tools able at reproducing the C-fluxes exchanges from olive orchard that could guarantee the same measures but in a more simple and cheaper way. Currently, several mathematical models able to predict C-fluxes from agricultural systems were widely developed and applied (e.g. DNDC, RothC, ECOSSE, ECOSYS, COMP, etc.). Among all of these models, Daycent (Parton et al., 1994) was chosen because it was considered as the most suitable to reproduce C-fluxes from orchard systems. In particular the "savanna sub-model" contained into Daycent allows for the interaction between the grassland/crop and forest subsystems through shading effects and nitrogen competition. Based on these premises, the objective of this paper was to calibrate and validate Daycent model over olive orchard. In this work, 3 years of Net Ecosystem Exchange (NEE) measures from eddy covariance were used to test the model over a typical managed olive orchard in Tuscany (central Italy). We first calibrated the model over the first year of study (2010), then it was validated over the two remaining years. We addressed the level of expected accuracy of the model and its suitability for C-sequestration prediction by means of statistical analysis (r, RMSE) carried out on different time intervals. Once the model was validated, a weather generator LARS-WG was used to generate 100 years of synthetic weather data under the SRES emission scenario A1B for 4 time slices (Baseline 1981-2010; 2011-2030; 2045-2064; 2080-2099) with the aim to assess the C-sequestration capacity that will be lost from olive orchard compared to the baseline.

5.2. Materials and methods

5.2.1. Study area

The Study area is located at Follonica (42°56' N , 10°46' E), a small village in Central Italy (Tuscany). The local climate is characterized by high temperatures and prolonged periods of drought during summer, whilst typically mild wintertime. The lowest monthly mean temperature is usually recorded on January (7.5°C), while the highest on August (30.9°C). Precipitations

represent the typical Mediterranean trend, with the main peaks recorded in fall and early spring. The long-term precipitation average (PP-LTA) calculated over the period 1981-2009 is 626 mm (MARS JRC). Test study site is an adult olive extended for about 6 ha and containing more than 1500 plants of 4-5 meters in height. Trees have same ages (20 years) and plant density (7x5m), and their canopies cover about 25% of the whole orchard (Maselli et al., 2012). Soil characteristics were obtained through the analysis of 10 soil samples taken in different part of the orchard. The sampling was done for four different soil depth are reported in Tab. 5. Results showed that orchard mainly consists of clay-sand textural class (50% clay and 30% sand), the average pH value is about 7, whilst bulk density (BD) is 1.27 Mg m⁻³ (Tab. 5.1). Moreover, the available water capacity of the area ranges from 90 to 120 mm/m (Harmonized World Soil Database, FAO/IIASA/ISRIC/ISS-CAS/JRC, 2009).

	Sand	Silt	Clay	pH	BD
Deep (cm)	g/kg⁻¹	g/kg⁻¹	g/kg⁻¹		Mg m⁻³
0-15	329 ± 22	233 ± 19	438 ± 34	7.2 ± 0.12	1.13 ± 0.11
15-30	310 ± 28	262 ± 25	428 ± 53	7.1 ± 0.21	1.26 ± 0.15
30-50	279 ± 19	200 ± 33	521 ± 42	6.8 ± 0.13	1.29 ± 0.14
50-70	250 ± 18	181 ± 37	569 ± 23	6.5 ± 0.11	1.42 ± 0.18

Table 5.1 - Soil characteristics of test site. Texture, pH and Bulk density were provided for 4 different soil layers.

Agricultural practices reflect the ancient tradition of olive tree cultivation, characterized by inter-row superficial tillage, fertilization at the beginning of the growing season (early spring), without irrigation. During the 3 years of study (from 2010 to 2012) tillage practices have been carried out 1 time per year using disk-harrowing. Inter-row orchard were ploughed in early May 2010, in February 2011 and in late May 2012. Similarly, fertilizer was applied at the end of February (2011) or in May (2010 and 2012). Mechanical harvesting was in 2010 and 2012 in November. Conversely in 2011, harsh meteorological conditions coupled with alternate bearing have caused extremely low production, therefore fruits were left on the trees. All remaining vegetation components within the orchard (i.e. weeds, litter, residues due to mechanical harvesting such as leaves, small branches, fruits, etc.) were incorporated into the soil during tillage.

5.2.2. Eddy Covariance data and processing

Eddy covariance (EC) is a micrometeorological technique that allow to measure ecosystem carbon (CO₂) and energy exchange (H₂O, H, LE) between the ecosystem and the atmosphere (Baldocchi et al., 1996). The EC system consisted of a mobile carriage equipped with a mast and it was placed in the central part of the olive orchard to obtain the net CO₂ exchange of the entire ecosystem. Data were recorded from March 2010 through October 2012. The fast sensors (i.e. a Metek USA 1 triaxial sonic anemometer and a Licor 7500 open path infra-red CO₂-H₂O analyzer) were mounted on the mast at a height of 7 m, about 2 m above canopy top. These data were acquired at high frequency (20 Hz) and then stored on an handheld low consumption computer (Matese et al., 2009). Ancillary data included half-hour mean meteorological measurements such as soil temperature profiles from 5 to 20 cm (thermocouples J and T types), global and net radiation (CMP3 and NR LITE Kipp & Zonen), air temperature and humidity (HMP45 Vaisala), and rainfall (rain gauge Davis 7852). These data were stored on half-hourly basis on a data logger (Campbell CR10X). The entire instrumentations was electricity supplied through a battery system charged by 3 solar panels with 90 A/h capacity. However, this setup caused some power outages especially during wintertime. Eddy covariance raw data were then analysed and processed. First step concerned the analysis of footprint through an analytical model (Hsieh et al., 2000) that computed footprint distances as a function of several parameters (i.e. wind speed and direction, atmospheric stability, measurement height and surface roughness). Doing so, we evaluated the extent of the area surrounding the tower where the observed fluxes originated from. This methods pointed out that the area containing 90% of the observed flux is almost entirely contained within the olive orchard edges. Then, the Eddy Pro® Software was used to process binary files and meteorological data collected by E.C. tower for all the 3 years of study. Eddy Pro® Software has been run in Express Mode that considered several procedures such as spectral corrections to compensate flux underestimations, despiking for detecting and eliminating short-term outranged values in the time series and control tests for fluxes according to Foken et al. (2004). Final outputs from Eddy Pro® consisted of gap-filled NEE data at half-hour resolution. These outputs were then aggregated both on daily and 10-days totals. During the 3 years of experiment, data losses were mainly concentrated in early 2010 and at the end of 2012. This condition did not allow a reliable assessment for those months in which the concentration of missing data was particularly high.

5.2.3. Daycent overview

Daycent (ver. 4.5), the daily time-step version of the biogeochemical Century model (Parton et al., 1994), has been designed to simulate soil C dynamics, nutrient flows (N, P, S), and trace gas fluxes (CO_2 , CH_4 , N_2O , NO_x , N_2) between soil and the atmosphere (Parton et al., 1998, Del Grosso et al. 2001a). The main inputs concern site specific soil properties, current and historical land use (i.e. vegetation type, management schedules, amount and timing of nutrient amendments, etc.), and specific meteorological parameters reported at daily time (i.e. maximum and minimum air temperature and precipitation). Daycent includes four major sub-models: *a) Plant productivity and allocation of net primary production (NPP)*. It is a function of genetic potential, phenology, nutrient availability, abiotic stresses (water and temperature), and solar radiation. The NPP is allocated within different plant compartments (i.e. roots, branches, shoots, etc.) based on vegetation type, phenology, and water/nutrient stress; *b) Decomposition of dead plant material (litter) and SOM*. They are functions of substrate availability and quality (lignin %, C/N ratio) as well as water/temperature stress. The SOM pools are 3 and they are defined as active, slow or passive pool depending on their turn over time; *c) Soil water and temperature dynamic*; *d) Trace gas fluxes*. The latter is driven by soil NH_4 and NO_3 concentrations, water content, temperature, texture, and labile C availability (Parton et al., 2001). Model outputs include several daily N-gas flux (N_2O , NO_x , N_2), CO_2 flux from heterotrophic soil respiration, soil organic C and N, NPP, NEE, H_2O and NO_3 leaching, and other ecosystem parameters. According to Del Grosso et al. (2002, 2005) Daycent model can be considered as a reliable tool for simulating crop yield, SOM levels, and trace gas flux for various native and managed systems.

5.2.4. Future climate scenarios

The climatic scenarios for present and future periods were created using the stochastic weather generator LARS-WG (Semenov and Barrow, 1997). Once calibrated on a specific site, LARS-WG is able to generate daily time series of minimum and maximum temperatures, precipitation and global radiation with statistical properties similar to those observed at the site (Semenov and Doblas-Reyes, 2007). In this study, the latest version of LARS-WG was adopted (Semenov and Stratonovitch, 2010). This latter allows the user to generate scenarios of climatic change since it incorporates future climate projections from several global simulation models. For this study, LARS-WG was used to generate 100 years of synthetic weather data for each of the following

time slices: present period (1981-2010, PP), and 3 future time slices (2010-2030, FP1; 2045-2064, FP2 and 2080-2099, FP3). Specifically, future climate scenarios were generated using the HADCM3 projections (Pope et al., 2000) under the SRES emission scenario A1B (Nakicenovic and Swart, 2000).

5.2.5. Daycent calibration and validation

Daycent was calibrated by matching simulating daily NEE data with corresponding observed values from eddy covariance for the entire year 2010. The daily weather data file taken into account minimum and maximum air temperature and precipitation, whilst solar radiation, relative humidity and wind speed were not used. The soil file was compiled based on field data collected within the test site. The schedule files for spin up and test site were built to reflect as nearly as possible the historical and current land use, vegetation type and management. Daycent was brought to an equilibrium state by simulating almost 2000 year consisting of continuous forest (1-1930) followed by low yield wheat (1931-1992). The current land use (1993–2012) was built for reflecting olive orchard system (i.e. mixed grass + olive trees). Then, we tuned the model as necessary within acceptable ranges to match observed NEE data more closely. The parameters changed were described in the tables reported in section 3 (Tab. 5.2 and 5.3), where were also indicated the recommended ranges of crop and tree parameters and the selected parameters based on matching the NEE for calibration. These key factors were identified as critical in explaining global variations in daily NEE. Finally, once the best calibration was found, the key parameters remained unchanged and the model was thus validated over the years 2011 and 2012.

5.2.6. Statistical analysis

In order to evaluate model performances different statistics were used. In particular, accuracy of NEE estimates from the model included correlation coefficients (r) and root mean square error (RMSE). According to Del Grosso et al. (2011), for vectors that are highly variable in time such as N₂O or CO₂ emissions and C-fluxes, the model could have some problem to well represent the timing at the daily scale, whilst it could represent more correctly treatment impacts at seasonal scale. All statistics were therefore applied also at different time intervals (daily, 5-10-days and monthly).

5.3. Results

5.3.1. Sensitivity analysis

Sensitivity analysis allowed to determine the key factors controlling C exchange in olive orchard. Different series of key factors were identified both for ground vegetation and trees. These factors were identified as the mostly critical in explaining variations in daily NEE, while the remaining had no great influence on modelled NEE.

The most sensitive controls were identified as the potential aboveground monthly production, temperature effect on growth, C/N ratio under different plant compartments and LAI. The optimized values of most parameters were significantly changed from their initial default values and adapted based on the different physiological characteristics of both layers.

The changed values of all sensitive parameters along with their initial values as well as their upper and lower limits are given in Tab. 5.2.

ID_Crop	Parameter	Description	Range	Selected
Mix grass	PRDX (1)	Coefficient used for calculating potential aboveground monthly production as a function of solar radiation	0.1 - 2.0	0.95
	PPDF (1)	Optimum temperature for production for parameterization of a Poisson Density Function curve to simulate temperature effect on growth	10 - 40	24
	PPDF (2)	Maximum temperature for production for parameterization of a Poisson Density Function curve to simulate temperature effect on growth	20 - 50	40
	PPDF (3)	Left curve shape for parameterization of a Poisson Density. Function curve to simulate temperature effect on growth	0 - 1	0.9
	PPDF (4)	Right curve shape for parameterization of a Poisson Density. Function curve to simulate temperature effect on growth	0 - 10	2.5
	BIOK5	Level of aboveground standing dead + 10% struce(1) C at which production is reduced to half maximum due to physical obstruction by the dead material	0 - 2000	1
	FRTCINDEX	Plant growth type: 0= use Great Plains equation; 1= perennial plant; 2= annual plant; 3= perennial plant, growing degree day	0 - 6	1

		implementation and dynamic carbon allocation; 4= non-grain filling annual plant and growing degree day implementation, dynamic carbon allocation; 5= grain filling annual plant, growing degree day implementation, dynamic carbon allocation; 6= grain filling annual plant that requires a vernalization period (i.e. winter wheat), growing degree day implementation, dynamic carbon allocation.		
	CLAYPG	Number of soil layers used to determine water and mineral N, P, and S that are available for crop growth.	1 - 9	4

Table 5.2 - Parameters changed in the file "crop.100" to adjust biomass production for grass layer (Mixed grass from crop default file with 50% warm and 50% cool, N fixation).

ID_Crop	Parameter	Description	Range	Selected
Olive tree	DECID	Type of forest: 0= continuous; 1= temperate-deciduous; 2= drought-deciduous	0 - 2	0
	PRDX (1)	Coefficient used for calculating potential aboveground monthly production as a function of solar radiation	0.1 - 2.0	0.93
	PPDF (1)	Optimum temperature for production for parameterization of a Poisson Density Function curve to simulate temperature effect on growth	10 - 40	30
	PPDF (2)	Maximum temperature for production for parameterization of a Poisson Density Function curve to simulate temperature effect on growth	20 - 50	45
	PPDF (3)	Left curve shape for parameterization of a Poisson Density. Function curve to simulate temperature effect on growth	0 - 1	1
	PPDF (4)	Right curve shape for parameterization of a Poisson Density. Function curve to simulate temperature effect on growth	0 - 10	3.9

CERFOR(2,1,1)	Maximum C/N ratio for leaves	1 - 200	90
LEAFDR	Monthly death rate fraction for leaves (1 - 12)	0 - 1	Jan= 0.060 Feb= 0.050 Mar= 0.070 Apr= 0.000 May= 0.070 Jun= 0.009 Jul= 0.040 Aug= 0.085 Sep= 0.060 Oct= 0.050 Nov= 0.040 Dec= 0.030
BTOLAI	Biomass to leaf area index (LAI) conversion factor for trees.	0.01 - 0.008	0.007
KLAI	Large wood mass (gC/m ²) at which half of the theoretical maximum <i>maxlai</i> is achieved		4500
LAITOP	Parameter determining relationship between LAI and forest production: LAI effect = $1 - \exp(\text{laitop} * \text{LAI})$		-0.47
MAXLAI	Theoretical maximum leaf area index achieved in mature forest	0 - 50	6
WDLIG(1)	Lignin fraction for leaf component	0 - 1	0.203
TLAYPG	Number of soil layers used to determine water and mineral N, P, and S available for growth	1 - 9	3

Table 5.3 - Parameters changed in the file "tree.100" to adjust biomass production for tree layer (Olive tree from tree default file based on century data).

5.3.2. Calibration and validation

Calibration was reported at daily time step in Fig. 5.1. Comparison between observed and simulated daily NEE showed that the model well represents the general behaviour of the olive orchard with the only exception in summer, where NEE is underestimated and the model shows little NEE variability compared to observed values.

More specifically, during summer the simulated daily NEE ($\sim -2 \text{ gC m}^{-2} \text{ d}^{-1}$) was, on average, the half of the NEE observed ($\sim -4.5 \text{ gC m}^{-2} \text{ d}^{-1}$). Different NEE was also observed during Spring and particular in May, where the daily simulated NEE was on average ($\sim 12 \text{ gC m}^{-2} \text{ d}^{-1}$) about 2 times greater than NEE observed ($\sim 6 \text{ gC m}^{-2} \text{ d}^{-1}$).

Despite the absolute values simulated by the model over these 2 periods did not match with those observed, statistical analysis (Tab 5.4) confirmed the good agreement between observed and modelled NEE trend at daily scale ($r= 0.5$) along the whole year.

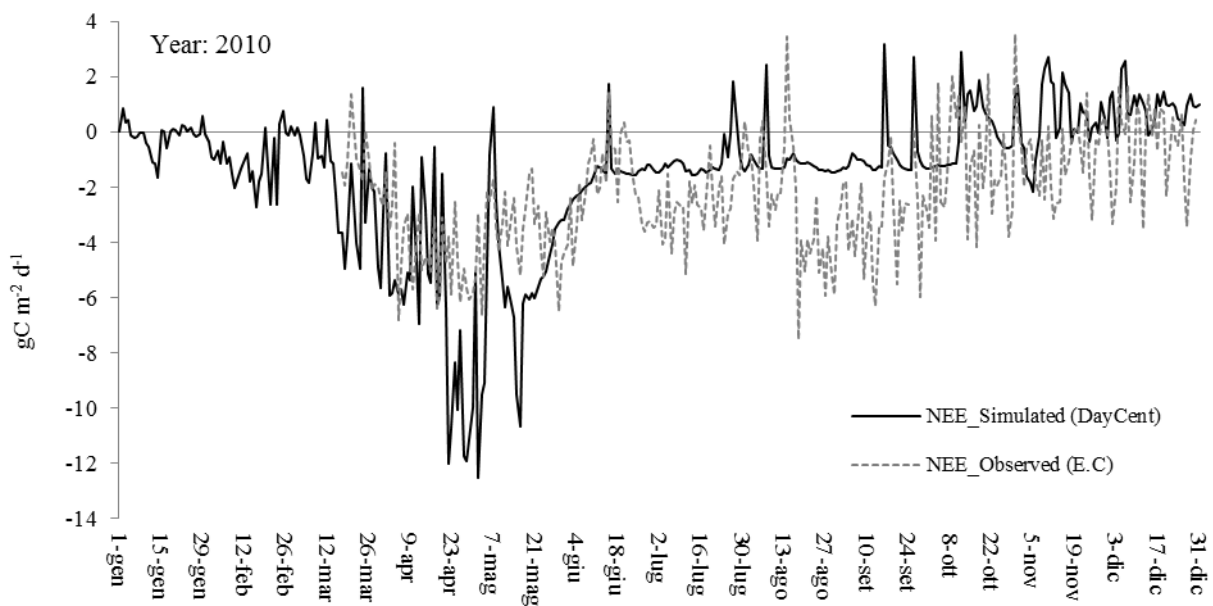


Figure 5.1 - Model calibration reported at daily time step.

Moreover, the correlation was found higher increasing the time step (i.e. 5, 10 days or monthly). However, based on an annual scale, the model resulted to underestimate the NEE. More specifically the total annual NEE simulated by the model (-553 gC m^{-2}) resulted to be 17% lower compared to that observed (-647.2 gC m^{-2}) (Tab. 5.5).

Daycent has been then validated over the two remaining years (2011 and 2012). As shown in Fig. 5.2, the NEE trend simulated by the model was found in good agreement with the observed NEE.

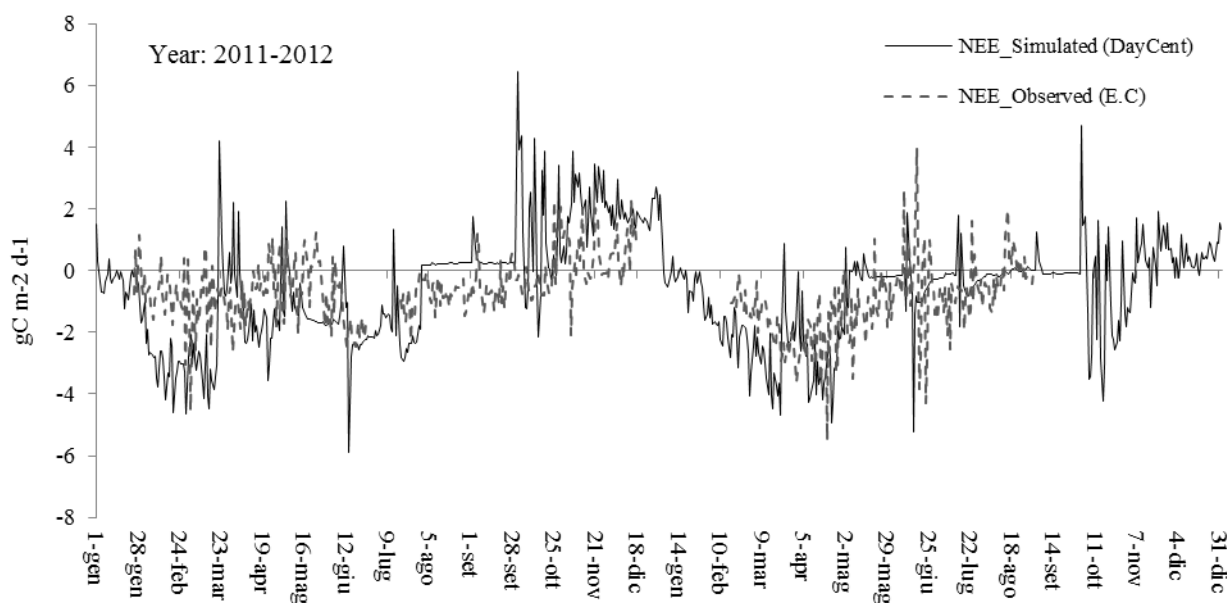


Figure 5.2 - Model validation reported at daily time step.

In particular, with the only exception of the early 2011 where the model overestimated the NEE, Daycent seems to well reproduces also emissions peak recorded during winter and summer. Similarly as observed during model calibration, the correlation between simulated and observed NEE enhances by increasing the time step. By contrast, based on an annual scale the model resulted to be perfectly consistent with the NEE observed in 2011 and 2012. More specifically the total annual NEE simulated by the model for both years (-157 and -227.6 gC m⁻²) resulted to be only 4% higher compared to that observed (-149.3 and -218.3 gC m⁻²) (Tab. 5.5).

NEE	Time Interval	r	RMSE (g C m ⁻² day ⁻¹)
Calibration (2010)	Daily	0.498	1.931
	5-days	0.623	1.375
	10-days	0.667	1.243
	Monthly	0.765	0.909
Validation (2011-2012)	Daily	0.412	0.625
	5-days	0.563	0.690
	10-days	0.634	0.635
	Monthly	0.915	0.399

2011	Daily	0.39	0.844
	5-days	0.541	0.559
	10-days	0.638	0.505
	Monthly	0.823	0.305
2012	Daily	0.416	1.013
	5-days	0.579	0.771
	10-days	0.647	0.698
	Monthly	0.888	0.386

Table 5.4 - Statistical analysis concerning model calibration and validation carried out at different time step.

Based on the whole period of study, Daycent model resulted to be able to reproduce NEE trend with high accuracy. More specifically taking in account the same days during the 3 years of study, the simulated NEE resulted to underestimate the observed NEE of only 8%.

NEE			
	Simulated (Daycent)	Observed (E.C)	Diff (%) Sim/Obs
2010	-552.97	-647.17	-17.04
2011	-157.02	-149.31	4.91
2012	-227.59	-218.35	4.06
SUM	-937.6	-1014.8	-8.24

Table 5.5 - Total annual NEE simulated by Daycent model and observed from Eddy Covariance. Total annual NEE was reported considering the same days for observed an simulated.

5.3.3. NEE: future projections

Once the model has been calibrated and validated, 4 different timeline under A1B scenario were used to estimate future NEE from olive orchard (Fig. 5.3). The NEE simulated by the 3 future scenarios (2011-2030; 2045-2064 and 2080-2099) was found close to the NEE simulated using the baseline (1981-2010), with the maximum sequestration during spring and a little vegetation recovery at the end of summer. The major differences were observed during dry period (summer).

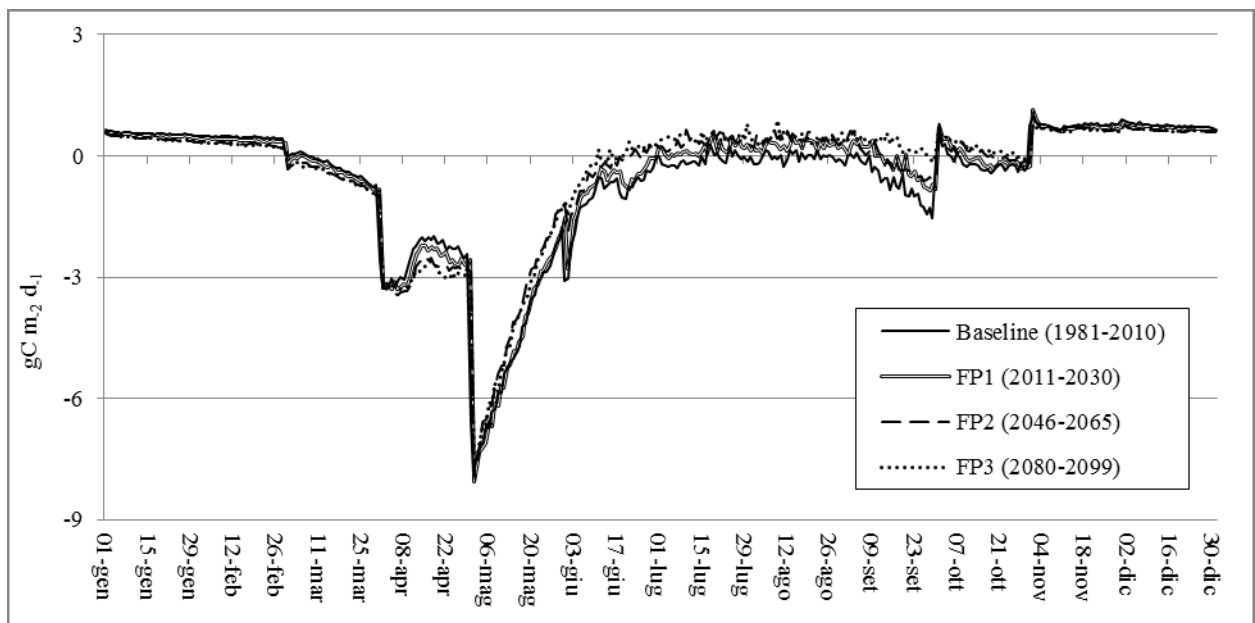


Figure 5.3 - Average daily NEE reported for the 4 different timeline under A1B scenario.

Based on a monthly scale (Fig. 5.4), the major differences among the baseline and all the three future scenarios were more clear compared to the analysis at daily scale.

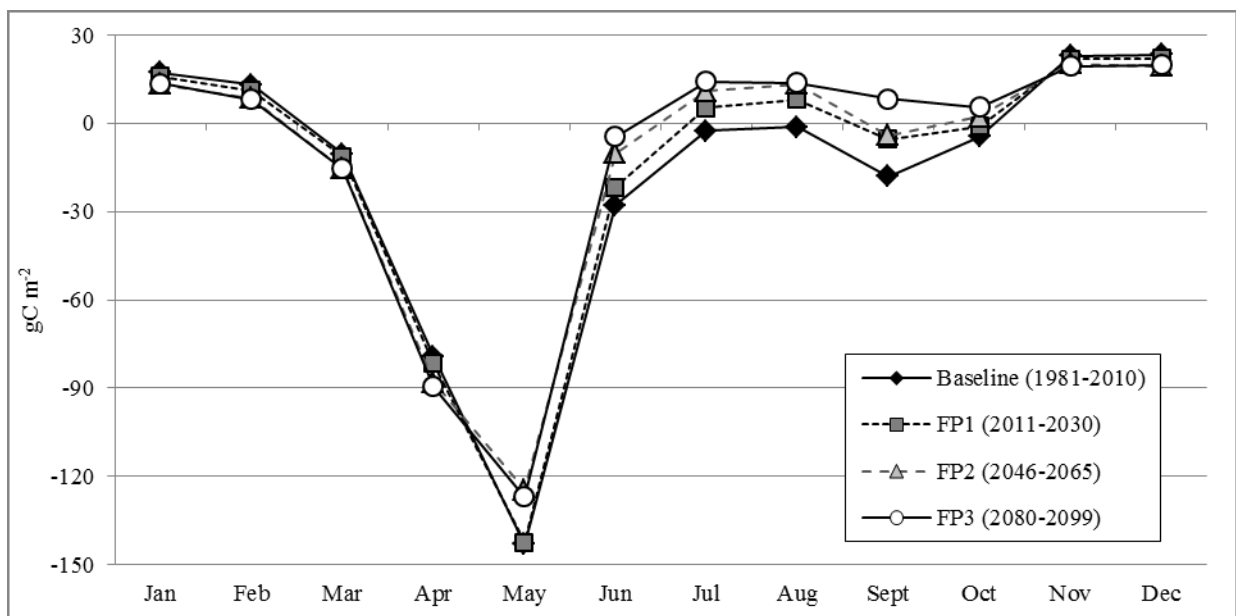


Figure 5.4 - Average monthly NEE reported for the 4 different timeline under A1B scenario.

The first clear difference was observed in May, where the cumulated NEE observed under the baseline and 2011-2030 scenario was similar and it was also lower compared to the other scenarios (2045-2064 and 2080-2099) of about 14%. Then, during the hottest period (i.e. July and August) the cumulated NEE showed positive values under all the 3 future scenarios with the only exception of the baseline, where a slight but continuative C-sequestration was observed. The cumulated NEE for the baseline was observed strongly increase again in September (-18.2 gC m⁻²) as typical for Mediterranean ecosystem, while it poorly increased for the periods 20011-2030 (-5.5 gC m⁻²) and 2045-2064 (-4 gC m⁻²). The only exception resulted to be the period 2080-2099, where the typical recovery result to be absent and a continuative C-emission was observed (8.2 gC m⁻²). According to Tab. 5.6, the olive orchard under investigation is expected to lose its C-sequestration capacity approaching the end of the century. More specifically based on our analysis the C-sequestration capacity of the olive orchard is expected to be reduce of 14.8, 26.6 and 36.3% for 2011-2030, 2046-2065 and 2080-2099 compared to the baseline scenario (1981-2010).

NEE (gC m⁻²)				
Time-Step	Baseline (1981-2010)	FP1 (2011-2030)	FP2 (2046-2065)	FP3 (2080-2099)
Jan	17.22	15.99	13.37	13.51
Feb	13.07	11.17	8.43	8.05
Mar	-10.46	-11.30	-15.53	-15.56
Apr	-79.17	-81.62	-88.06	-89.54
May	-143.14	-142.47	-124.60	-126.87
Jun	-27.89	-21.70	-10.22	-4.49
Jul	-2.56	5.14	10.89	14.06
Aug	-1.24	8.16	13.17	13.73
Sept	-18.16	-5.50	-4.05	8.21
Oct	-4.52	-1.09	2.22	5.46
Nov	22.94	21.73	20.30	19.45
Dec	23.20	21.93	19.42	19.80
	<i>-210.72</i>	<i>-179.54</i>	<i>-154.66</i>	<i>-134.17</i>

Table 5.6 - Monthly NEE simulated by Daycent model for the baseline and the 3 future timeline under AIB scenario

5.4. Discussion

5.4.1. Calibration and validation

Cultivar-specific plant parameters for olive tree and grass were calibrated across a site specific area in Tuscany (Italy). Overall, the modelled NEE agreed well with the observed NEE (Tab. 5.4). The model, however, appeared to overestimate the range of NEE variation during late spring when tillage was done, whilst it seems to underestimate the NEE during dry period.

These issues were probably due to different causes. During springtime, the NEE overestimation was observed especially in April and May. In April the maximal rate of photosynthesis adjusted to reflect the general length of the growing season across the year could be resulted higher in respect of those observed. This could be explained by the fact that the maximal rate of photosynthesis simulated by the model is mainly driven by precipitation and air temperature. In this context these two climate parameters recorded over April could have lead the model to overestimate the NEE during this period. During May the main issues was probably due to the effect of cult.100 file. This file was used to simulate tillage practice that was done at the begin of May. This practice was done in a period with high water availability in conjunction with the increase of air temperature. This could have enhance soil microbial biomass and its relative activity, leading to a quickly vegetation growth and SOM decomposition. This is in agreement with Parton et al. (1987) that suggested as soil carbon sequestration in Daycent model is a function of plant productivity and SOM decomposition.

During the hottest period of the year (i.e. July and august) Daycent model does not follow the NEE trend, underestimating the observed NEE. More specifically, in these months the simulated NEE shows low variability compared to the direct measurement. Doing so, Daycent model does not reflect the vegetation activity that, by contrast, it is clearly indicated by the direct measurements. This disagreement can be observed in a period where the most limiting factor for vegetation activity is water availability. According to some recent studies (Nardino et al., 2013; Brilli et al., forthcoming), during the growing season the olive orchard NEE dynamics are mainly influenced by the availability of water. On these basis, therefore, the main issues could be due to a synergy of input factors that concern both soil characteristics and olive tree physiology.

Besides to basic soil parameter such as texture, pH and bulk density, Daycent soil file allows to indicate also number and depth of soil layers as well as the percentage of roots that are in each of those. Similarly, within the tree.100 file it is possible to indicate the number of the soil layers that are used to determine the available water and mineral N, P, and S for tree and grass growth.

These input parameters are useful to better define the structure of the system, arranging the roots in the most superficial layers (i.e. 30 centimetres) and by indicating these layers as the more important relating to water availability. Despite these parameters have been chosen through field analysis and literature and therefore they can be considered as highly suitable to represent the olive orchard ground structure, the model could not reflect the observed NEE since the tree.100 file parameters does not take in account specific intrinsic olive tree physiological characteristics. For instance, olive trees usually rely on conservative water use in Spring thus reducing the extent and intensity of the summer drought (Connor, 2005). This behaviour allows a continuative photosynthetic activity also during the driest period. This is possible thanks to adjustments that are typical of xerophil plants. These species, indeed, is usually characterized by high resistance to gas diffusion in the leaf since they can reduce their intercellular volume spaces within tissues (Bongi et al., 1987; Gucci, 1998). Daycent model, therefore, could have several problems at reproducing the NEE of those species that are particularly good in water use efficiency. Changing the number of soil layers that are used to determine the available water and mineral for tree and grass growth model performance improved. This may be due to the increase of the roots percentage in soil layers that may have allow an increase of water and mineral supply for tree and grass growth.

5.4.2. Future NEE projections

Once model was calibrated and validated, it was applied to simulate future NEE from the same olive orchard. As it was expected, results showed a progressive decrease in NEE approaching the end of the century. This is consistent with the precipitation and air temperature trend for future period. More specifically according to several studies (IPCC, 2013) these trends are expected to show air temperature increase and a strong precipitation reduction over Mediterranean basin and, consequently, over the study area. Compared to the baseline, the greatest changes in NEE were observed in FP2 and FP3 during the whole growing season (Fig 5.4). Both time slices showed a similar trend characterized by a slight NEE increase during early spring followed by a reduction during May. As previously indicated, since the rate of photosynthesis simulated by the model is mainly driven by precipitation and air temperature, an increase in daily air temperature in conjunction with precipitation reduction expected for future period may have anticipated the period where the maximum physiological activity is usually observed, thus showing an highest NEE compared to the baseline during the early Spring. Similarly, the precipitation decrease

expected for summer months may have strongly influence the NEE during summer months. This was clearly observed over each one of the future scenarios. Indeed, a continuative decrease of precipitation coupled with the increase in temperature led to stomatal closure with the consequent reduction in C fixation and an increase in ecosystem respiration.

5.5. Conclusions

The development of tools able to predict C-sequestration capacity and C-fluxes dynamics from several ecosystem it is a fundamental field of research to cope with the current issue of climate change. Understanding and prediction of these parameters could be fundamental to assess the role that specific ecosystems may have in climate mitigation. In this context, our study has been focused on the calibration and validation of the biogeochemical model Daycent. This model was considered as one of the most suitable to assess the mitigative potential of a complex system such as olive orchard. Statistical analysis confirmed that Daycent was able at reproducing daily olive orchard NEE with a good accuracy ($r=0.5$ and $RMSE=1.93$ and $r=0.41$ and $RMSE=0.62$ g C m⁻² day⁻¹, for calibration and validation respectively) during the whole period of study. These results suggested that the model properly tuned for the two components of this system (i.e. tree and grass) can be used to simulate NEE dynamics from olive orchard and for estimating the influences of agronomic management, soil and climatic on GHG emissions from Mediterranean olive orchards. The results also suggested that for the selected future climate scenarios over the study area, the C-sequestration capacity of the olive orchard is expected to be reduced of 14.8, 26.6 and 36.3% for 2011-2030, 2046-2065 and 2080-2099 compared to the baseline scenario (1981-2010). Model calibration and validation reported in our study can be considered quite good to fully simulate the influence of climate conditions or the effects of tillage and other management operations on carbon cycle. However, given the still scarce knowledge on carbon fluxes dynamics in agro-ecosystems such as olive orchards, further studies should be conducted to assess the possibility of further improving the model performances through tuning or algorithms implementation, or with the aim to test the efficiency of new mitigation strategies.

Chapter 6

General discussion and conclusions



Chapter 6.

General discussion and conclusions

6.1. Main theme and questions

The main theme of this work was to assess the role that one of the most important fruit orchards (olive orchard) cultivated over Mediterranean area can play in climate mitigation. Starting with this aim that is in perfect line with the current issue of climate changes, this work followed a research path that has addressed 2 main questions:

- 1. Which is the current C-sequestration sequestration capacity provided by a typical Mediterranean olive orchard? How climate conditions and management can affect the C-sequestration capacity of this crop system?*
- 2. Can olive orchard system being modelled? Which are the current mathematical tools able to reproduce C-dynamics of this system?*

This final chapter gives a synthesis of all results reported into the chapters 3, 4 and 5 of this thesis, closing with broader thought about the contribute that olive orchard systems may play in climate mitigation and, based on our results, on the need of developing or improving mitigation strategies concerning this ecosystem to cope with climate change.

6.1.1. Role of olive orchards in C-sequestration capacity and influence of climate conditions and management.

Results reported in this thesis indicated that C-sequestration capacity of our olive orchard test was about 3.5 tC/ha yr⁻¹ on average, thus resulting almost comparable to forestry systems. This result, besides to indicate that this agro-system currently highly contributes to climate mitigation, also suggests the needs of a further development of mitigation strategies that take in account this agro-ecosystem especially over areas where climate change is particularly detrimental (i.e. Mediterranean basin) (Chapter 3). Moreover, during the 3 years of study the inter-year and intra-seasonal variability in climate conditions were observed to highly affect the magnitude and pattern of NEE. More specifically, whilst the magnitude of yearly NEE has been found highly correlated with annual rainfall regimes, spring rainfall resulted to be the main driver of NEE both for spring and summer (Chapter 3). This may be due to besides soil characteristics of the test

site, also for eco-physiology of the specie. Looking at future predictions, these systems might encounter consistent loss in C-sequestration capacity due a strong decrease in rainfall expected over Mediterranean basin in the next decades.

In addition to climate conditions, also management practices were observed to strongly influence the magnitude and pattern of NEE, particularly affecting the soil C-cycle. More specifically these practices through the removal of ground vegetation can cause a reduced carbon sequestration due to less quantity vegetation able to fix atmospheric carbon. Moreover, the conjunction between tillage practices and climate conditions can also influence soil respiration (Chapter 4). As described in section 4.4.1, indeed, "in periods with high temperatures and high water soil content, tillage can induce large carbon loss due to increased bacterial growth in the short-term. The higher bacterial activity increases oxidation of soil organic matter causing a loss of soil carbon and consequently a higher ecosystem respiration. On the other hand, when tillages are done in periods with low temperature, their influence on ecosystem respiration and maximum microbial activity is reduced".

6.1.2. Current status, calibration, validation and application of the most suitable tool able at reproducing C-fluxes from a complex system such as olive orchard.

Nowadays, development and application of tools able to predict C-fluxes from agricultural or natural ecosystem it is a fundamental field of research to cope with the issue of climate change. In particular the application of these tools can improve the understanding of the role that these systems can play in climate mitigation. These tools may have a different level of complexity and simulate processes such as whole-plant photosynthesis and heterotrophic/autotrophic respiration. The modified version of a simple parametric model C-Fix allowed to estimate daily GPP by separating the contribution of the autotrophic components dominating this ecosystem (trees and ground vegetation). Results confirmed that C-fix model was able to reproduce the GPP trend from the orchard and that the major discrepancies where observed for post-tillage periods. Being a model based on remote sensing, some of the limitations were related to the low resolution of satellite data that were not capable of separately resolving tree canopies and soil (Chapter 4). By contrast, the calibration and validation of the biogeochemical model Daycent allowed to overcome limitations or constraints typical of remote sensing models. More specifically the "savanna sub-model" contained into Daycent allowing for the interaction between the grassland/crop and forest subsystems through shading effects and nitrogen competition, it

allowed to deeply analyse the effect of agricultural practices and climate conditions on the whole C-cycle of the orchard as well as the single behaviour of the two autotrophic components (i.e. olive trees and grass) (Chapter 5). Statistical analysis confirmed that Daycent was able at reproducing daily olive orchard NEE with a good accuracy ($r=0.5$ and $RMSE=1.93$ and $r=0.41$ and $RMSE=0.62$ g C m⁻² day⁻¹, for calibration and validation respectively). The higher suitability of Daycent model compared to C-fix model, also considering the its ability to reproduce the soil C dynamics, suggests its use for testing the efficiency of new mitigation strategies or with the aim to evaluate predicted changes in mitigation capacity provided by this long term agro ecosystems in the next decades.

6.2. Conclusions

Several worldwide studies have analysed the magnitude that forests can provide in terms of C-sequestration capacity and, consequently, how these systems can contribute to climate change mitigation. By contrast, the role and contribution in climate mitigation played by crop systems such as orchards has often been neglected. These systems, indeed, have always been investigated for their economic importance (i.e. fruits production), whilst their long term carbon storage capacity in soil or woody compartments has not been taken into account.

The mid-term experiment (3 years) carried out on a typical Mediterranean olive orchard allowed a complete overview about the role that this system could play in climate mitigation. More specifically by integrating C-fluxes measures with short and long term meteorological analysis has been possible to assess the C-sequestration capacity provided by a typical Mediterranean olive orchard as well as evaluating how climate conditions and management can affect it. Results indicated that under current climate conditions olive orchard can be considered, on average, a carbon sink almost comparable to Italian forestry systems and therefore highly suitable for climate mitigation. The influence of climate and management highly affected the magnitude and pattern of C-sequestration capacity of the olive orchard. Despite changes in magnitude and pattern of C-sequestration were as higher as the time-scale was lower (i.e. from half-hour to monthly scale) they strongly affected the yearly C sequestration capacity. This aspect, therefore, should be retained fundamental in order to improve or develop new mitigation strategies involving olive orchard systems.

The major issue to obtain a more detailed overview about the role that olive orchard plays in climate mitigation is related to time and space limitations. Our work, indeed, was focused on the

assessment of the contribution provided from only one olive orchard (i.e. test site) through eddy covariance measurements that, as is known, are site-specific measurements challenging and expensive to obtain. For overcoming these limitations and obtaining the C-sequestration capacity of olive orchards at higher scale (i.e. from regional to global) as well as expected changes in C-sequestration over the next decades, olive orchard system modelling was retained to be needed. On these premises, two different tools were taken into account: the first one was a simple parametric model C-Fix that was modified and then applied to estimate daily GPP; the second was the biogeochemical model Daycent that was calibrated and validated to estimate daily NEE. Our results indicated that both models, once properly tuned, resulted to be suitable tools to assess C-fluxes from olive orchard systems.

This work, by providing a complete overview about the current contribution of C-sequestration capacity of a typical Mediterranean olive orchard and on the tools able to reproduce the behaviour of this system, it should be retained as an early step to enhance the knowledge about the role that olive orchard systems could play in climate mitigation. Moreover, the development of new mitigation strategies and climate policies concerning olive orchard systems as well as the improvement of those already existing should be increased. This aspect should be taken into account especially by those countries that lie over Mediterranean areas and where climate change is the main issue for agriculture and environment.

Chapter 7

References

- Adler, P.R., Del Grosso, S.J. and Parton, W.J. (2007). Life-Cycle Assessment of net greenhouse-gas flux for bioenergy cropping systems. *Ecological Applications* 17(3): 675-691.
- AGEA, Consorzio olivicolo italiano. (2010). Lo scenario economico di settore “Olivicoltura da olio”.
- Angassa A. and Oba, G. (2008). Effects Of Management And Time On Mechanisms Of Bush Encroachment In Southern Ethiopia. *African Journal Of Ecology* 46: 186-196 doi: 10.1111/J.1365-2028.2007.00832.X, ISSN: 1365-2028.
- Archer, S., Scifres, C.J., Bassham, C.R. and Maggio, R. (1988). Autogenic succession in a subtropical savanna: conversion of grassl and to thorn woodland. *Ecol. Monogr* 58:111-27.
- Artale, V., Calmanti, S., Carillo, A., Dell’Aquila, A., Herrmann, M., Pisacane, G., Ruti, P.M., Sannino, G., Struglia, M.V., Giorgi, F., Bi, X., Pal, J.S. and Rauscher, S. (2010). The Protheus Group. An atmosphere–ocean regional climate model for the Mediterranean area: assessment of a present climate simulation. *Clim. Dyn.*, 35: 721–740.
- Aubinet, M., Grelle, A., Ibrom, A., Rannik, U., Moncrieff, J., Foken, T., Kowalsk, I A.S., Martin, P.H., Berbigier, P., Bernhofer, C., Clement, R., Elbers, J., Granier, A., Grunvald, T., Morgenstern, K., Pilegaard, K., Rebmann, C., Snijders, W., Valentini, R. and Vesala, T. (2000). Estimates of the annual net carbon and water exchange of European forests: the EUROFLUX methodology. *Ecol. Res.* 30: 113-175.
- Baker, J.M. and Griffis, T.J. (2005). Examining strategies to improve the carbon balance of corn/soybean agriculture using eddy covariance and mass balance techniques. *Agric. For. Meteorol.* 128: 163–177.
- Baldocchi, D. and Meyers, T.D. (1988). A spectral and lag-correlation analysis of turbulence in a deciduous forest canopy. *Boundary-Layer Meteorology*, 45: 31-58.

- Baldocchi, D., Valentini, R. and Running, S. (1996). Strategies for measuring and modeling carbon dioxide and water vapour fluxes over terrestrial ecosystem. *Glob. Change Biology*, 2: 159–168, doi: 10.1111/j.1365-2486.1996.tb00069.x.
- Baldocchi, D.D., Vogel, C.A. and Hall, C. (1997). Seasonal variation of carbon dioxide exchange rates above and below a boreal jack pine forest. *Agricultural and Forest Meteorology* 01/1997; 83:147-170. doi: 10.1016/S0168-1923(96)02335-0.
- Baldocchi, D. (2003). Assessing the eddy covariance technique for evaluating carbon dioxide exchange rates of ecosystems: past, present and future. *Global Change Biology*, 9: 479-492.
- Baldocchi, D. (2005). *Advanced Topics in Biometeorology and Micrometeorology*. Lecture 2, pages 3-4.
- Bauer, M.E. (1975). The role of remote sensing in determining the distribution and yield of crops. *Advances in Agronomy*, 27: 271–304.
- Beach, R.H., Deangelo, B.J., Rose, S., Li, C., Salas, W. and Del Grosso, S.J. (2008). Mitigation potential and costs for global agricultural greenhouse gas emissions. *Agricultural Economics* Vol 38, Issue 2: 109-115.
- Behrenfeld, M. J., Randerson, J. T., McClain, C. R., Feldman, G. C., Los, S. O., Tucker, C. J., Falkowski, G.P., Field, B.C., Frouin, R., Esaias, E.W., Kolber, D.D. and Pollack, H.N. (2001). Biospheric primary production during an ENSO transition. *Science* 291: 2594–2597.
- Bennetzen, H.E., Smith, P., Soussana, J.F. and Porter, J.R. (2012). Identity-based estimation of greenhouse gas emissions from crop production: case study from Denmark. *European Journal Of Agronomy*, 41: 66–72.

- Bindi, M. and Olesen, J.E.(2011). The responses of agriculture in europe to climate change. *Reg Environ Change*, 11: S151–S158.
- Bongi, G. and Long, S.P. (1987). Light dependent damage to photosynthesis in olive trees during chilling and high temperatures stress, *Plant. Cell. Environment*, 14: 127-132, doi: 10.1111/1365-3040.ep11602267.
- Bouman, B.A.M. (1992). Linking physical remote sensing models with crop growth simulation models, applied for sugar beet. *Int. J. of Remote Sensing*, Vol. 13 (14), 1: 2565-2581.
- Boutton, T.W., Liao, J.D., Filley, T.R. and Archer, S.R. (2009). Belowground carbon storage and dynamics accompanying woody plant encoachment in a subtropical savanna. *SSSA Special Publications*. In: *Soil carbon sequestration and the greenhouse effect*. Soil Science Society Of America, Madison, WI, USA, pp.181–205.
- Brilli, L., Chiesi, M., Maselli, F., Moriondo, M., Gioli, B., Toscano, P., Zaldei, A., and Bindi, M. (2013). Simulation of olive grove gross primary production by the combination of ground and multi-sensor satellite data, *Int. J. Appl. Earth Obs. Geoinf.*, 23: 29–36, doi: 10.1016/j.jag.2012.11.006.
- Brilli, L., Moriondo, M., Ferrise, R., Dibari, C. and Bindi, M. (2014). Climate change and Mediterranean crops: 2003 and 2012, two possible examples of the near future. *Agrochimica*, Vol. LVIII – Special Issue.
- Brilli, L., Gioli, B., Toscano, P., Moriondo, M., Zaldei, A., Cantini, C. and Bindi, M. Effects of inter annual and inter-seasonal variability in rainfall regimes on C-exchanges of a rainfed Olive orchard. (forthcoming).
- Budyko, M. I. (1974). *Climate and Life*. 508 pp., Academic Press, New York, 1974.

- Burba, G. (2013). *Eddy Covariance Method for Scientific, Industrial, Agricultural, and Regulatory Applications: A Field Book on Measuring Ecosystem Gas Exchange and Areal Emission Rates*. LI-COR Biosciences, Lincoln, NE, USA, 331 pp.
- Burgess, T.L. (1995). Desert grassland, mixed shrub savanna, shrub steppe, or semidesert scrub? the dilemma of coexisting growth forms. In *The Desert Grasslands*, Ed. MP Mcclaran, TR Van De Vender, pp. 31-67. Tucson: Univ. Ariz. Press.
- Canadell, J.G., Mooney, H.A., Baldocchi, D.D., Berry, J.A., Ehleringer, J.R., Field, C.B., Gower, S.T., Hollinger, D.Y., Hunt, J.E., Jackson, R.B., Running, S.W., Shaver, G.R., Steffen, W., Trumbore, S.E., Valentini, R. and Bond, B.Y. (2000). Carbon metabolism of the terrestrial biosphere: a multi-technique approach for improved understanding. *Ecosystems*, 3: 115-130.
- Castro, J., Fernández-Ondoño, E., Rodríguez, C., Lallena, A.M., Sierra, M. and Aguilar, J. (2008). Effects of different olive-grove management systems on the organic carbon and nitrogen content of the soil in Jaén (Spain), *Soil Till. Res.*, 98: 56-67, doi: 10.1016/j.still.2007.10.002.
- Cavallero, A. and Ciotti, A. (1991). Aspetti agronomici dell'utilizzazione dei prati e dei pascoli. *Riv. di Agron.* 25: 2, 81-126.
- Chaves, M.M., Pereira, J.S., Maroco, J., Rodrigues, M.L., Ricardo, C.P.P., Osorio, M.L., Carvalho, I., Faria, T. and Pinheiro, C. (2002). How plants cope with water stress in the field. Photosynthesis and growth. *Ann. Bot.*, 89,907-916, doi: 10.1093/aob/mcf105.
- Chiesi, M., Fibbi, L., Genesio, L., Gioli, B., Magno, R., Maselli, F., Moriondo, M. and Vaccari, F.P. (2011). Integration of ground and satellite data to model Mediterranean forest processes. *Int. J. Appl. Earth Observ. Geoinform.* 13: 504-515.

- Chmielewski, F.M., Müller, A. and Bruns, E. (2004). Climate changes and trends in phenology of fruit trees and field crops in Germany, 1961–2000. *Agricultural and Forest Meteorology*, 121:69–78.
- Cole, M.M. (1986). *The savannas: Biogeography and geobotany*. Orlando, FL: Academic.
- Conant, R.T., Paustian, K., Del Grosso, S.J. and Parton, W.J. (2005). Nitrogen pools and fluxes in grassland soils sequestering carbon. *Nutrient Cycling in Agroecosystems*, 71: 239-248.
- Conese, C. and Maselli, F. (1992). Use of error matrices to improve area estimates with maximum likelihood classification procedures. *Remote Sens. Environ.* 40: 113-124.
- Connor, J.D. (2005). Adaptation of olive (*Olea europaea* L.) to water-limited environments. *Aust. J. of Agric. Res.*, 56: 1181–1189.
- Davis, A.S., Cousens, R.D., Hill, J.H., Mack, R.N., Simberloff, D. and Raghu, S. (2010). Screening bioenergy feedstock crops to mitigate invasion risk *Front. Ecol. Environ.* 8 533–9.
- De Graaff, J. and Eppink, L.A.A.J. (1999). Olive oil production and soil conservation in southern Spain, in relation to EU subsidy policies. *Land Use Policy*, 16: 259–267, doi: 10.1016/S0264-8377(99)00022-8.
- De Marco, A., Meola, A., Esposito, F. and Virzo De Santo, A. (2008). Productivity and modifications of ecosystem processes in gaps of a low Macchia in southern Italy. *Web Ecol.* 8: 55–66.
- Del Grosso, S.J., Parton, W.J., Mosier, A.R., Hartman, M.D., Brenner, J., Ojima, D.S. and Schimel, D.S. (2001). Simulated interaction of carbon dynamics and nitrogen trace gas fluxes using the DAYCENT model. In: M. Schaffer, M. L. Ma, L. S. Hansen, S. (Eds.), *Modeling Carbon and Nitrogen Dynamics for Soil Management*. CRC Press, Boca Raton, Florida, pp. 303-332.

- Del Grosso, S.J., Parton, W.J., Mosier, A.R., Hartman, M.D., Keough, C.A., Peterson, G.A., Ojima, D.S. and Schimel, D.S. (2001b). Simulated effects of land use, soil texture, and precipitation on N gas emissions using DAYCENT. In: R.F. Follett, R.F., Hatfield, J.L. (Eds.), Nitrogen in the Environment: Sources, Problems, and Management. Elsevier Science Publishers, The Netherlands, pp. 413-431.
- Del Grosso, S.J., Ojima, D.S., Parton, W.J., Mosier, A.R., Peterson, G.A. and Schimel, D.S. (2002). Simulated effects of dryland cropping intensification on soil organic matter and greenhouse gas exchanges using the DAYCENT ecosystem model. *Environ. Pollut.* 116: S75-S83.
- Del Grosso, S.J., Mosier, A.R., Parton, W.J. and Ojima, D.S. (2005). DAYCENT model analysis of past and contemporary soil N₂O and net greenhouse gas flux for major crops in the USA. *Soil Tillage and Research* 83: 9-24, doi:10.1016/j.still.2005.02.007.
- Del Grosso, S.J., Parton, W., Mosier, A.R., Walsh, M.K., Ojima, D. and Thornton, P.E. (2006). DAYCENT national scale simulations of N₂O emissions from cropped soils in the usa. *Journal of Environmental Quality*. 35: 1451-1460.
- Del Grosso, S.J., Ogle, S., Wirth, J. and Skiles, S. (2008). U.S. Agriculture and Forestry Greenhouse Gas Inventory: 1990-2005. United States Department of Agriculture Technical Bulletin 1921.
- Del Grosso, S.J., Ogle, S., Wirth, S. and Skiles, S. (2008). Chapter 2: Livestock and grazed land emissions. U.S. Agriculture and Forestry Greenhouse Gas Inventory: 1990-2005. Technical bulletin 1921. United States Department of Agriculture Technical Bulletin 1921.
- Del Grosso, S.J., Ojima, D.S., Parton, W.J., Stehfest, E., Heistemann, M., DeAngelo, B. and Rose, S. (2009). Global Scale DAYCENT Model Analysis of Greenhouse Gas Mitigation Strategies for Cropped Soils. *Global and Planetary Change*, 67: 44-50.

- Del Grosso, S.J., Ogle, S.M., Parton, W.J. and Breidt, F.J. (2010). Estimating Uncertainty in N₂O Emissions from US Cropland Soils. *Global Biogeochemical Cycles* Vol. 24: GB1009, 12 pp, doi:10.1029/2009GB003544.
- Del Grosso, S.J., Parton, W.J., Keough, C.A. and Reyes-Fox, M. (2011). Special features of the Daycent modeling package and additional procedures for parameterization, calibration, validation, and applications. *Methods of introducing system models into agricultural research*. Published by: American Society of Agronomy, Crop Science Society of America, Soil Science Society of America.
- Del Río, S., Herrero, L., Pinto-Gomes, C. and Penas, A. (2011). Spatial analysis of mean temperature trends in Spain over the period 1961–2006. *Global And Planetary Change* 79: 65–75, doi: 10.1016/j.gloplacha.2011.05.012.
- Denman, K.L., Brasseur, G., Chidthaisong, A., Ciais, P., Cox, P.M., Dickinson, R.E., Hauglustaine, D., Heinze, C., Holland, E., Jacob, D., Lohmann, U., Ramachandran, S., Da Silva Dias, P.L., Wofsy, S.C. and Zhang, X. (2007). Couplings between changes in the climate system and biogeochemistry. In: Solomon, S., Qin, D., Manning, M., Chen, Z., Marquis, M., Averyt, K.B., Tignor, M. and Miller H.L. (Ed.). *Climate Change 2007: The Physical Science Basis. Contribution Of Working Group I To The Fourth Assessment Report Of The Intergovernmental Panel On Climate Change*. Cambridge University Press, Cambridge, United Kingdom And New York, NY, USA.
- Denney, J.O. and McEachern, R. (1983). An analysis of several climatic temperature variables dealing with olive reproduction. *J. Am. Soc. Hort. Sci.* 108 (4): 578–581.
- Dichio, B., Xiloyannis, C., Sofo, A. and Montanaro, G. (2005). Osmotic regulation in leaves and roots of olive trees during a water deficit and rewatering. *Tree physiology* 26: 179-185, doi: 10.1093/treephys/26.2.179.

- Dickie, A., Streck, C., Roe, S., Zurek, M., Haupt, F. and Dolginow, A. (2014). “Strategies for mitigating climate change in agriculture: Abridged Report.” Climate Focus And California Environmental Associates, Prepared With The Support Of The Climate And Land Use Alliance. Report And Supplementary Materials Available At: www.Agriculturalmitigation.Org.
- Durao, R.M., Pereira, M.J., Costa, A., Delgado, J., Del Barrio, G. and Soares A. (2010). Spatial-temporal dynamics of rainfall extremes in southern Portugal: a geostatistical assessment study. *Int. J. Climatol.*, 30: 1526–1537, doi: 10.1002/joc.1999.
- Dyer, A.R. and Rice, K.J. (1999). Effects of competition on resource availability and growth in a native bunchgrass in two California grasslands. *Ecol.* 80: 2697-2710.
- EPA (2010). Carbon Content Coefficients Developed for EPA's Mandatory Reporting Rule. Office of Air and Radiation, Office of Atmospheric Programs, U.S. Environmental Protection Agency, Washington, D.C.
- Falge, E., Baldocchi, D., Tenhunen, J., Aubinet, M., Bakwin, P., Berbigier, P., Bernhofer, C., Burba, G., Clement, R., Davis, K. J., Elbers, J. A., Goldstein, A. H., Grelle, A., Granier, A., Guomundsson, J., Hollinger, D., Kowalski, A.S., Katul, G., Law, B.E., Malhi, Y., Meyers, T. and Monso, R.K. (2002a). Seasonality of ecosystem respiration and gross primary production as derived from FLUXNET measurements. *Agricultural and Forest Meteorology*, 113(1-4): 53-74.
- Falge, E., J. Tenhunen, D. Baldocchi, M. Aubinet, P. Bakwin, P. Berbigier, C. Bernhofer, J. M. Bonnefond, G. Burba, R. Clement, K. J. Davis, J. A. Elbers, M. Falk, A. H. Goldstein, A. Grelle, A. Granier, T. Grunwald, J. Gudmundsson, D. Hollinger, Janssens, I.A. and Keronen, P. (2002b). “Phase and amplitude of ecosystem carbon release and uptake potentials as derived from FLUXNET measurements”. *Agricultural and Forest Meteorology*, 113 (1-4): 75-95.

- FAO/IIASA/ISRIC/ISS-CAS/JRC (2009). Harmonized World Soil Database (version 1.1). FAO, Rome, Italy and IIASA, Laxenburg, Austria.
- FAOSTAT (2013). FAO statistical databases. Agriculture data collection (crops).
- Fereres, E. and Goldhamer, D.A. (1990). Deciduous fruit and nut trees. In: Stewart BA, Nielsen DR (eds). Irrigation of agricultural crops, vol 30. ASA, Madison, pp 987–1017.
- Fereres, E., Ruz, C., Castro, J., Gómez, J.A. and Pastor, M. (1996). Recuperación del olivo después de una sequía extrema. Proceedings of the XIV. Congreso Nacional de Riegos, Aguadulce (Almería), 11–13 June, 1996, pp. 89–93.
- Fiorino, P. (2003). Olea. Trattato di olivicoltura. – Il sole 24 ore Edagricole (Ed.), Roma, 2003.
- Fisher, A.C., Hanemann, W.M., Roberts, M.J. and Schlenker, W. (2012). The economic impacts of climate change: evidence from agricultural output and random fluctuations in weather: Comment. *The American Economic Review*, 102: 3749-3760.
- Fitzpatrick, B.T., Hill, G.J.E. and Kelly, G.D. (1990). Mapping and monitoring of weed infestations using satellite remote sensing data. In Proceedings 5th Australasian Remote Sensing Conference, Perth, Western Australia, 8th-12th October 1990, pp. 598-601.
- Fleskens, L., Duarte, F., and Eicher, I. (2008). A conceptual framework for the assessment of multiple functions of agro-ecosystems: A case study of Trás-os-Montes olive groves. *Journal of Rural Studies*. 25(1), 141–155.
- Foken, T. and Wichura, B. (1996). Tools for quality assessment of surface-based flux measurements. *Agric. For. Meteorol.*, 78: 83-105.
- Foken, T., Gockede, M., Mauder, M., Mahrt, L., Amiro, B.D. and Munger, J.W. (2004). Post-field data quality control. In: Lee, X. (Ed.), *Handbook of Micrometeorology: A Guide for Surface Flux Measurements*. Kluwer Academic Publishers, Dordrecht, pp. 81–108.

- Giorgi, F. and Lionello, P. (2008). Climate change projections for the Mediterranean region. *Global Plant Change*, 63: 90-104.
- Gitelson, A.A., Gritz, Y. and Merzlyak, M.N. (2003). Relationships between leaf chlorophyll content and spectral reflectance and algorithms for non-destructive chlorophyll assessment in higher plant leaves. *J. Plant Physiol.* 160: 271-282.
- Gómez, A.J., Sobrinho, T.A., Giráldez, J.V., and Fereres, E. (2009). Soil management effects on runoff, erosion and soil properties in an olive grove of Southern Spain. *Soil and Tillage Research*, 102: 5-13, doi: 10.1016/j.still.2008.05.005.
- Grossoni, P., and Gellini, R. (1997). *Botanica Forestale*. Vol II. Cedam (ed), Roma.
- Gucci, R. (1998). Assimilazione e ripartizione del carbonio in foglie di olivo. *Frutticoltura*, 7-8, 77-82.
- Haylock, M.R., Hofstra, N., Klein Tank, A.M.G., Klok, E.J., Jones, P.D. and New, M. (2008). A European daily high-resolution gridded data set of surface temperature and rainfall for 1950–2006. *Journal Of Geophysical Research* 113: D20119, doi: 10.1029/2008JD010201.
- Hsieh, C.I., Katul, G.G. and Chi, T.W. (2000). An approximate analytical model for footprint estimation of scalar fluxes in thermally stratified atmospheric flows. *Advances in Water Resources*, 23: 765-772, doi: 10.1016/S0309-1708(99)00042-1.
- Hughes, R.F., Archer, S.R., Asner, G.P., Wessman, C.A., Mcmurtry, C., Nelson, J. and Ansley, R.J. (2006). Changes in aboveground primary production and carbon and nitrogen pools accompanying woody plant encroachment in a temperate savanna. *Global Change Biology*, 12:1733–1747, doi: 10.1111/J.13652486.2006.01210.X, ISSN: 1365-2486.
- IPCC 2007. (2007). *Climate Change 2007: The Physical Science Basis*. Contribution of working group I to the fourth assessment report of the intergovernmental panel on climate change (Cambridge: Cambridge University Press) pp. 996.

IPCC, 2013. Climate Change 2013: The Physical Science Basis. 2013.

Iraldo, F., Testa, F. and Bartolozzi, I. (2013). An application of Life Cycle Assessment (LCA) as a green marketing tool for agricultural products: the case of extra-virgin olive oil in Val di Cornia, Italy. *Journal of Environmental Planning and Management*, 57 (1): 78-103, doi:10.1080/09640568.2012.735991.

IRPET (2011). Rapporto sul sistema rurale toscano. Economia, politiche, filiere e produzioni di qualità.

ISTAT 2010. (Italian National Institute of Statistics) (2010) 6th National Agricultural Census (<http://www.istat.it/en/agricultural-census>).

ISTAT (2011). Italian National Institute for Statistics.

Jackson, R.D. (1983). Spectral indices in n- space. *Remote Sens. Environ.* 13: 409-421.

Jacob, D. and Podzun, R. (2010). Global warming below 2°C relative to pre-industrial level: how might climate look like in Europe. *Nova Acta Leopoldina*, NF: 71-76.

Janicka, M. (2005). Re-growth of original sward following meadow renovation by the over drilling- central Poland. *Grassland Sci. Eur.* 10: 625-629.

Jia, X., Zha, T. S., Wu, B., Zhang, Y. Q., Gong, J. N., Qin, S. G., Chen, G. P., Kellomäki, S. and Peltola, H. (2014). Biophysical controls on net ecosystem CO₂ exchange over a semiarid shrubland in northwest China. *Biogeosciences Discuss.*, 11: 5089–5122, doi:10.5194/bgd-11-5089.

Johnson, R.W. and Tothill, J.C. (1985). Definition and broad geographic outline of savanna lands. in *ecology and management of the world's savannas*. (Ed. JC Tothill, JJ Mott, pp. 1-13). Canberra, ACT: Aust. Acad. Sci.

- Joseph, S., Laake P.E., Thomas, A.P. and Eklundh, L. (2012). Comparison of carbon assimilation estimates over tropical forest types in India based on different satellite and climate data products. *Int. J. Appl. Earth Observ. Geoinform.* 18: 557-563.
- Kaimal, J.C. and Finnigan, J.J. (1994). *Atmospheric boundary layer flows: their structure and measurement.* Oxford University Press, Oxford, UK. 289 pp.
- Keenan, T.F., Baker, I., Barr, A., Ciais, P., Davis, K.J., Dietze, M., Dragon, D., Gough, C.M., Grant, R., Hollinger, D.Y., Hufkens, K., Poulter, B., McCaughey, H., Raczka, B.M., Ryu, Y., Schaefer, K., Tian, H., Verbeeck, H., Zhao, M. and Richardson, A.D. (2012). Terrestrial biosphere model performance for inter-annual variability of land-atmosphere CO₂ exchange. *Global Change Biol.* 18: 1971-1987.
- Kelly, P. M. (2000). Towards a Sustainable Response to Climate Change. In Huxham, M. and Sumner, D. (eds.), *Science and Environmental Decision-Making*, Pearson Education, Harlow, pp. 118–141.
- Kjellström, E., Nikulin, G., Hansson, U., Strandberg, G. and Ullerstig, A. (2011). 21st century changes in the European climate: uncertainties derived from an ensemble of regional climate model simulations. *Special Issue On Regional Climate Studies Using The Smhi-Rosby Centre Models* 63, 24–40, doi: 10.1111/j.1600-0870.2010.00475.x.
- Knipling, E.B. (1970). Physical and physiological basis for the reflectance of visible and infrared radiation from vegetation. *Rem. Sens. Env.* 1(3): 155-159.
- Kotchenova, S.Y., Song, X., Shabanov, N.V., Potter, C.S., Knyazikhin, Y. and Myneni, R.B. (2004). Lidar remote sensing for modelling net primary productivity of deciduous forests. *Remote Sens. Environ.* 92: 158-172.
- Kumar, M. and Monteith, J.L. (1981). Remote sensing of crop growth. In: H. Smith (ed.). *Plants and the daylight spectrum.* Academic Press, San Diego, California. pp. 133-144.

- Kwon, H., Pendall, E., Ewers, B.E., Cleary, M., and Naithani, K. (2008). Spring drought regulates summer net ecosystem CO₂ exchange in a sagebrush-steppe ecosystem. *Agr. For. Met.*, 148, 381-391, doi: 10.1016/j.agrformet.2007.09.010.
- Lamb, D.W. (1998). Opportunities for satellite and airborne remote sensing of weeds in Australian crops. In: Medd, R.W. & Pratley, J.E. (eds.). *Precision weed management in crops and pastures*. CRC for Weed Management Systems, Adelaide, Australia. pp. 48-54.
- Lee, X., Massman, W. and Law, B.E. (2004). *Handbook of micrometeorology. A guide for surface flux measurement and analysis*. Kluwer Academic Press, Dordrecht, 250 pp.
- Lenderink, G. and Van Meijgaard, E. (2008). Increase in hourly rainfall extremes beyond expectations from temperature changes. *Nature Geoscience*, 1: 511-514, doi:10.1038/ngeo262.
- Liao, J.D., Boutton, T.W. and Jastrow, J.D. (2006). Storage and dynamics of carbon and nitrogen. In: soil physical fractions following woody plant invasion of grassland. *Soil Biology And Biochemistry*, 38: 3184-3196 doi: 10.1016/J.Soilbio.2006.04.003, ISSN: 00380717.
- Liguori, G., Gugliuzza, G., and Inglese, P. (2009). Evaluating carbon fluxes in orange orchards in relation to planting density. *J. Agr. Sci.* 147: 637-645, doi: <http://dx.doi.org/10.1017/S002185960900882X>.
- Lloyd, J. and Taylor, J.A. (1994). On the temperature dependence of soil respiration. *Funct. Ecol.* 8: 315-323.
- Lomou, A. and Giourga, C. (2003). Olive groves: The life and identity of the Mediterranean. *Agriculture and Human Values*, 20: 87-95.

- Lotze-Campen, H., Müller, C., Bondeau, A., Jachner, A., Popp, A. and Lucht, W. (2008). Food demand, productivity growth and the spatial distribution of land and water use: a global modelling approach. *Agricultural Economics* 39: 325–338.
- Lotze-Campen, H., Popp, A., Beringer, T., Müller, C., Bondeau, A., Rost, S. and Lucht, W. (2010). Scenarios of global bioenergy production: the trade-offs between agricultural expansion, intensification and trade. *Ecol. Model.*, 221: 2188–2196, doi:10.1016/j.ecolmodel.2009.10.002.
- Loumou, A. and Giourga, C. (2003). Olive groves: The life and identity of the Mediterranean. *Agric. Human Values* 20: 87–95.
- Lunt, I.D., Winsemius, L.M., Mcdonald, S.P., Morgan, J.W. and Dehaan, R.L. (2010). How widespread is woody plant encroachment in temperate Australia? changes in woody vegetation cover in lowland woodland and coastal ecosystems in Victoria from 1989 to 2005. *Journal Of Biogeography*, 37: 722–732, doi: 10.1111/J.1365-2699.2009.02255.X, ISSN: 1365-2699.
- Luo, H., Oechel, W.C., Hastings, S.J., Zulueta, R., Qian, Y. and Kwon, H. (2007). Mature semiarid chaparral ecosystems can be a significant sink for atmospheric carbon dioxide. *Global Change Biology*, 13: 386-396, doi:10.1111/j.1365- 2486.2006.01299.x7.
- Ma, S., Baldocchi, D.D., Xu, L., and Hehn, T. (2008). Inter-annual variability in carbon dioxide exchange of an oak/grass savanna and open grassland in California. *Agr. For. Met.*, 147: 157–171, doi: 10.1016/j.agrformet.2007.07.008.
- Maselli, F. (2001). Definition of spatially variable spectral end-members by locally calibrated multivariate regression analyses. *Remote Sens. Environ.* 75: 29-38.
- Maselli, F., Chiesi, M., Fibbi, L., and Moriondo, M. (2008). Integration of remote sensing and ecosystem modelling techniques to estimate forest net carbon uptake. *Int. J. Remote Sens.*, 29(8), 2437-2443.

- Maselli, F., Papale, D., Puletti, N., Chirici, G. and Corona, P. (2009). Combining remote sensing and ancillary data to monitor the gross productivity of water-limited forest ecosystems. *Remote Sens. Environ.* 113: 657-667.
- Maselli, F., Chiesi, M., Brilli, L., and Moriondo, M. (2012a). Simulation of olive yield in Tuscany through the integration of remote sensing and ground data. *Ecol. Model.* 244: 1–12, doi: 10.1016/j.ecolmodel.2012.06.028.
- Maselli, F., Argenti, G., Chiesi, M., Angeli, L. and Papale, D. (2013). Simulation of grassland productivity by the combination of ground and satellite data. *Agr. Ecos. Environ.*, vol. 165: 163-172, doi: ISSN:0167-8809.
- Massman, W.J. and Lee, X. (2002). Eddy covariance flux corrections and uncertainties in long-term studies of carbon and energy exchanges. *Agricultural and Forest Meteorology*, 113(1-4): 121-144.
- Matese, A., Gioli, B., Vaccari, F.P., Zaldei, A. and Miglietta, F. (2009). Carbon dioxide emissions of the city center of Firenze, Italy: measurement, evaluation, and source partitioning. *Journal of Applied Meteorology and Climatology*, 48(9): 1940-1947, doi: <http://dx.doi.org/10.1175/2009JAMC1945.1>.
- Matteucci, G. and Scarascia Mugnozza, G. (2007). Ecosistemi forestali e mitigazione dei cambiamenti ambientali: sequestro di carbonio in foreste italiane. In: *Clima e cambiamenti climatici: le attività di ricerca del CNR*. (Carli B., Cavarretta G., Colacino M., Fuzzi S., eds.) ISBN 978-88-8080-075-0, pp. 709-712.
- Medrano, H., Flexas, J. and Galmés, J. (2009). Variability in water use efficiency at the leaf level among Mediterranean plants with different growth forms. *Plant Soil* 317:17–29, doi: 10.1007/s11104-008-9785-z.

- Menaut, J.C., Gignoux, J., Prado, C. and Clober, J. (1990). Tree community dynamics in a humid savanna of the Cote d' Ivoire: modelling the effects of fire and competition with grass and neighbors. *J. Biogeogr.*, 17: 471-81.
- MIPAAF. (2010). Ministero delle politiche agricole e culturali.
- Moncrieff, J., Massheder, J.M., de Bruin, H., Elbers, J., Friborg, T., Heusinkveld, B., Kabat, P., Scott, S., Soegaard, H. and Verhoef, A. (1997). A system to measure surface fluxes of momentum, sensible heat, water vapour and carbon dioxide. *Journal of Hydrology*, 188-189, 589-611, doi: 10.1016/S0022-1694(96)03194-0.
- Montania, C. (1992). The colonization of bare areas in two-phase mosaics of an arid ecosystem. *J. Ecol.*, 80: 315-27.
- Morgan, J.A., Mosier, A.R., Milchunas, D.G., LeCain, D.R., Nelson, J.A. and Parton, W.J. (2004). CO₂ enhances productivity of the shortgrass steppe, alters species composition, and reduces forage digestibility. *Ecological Applications* 14: 208-219.
- Moriondo, M., Stefanini, F.M. and Bindi, M. (2008). Reproduction of olive tree habitat suitability for global change impact assessment. *Ecol. Model.* 218: 95-109.
- Myneni, R.B. and Williams D.L. (1994). On the relationship between FAPAR and NDVI. *Remote Sensing of Environment*, 49: 200-211.
- Nakićenović, N. and Swart, R. (2000). Special report on emissions scenarios. Cambridge University Press, Cambridge, pp. 599.
- Nardino, M., Pernice, F., Rossi, F., Georgiadis, T., Facini, O., Motisi, A. and Drago, A. (2013). Annual and monthly carbon balance in an intensively managed Mediterranean olive orchard. *Photosynthetica* 51, 63-74.

- Nieto, O.M., Castro, J., Fernández, E. and Smith, P. (2010). Simulation of soil organic carbon stocks in a Mediterranean olive grove under different soil-management systems using the RothC model. *Soil Use and Management* 26 (2): 118–125, doi: 10.1111/j.1475-2743.2010.00265.x.
- Nitsch, B., Kemmesies, O. and Graeber, P.W. (2013). Groundwater recharge balancing under the conditions of climatic changes. Available at http://tudresden.de/die_tu_dresden/fakultaeten/fakultaet_forst_geo_und_hydrowissenschaften/fachrichtung_wasserwesen/iaa/systemanalyse/publikationen/Nitsch%20Jaipur08.pdf (accessed Dec 11, 2013).
- Noy-Meir, I. (1973). Desert ecosystems: environment and producers. *Annual Review of Ecology and Systematics*, 4, 25-51, doi:10.1146/annurev.es.04.110173.000325.
- Olesen J.E., Trnka M., Kersebaum K.C., Skjelvåg A.O., Seguin B., Peltonen-Osmond, B., Ananyev, G., Berry J.A., Langdon, C., Kolber, Z., Lin, G., Monson, R., Nichol, C., Rascher, U., Schurr, U., Smith, S. and Yakir, D. (2004). Changing the way we think about global change research: scaling up in experimental ecosystem science. *Global Change Biol.* 10: 393-407.
- Palese, A. M., Nuzzo, V., Dichio, B., Celano, G., Romano, M. and Xiloyannis, C (2000). The influence of soil water content on root density in young olive trees. *Acta Horticulturae*, 537: 329–336.
- Palese, A.M., Pergola, M., Favia, M., Xiloyannis, C. and Celano, G. (2013). A sustainable model for the management of olive orchards located in semi-arid marginal areas: Some remarks and indications for policy makers. *Environmental Science & Policy*, 27, 81–90, doi: 10.1016/j.envsci.2012.11.001.
- Parsons, A.J. (1988). The effect of season and management on the growth of temperate grass swards. In: Jones M.B. and Lazenby A. (eds.) *The Grass Crop – the Physiological Basis of Production*. pp. 129–177. Chapman and Hall, London.

- Parton W. J., Schimel D. S., Cole C. V. and Ojima D. S. (1987) Analysis of factors controlling soil organic matter levels in great plains grasslands. *Soil Science Society of America Journal* 51: 1173-1 179.
- Parton, W.J., Hartman, M.D., Ojima, D.S. and Schimel, D.S. (1998). DAYCENT: Its land surface submodel: description and testing. *Glob. Planet. Chang.* 19: 35-48.
- Parton, W.J., Holland, E.A., Del Grosso, S.J., Hartman, M.D., Martin, R.E., Mosier, A.R., Ojima and D.S. Schimel, D.S. (2001). Generalized model for NO_x and N₂O emissions from soils. *J. Geophys. Res.* 106 (D15): 17403-17420.
- Paustian, K., Babcock, B.A., Hatfield, J., Lal, R., Mccarl, B.A., Mclaughlin, S., Mosier, A., Rice, C., Robertson, G.P., Rosenberg, N.J., Rosenzweig, C., Schlesinger, W.H. and Zilberman, D. (2004). Agricultural mitigation of greenhouse gases: science and policy options. CAST (Council On Agricultural Science And Technology) Report, 120 pp.
- Pavel, E.W. and Fereres, E. (1998). Low soil temperatures induce water deficit in olive (*Olea Europaea*) trees. *Physiologia Plantarum*, 104: 525-532, doi: 10.1034/j.1399-3054.1998.1040402.x.
- Peacock, J.M. (1976). Temperature and leaf growth in four grass species. *J. of Appl. Ecol.* 13: 225-232.
- Pepper, D.A., Del Grosso, S.J., McMurtrie, R.E. and W.J. Parton. (2005). Simulated carbon sink response of shortgrass steppe, tallgrass prairie and forest ecosystems to rising CO₂, temperature and nitrogen input. *Global Biogeochem. Cycles* 19:GB1004. doi:10.1029/2004GB002226.
- Pinter, P.J., Hatfield, J.L., Schepers, J.S., Barnes, E.M., Moran, M.S., Daughtry, C.S.T. and Upchurch, D.R. (2003). Remote Sensing for Crop Management. *Photogrammetric Engineering and Remote Sensing* Vol. 69(6): 647–664.

- Pope, V.D., Gallani, M.L., Rowntree, P.R. and Stratton, R.A. (2000). The impact of new physical parameterizations in the Hadley Centre climate model: HadAM3. *Clim Dyn.* 16:123–146.
- Prince, S.D. (1990). High temporal frequency remote sensing of primary production using NOAA AVHRR. In: Steven, M.D., Clark J.A. (eds.), *Appl. Remote Sens. Agric.* pp. 169-183.
- Rallo, L. (1998). Frutification y production. In: D. Barranco, R. Fernandez-Escobar, and L. Rallo. (eds). *El cultivo del olivo*. Junta de Andalucía y Mundi-Prensa, Madrid, pp 112-144.
- Reichstein, M Tenhunen, J.D., Ourcival, J.M., Rambal, S., Dore, S. and Valentini, R. (2002a). Ecosystem respiration in two Mediterranean evergreen holm oak forests: drought effects and decomposition dynamics. *Functional Ecology*, 16, 27–39.
- Reichstein, M., Tenhunen, J.D., Roupsard, O., Ourcival, J.-M., Rambal, S., Miglietta, F., Peressotti, A., Pecchiari, M., Tirone, G. and Valentini, R. (2002b). Severe drought effects on ecosystem CO₂ and H₂O fluxes at three Mediterranean sites: revision of current hypothesis?. *Global Change Biology*, 8, 999–1017.
- Reichstein M., Falge E., Baldocchi D., Papale D., Aubinet M., Berbigier P., Bernhofer C., Buchmann N., Gilmanov T., Granier A., Grunwald T., Havrankova K., Ilvesniemi H., Dalibor J., Knohl A., Laurila T., Lohila A., Loustau D., Matteucci G., Meyer T., Miglietta F., Ourcival J.-M., Pumpanen J., Rambal S., Rotenberg E., Sanz M.J., Tenhunen J., Seufert G., Vaccari F., Vesala T. and Valentini R. (2005). On the separation of net ecosystem exchange into assimilation and ecosystem respiration: review and improved algorithm. *Global Change Biology* 11: 1–16, doi: 10.1111/j.1365-2486.2005.001002.x.
- Reicosky, D.C. (1997). Tillage-induced CO₂ emission from soil. *Nutrient Cycling in Agroecosystems* 49: 273-285.

- Reynolds, O. (1886). On the Theory of Lubrication and Its Application to Mr. Beauchamp Tower's Experiments, Including an Experimental Determination of the Viscosity of Olive Oil. *Philosophical Transactions of the Royal Society of London*
- Resco, V., Fischer, C., and Colinas, C. (2007). Climate change effects on Mediterranean forests and preventive measures. *New Forests*, 33: 29–40, doi 10.1007/s11056-006-9011-x, 2007.
- Robertson, G.P., Hamilton, S.K., Del Grosso, S.J. and Parton, W.J. (2010). Growing Plants for Fuel: Predicting Effects on Water, Soil, and the Atmosphere. In *Biofuels and Sustainability Reports*: Ecological Society of America.
- Robertson, G.P., Hamilton, S.K., Parton, W.J. and Del Grosso, S.J. (2011). The biogeochemistry of bioenergy landscapes: Carbon, nitrogen, and water considerations. *Ecological Applications* 21: 1005-1067.
- Rodda, J.C., Little, M.A., Harvey, J.E. and Mcsharry, P.E. (2010). A comparative study of the magnitude, frequency and distribution of intense rainfall in the United Kingdom. *International Journal of Climatology* 30: 1776-1783, doi: hdl:10101/npre.2009.3847.1.
- Rohde, R.F. and Hoffman, M.T. (2012). The historical ecology of namibian rangelands: vegetation change since 1876 in response to local and global drivers, *science of the total environment*, 416: 276– 288 doi: 10.1016/J.Scitotenv.2011.10.067, ISSN: 00489697.
- Rosset, M., Riedo, M., Grub, A., Geissmann, M. and Fuhrer, J. (1997). Seasonal variation in radiation and energy balances of permanent pastures at different altitudes. *Agric. For. Meteorol.* 86: 245–258.
- Ruimy, A. and Saugier, B. (1994). Methodology for the estimation of terrestrial net primary production from remotely sensed data. *J. Geophys. Res.* 99: 5263-5283.
- Running, S.W. (1999). A blueprint for improved global change monitoring of the terrestrial biosphere. *NASA Earth Observ.* 10: 8-11.

- Sainio P., Rossi F., Kozyra J. And Micale F. (2011). Impacts and adaptation of european crop production systems to climate change. *European Journal Of Agronomy*, 34: 96–112.
- San José, J.J., Farifias, M.R. and Rosales, J. (1991). Spatial patterns of trees and structuring factors in a trachypogon savanna of the orinoco llanos. *Biotropica*, 23:114-23.
- Sarmiento, G. (1984). *The ecology of neotropical savannas*. Cambridge, MA: Harvard Univ. Press. 235 pp.
- Scholes, R.J. and Archer, S. R. (1997). Tree grass interactions in savannas. *annual review of ecology and systematics*. Vol. 28 (1997), 517-544 url: <http://Www.Jstor.Org/Stable/2952503> .Accessed: 18/09/2013 05:15.
- Schroter, D., Cramer, W., Leemans, R., Prentice, I.C., Araujo, M.B., Arnell, N.W., Bondeau, A., Bugmann, H., Carter, T.R., Gracia, C.A., de la Vega-Leinert, A.C., Erhard, M., Ewert, F., Glendining, M., House, J.I., Kankaanpää, S., Klein, R.J., Lavorel, S., Lindner, M., Metzger, M.J., Meyer, J., Mitchell, T.D., Reginster, I., Rounsevell, M., Sabate, S., Sitch, S., Smith, B., Smith, J., Smith, P., Sykes, M.T., Thonicke, K., Thuiller, W., Tuck, G., Zaehle, S. and Zierl, B. (2005). Ecosystem service supply and vulnerability to global change in Europe. *Science*, 310: 1333–1337, doi: 10.1126/science.1115233.
- Schuepp, P.H., M.Y. Leclerc, J.I. Macpherson and Desjardins, R.L. (1990). Footprint Predictions of Scalar Fluxes from Analytical Solutions of the Diffusion Equation. *Boundary-Layer Meteorology*, 50: 355-373.
- Scott, R.L., Serrano-Ortiz, P., Domingo, F., Hamerlynck, E.P. and Kowalsky, A.S. (2012). Commonalities of carbon dioxide exchange in semiarid regions with monsoon and Mediterranean climates. *Journal of arid environments*, 84: 71-79, doi: 10.1016/j.jaridenv.2012.03.017.

- Seguin, B., Arrouays, D., Balesdent, J., Soussana, J.F., Bondeau, A., Smith, P., Zaehle, S., De Noblet, N. and Viovy, N. (2007). Moderating the impact of agriculture on climate. *Agricultural and Forest Meteorology*, 142: 278–287.
- Semenov, M. and Barrow, E.M. (1997). Use of a stochastic weather generator in the development of climate change scenarios. *Climate Change* 35: 397-414.
- Semenov, M. and Stratonovitch, P. (2010). Use of multi-model ensembles from global climate models for assessment of climate change impacts. *Clim Res.* 41:1–14(Scholes and Archer, 2013).
- Semenov, M.A. and Doblus-Reyes, F.J. (2007). Utility of dynamical seasonal forecasts in predicting crop yield. *Clim Res.* 34:71.
- Showengerdt, (2006). *Remote Sensing: Models and Methods for Image Processing*. Robert A. Schowengerdt Academic Press, pp 560.
- Sing, D. (2011). Generation and evaluation of gross primary productivity using Landsat data through blending with MODIS data. *Int. J. Appl. Earth Observ. Geoinform.* 13: 59-69.
- Smith, P., Martino, D., Cai, Z., Gwary, D., Janzen, H., Kumar, P., Mccarl, B., Ogle, S., O’Mara,, F., Rice, C., Scholes, B., Sirotenko, O., Howden, M., Mcallister, T., Pan, G., Romanenkov, V., Rose, S., Schneider, U., Towprayoon, S. and Wattenbach, M. (2007), “Agriculture”. In: B Metz, OR Davidson, PR Bosch, R Dave & LA Meyer (Ed). *Contribution Of Working Group Climate Change 2007: Mitigation Of Climate Change: Working Group III Contribution To The Fourth Assessment Report Of The IPCC*. Cambridge University Press, Cambridge, United Kingdom, pp. 497-540.
- Smith, P. and Olesen, J.E. (2010). Synergies between the mitigation of, and adaptation to, climate change in agriculture. *Journal Of Agricultural Science*, 148: 543-552.

- Sofo, A., Nuzzo, V., Palese, A.M., Xiloyannis, C., Celano, G., Zukowskyj, P. and Dichio, B. (2005). Net CO₂ storage in Mediterranean olive and peach orchards. *Horticultural Science* 107: 17–24, doi: 10.1016/j.scienta.2005.06.001.
- Sorrentino, G. (2001). Meccanismi fisiologici di recupero dal deficit idrico in Olivo. In: *Gestione dell'acqua e del territorio per un'olivicultura sostenibile*. (Napoli, 24 - 28 Settembre 2001).
- Stull, R.B. (1988). *An Introduction to Boundary Layer Meteorology*. Kluwer Acad. Publ., Dordrecht, Boston, London, pp. 666.
- Suyker, A.E., Verma, S.B., Burba, G.G. and Arkebauer, T.J. (2005). Gross primary production and ecosystem respiration of irrigated maize and irrigated soybean during a growing season. *Agric. For. Meteorol.* 131: 180-190.
- Swinbank, W.C. (1951). The measurement of vertical transfer of heat and water vapor by eddies in the lower atmosphere. *Journal of Meteorology*, 8: 135-145.
- Testi, L., Orgaz, F. and Villalobos, F. (2008). Carbon exchange and water use efficiency of growing irrigated olive orchard. *Environmental and experimental Botany*, 63: 168-177, doi: 10.1016/j.envexpbot.2007.11.006.
- Thorntwaite, C.W. (1948). An approach toward a rational classification of climate. *Geogr. Rev.*, 38, 55-94.
- Thornton, P.E., Running, S.W. and White, M.A. (1997). Generating surfaces of daily meteorological variables over large regions of complex terrain. *Journal of Hydrology*, 190: 214-251.
- Thornton, P.E. and Running, S.W. (1999). An improved algorithm for estimating incident daily solar radiation from measurements of temperature, humidity, and precipitation. *Agric. For. Meteorol.* 93: 211–228.

- Thornton, P.E., Hasenauer, H. and White, M.A. (2000). Simultaneous estimation of daily solar radiation and humidity from observed temperature and precipitation: an application over complex terrain in Austria. *Agricultural and Forest Meteorology*, 104: 255-271
- Throop, H.L. and Archer, S.R. (2008). Shrub (*Prosopis Velutina*) encroachment in a semidesert grassland: spatial-temporal changes in soil organic carbon and nitrogen pools. *Global Change Biology*, 14: 2420–2431 doi: 10.1111/J.1365 2486.2008.01650.X, ISSN: 1365-2486.
- Tongway, D.J. and Ludwig, J.A. (1990). Vegetation and soil patterning in semi-arid mulga lands of eastern Australia. *Aust. J. Ecol.* 15: 23-34.
- Tucker, C.J. (1979). Red and Photographic Infrared Linear Combinations for Monitoring Vegetation. *Remote Sensing of Environment*, 8(2):127-150.
- USDA-NRCS (2004). Soil Data Mart. United States Department of Agriculture, Natural Resources Conservation Service (<http://soildatamart.nrcs.usda.gov>).
- Valentini, R., Matteucci, G. and Dolmann, A.J. (2000). Respiration as the main determinant of carbon balance in European forests. *Nature*, 404: 861-865.
- Valentini, R., Matteucci, G., Dolman, A.J., Schulze, E.D., Rebmann, C., Moors, E. J., Granier, A., Gross, P., Jensen, N.O., Pilegaard, K., Lindroth, A., Grelle, A., Bernhofer, C., Grünwald, T., Aubinet, M., Ceulemans, R., Kowalski, A.S., Vesala, T., Rannik, Ü., Berbigier, P., Loustau, D., Guethmundsson, J., Thorgeirsson, H., Ibrom, A., Morgenstern, K., Clement, R., Moncrieff, J., Montagnani, L., Minerbi, S. and Jarvis, P.G. (2000). Respiration as the main determinant of carbon balance in European forests. *Nature*, 404: 861-865, doi:10.1038/35009084.
- Valentini, R. (2003). Castelporziano Euroflux dataset - The Euroflux dataset 2000. In: Valentini R. (ed.) *Fluxes of C, Water and Energy of European Forests*. Ecological Studies 163. Springer Verlag, pp 270.

- Vautard, R., Yiou, P., D'andrea, F., De Noblet, N., Viovy, N., Cassou, C., Polcher, J., Ciais, P., Kageyama, M. and Fan, Y. (2007). Summertime European heat and drought waves induced by wintertime mediterranean rainfall deficit. *Geophys. Res. Lett.*, 34: L07711, doi: 10.1029/2006GL028001.
- Veenendal, E.M., Ernst, W.H.O.E. and Modise, G.S. (1996). Effect of seasonal rainfall pattern on seedling emergence and establishment of grasses in a savanna in south-eastern Botswana. *J. Arid Environ.* 32: 305-317.
- Veroustraete, F., Patyn, J. and Myneni, R.B. (1994). Forcing of a simple ecosystem model with fAPAR and climatic data to estimate regional scale photosynthetic assimilation. In: *Vegetation, Modelling and Climate Change Effects*, (eds.) Veroustraete, F. et al., Academic Publishing, The Hague, the Netherlands, 151-177.
- Veroustraete, F., Patyn, J. and Myneni, R.B. (1996). Estimating net ecosystem exchange of carbon using the normalized difference vegetation index and an ecosystem model. *Remote Sens. Environ.*, 58:115-130.
- Veroustraete, F., Sabbe, H. and Eerens, H. (2002). Estimation of carbon mass fluxes over Europe using the C-Fix model and Euroflux data. *Remote Sensing of Environment*, Vol. 83,(3): 376–399.
- Veroustraete, F., Sabbe, H., Rasse, D.P. and Bertels, L. (2004). Carbon mass fluxes of forests in Belgium determined with low resolution optical sensors. *Intern. J. Rem. Sens.* 25: 769-792.
- Vignolio, O.R., Biel, C., De Heralde, F., Araújo-Alves, J.P.L. and Savè, R. (2002). Growth of *Lotus creticus creticus* and *Cynodon dactylon* under two levels of irrigation. *Austr. J. Agric. Res.* 53: 1375-1381.
- Villalobos, F.J., Perez-Priego, O., Testi, L., Morales, A. and Orgaz, F. (2012). Effects of water supply on Carbon and water exchange of olive trees. *European J. of Agronomy*, 40: 1-7, doi: 10.1016/j.eja.2012.02.004.

- Vossen, P. (2007). Olive oil: history, production, and characteristics of the world's classic oils. *Horticultural Science*, 42: 1093–1100.
- Webb, E.K., Pearman, G.I. and Leuning, R. (1980). Correction of flux measurements for density effects due to heat and water vapour transfer. *Q. J. R. Meteorol. Soc.* 106: 85–100.
- Wesely, M.L. (1970). Eddy correlation measurements in the atmospheric surface layer over agricultural crops. Dissertation, University of Wisconsin. Madison, WI.
- Wilson, K., Goldstein, A., Falge, E. and Baldocchi, D. (2002). Energy balance closure at FLUXNET sites. *Agricultural and Forest Meteorology*, 113(1-4): 223-243.
- Witt, G.B., Harrington, R.A. and Page, M.J. (2009). Is ‘Vegetation Thickening’ occurring in Queensland’s Mulga lands. A 50 year aerial photographic analysis. *Australian Journal Of Botany* 57: 572-582, doi.Org/10.1071/BT08217.
- Xiao, J., Zhuang, Q., Law, E.B., Chen, J., Baldocchi, D.D., Cook, D.R., Oren, R., Richardson, A.D., Wharton, S., Ma, S., Martin, T.A., Verma, S.B., Suyker, A.E., Scott, R.L., Monson, R.K., Litvak, M., Hollinger, D.Y., Sun, G., Davis, K.J., Bolstad, P.V., Burns, S.P., Curtis, P.S., Drake, B.G., Falk, M., Fischer, M.L., Foster, D.R., Gu, L., Hadley, J.L., Katul, G.G., Matamalay, R., McNulty, S., Meyers, P.T., Munger, J.W., Noormets, A., Oechel, W.C., Paw, K.T.U., Schmid, H.P., Starr, G., Torn, M.S. and Wofsy, S.C. (2010). A continuous measure of gross primary production for the conterminous United States derived from MODIS and AmeriFlux data. *Remote Sens. Environ.* 114: 576-591.
- Xiao, Y., Jacob, D.J., Wang, J.S., Logan, J.A., Palmer, P.I., Suntharalingam, P., Yantosca, R.M., Sachse, G.W., Blake, D.R. and Streets, D.G. (2004). Constraints on Asian and European sources of methane from CH₄-C₂H₆-CO correlations in Asian outflow. *J. Geophys. Res.* 109: D15S16.

- Xu, L., Baldocchi, D., and Tang, J. (2004). How soil moisture, rain pulses, and growth alter the response of ecosystem respiration to temperature. *Global. Biogeochem. Cycles*, 18: GB4002, doi:10.1029/2004GB002281.
- Yang, F., Ichii, K., White, M.A., Hashimoto, H., Michaelis, A.R., Votava, P., Zhu, A-X., Huete, A., Running, S.W. and Nemani, R.R. (2007). Developing a continental-scale measure of gross primary production by combining MODIS and AmeriFlux data through Support Vector Machine approach. *Remote Sens. Environ.* 110: 109-122.
- Zanotelli, D., Montagnani, L. Manca, G. and Tagliavini, M. (2013). Net primary productivity, allocation pattern and carbon use efficiency in an apple orchard assessed by integrating eddy covariance, biometric and continuous soil chamber measurements. *Biogeosciences*, 10: 3089–3108, doi: 10.5194/bg-10-3089.
- Zohary, D. and Spiegel Roy, P. (1975). Beginnings of fruit growing in the old world. *Science* 187: 319-327.

Acknowledgments

I wish to thank Prof. Marco Bindi and Prof.ssa Donatella Spano for their professional assistance.

I'm grateful to Dr. Alessandro Zaldei, Dr. Beniamino Gioli, Dr. Piero Toscano, (CNR-Ibimet), Dr. Claudio Cantini (CNR-Ivalsa), and Dr. Emanuele Lugato (FEM) for giving me the opportunity to collaborate with their research units and for their expertise.

Many thanks to my PhD thesis revisors Dr. Massimo Tagliavini and Andrea Pitacco for their useful advises and suggestions.

I wish to express my gratitude to all my colleagues Marco Moriondo, Roberto Ferrise, Camilla Dibari, Giacomo Trombi, Paolo Merante, Nicolina Staglianò, Luisa Leolini, Anna Dalla Marta, Giada Brandani, Marco Mancini, Ada Baldi, Simone Orlandini, Federico Guasconi, Francesca Natali and Alessandro Messeri for their friendship and support.

Annexes

Curriculum Vitae

Name: Lorenzo

Surname: Brilli

Place of birth: Fiesole (Firenze, Italia), il 18/6/1985

Adress: via Luciano Manara n° 19, 50135 (Firenze, Italy)

Phone: +39 0552755743

Mobile: +393402951633

E-mail: lorenzo.brilli@unifi.it

E-mail: lore.brilli@gmail.com



Dr. Lorenzo Brilli holds a degree in Agricultural Sciences in 2011 at University of Florence, Italy. He is working at University of Florence Department of Agri-Food Production and Environmental Sciences (DISPAA). He started its experience in 2010. From 2010 to November 2011 he collaborated with DiSPAA and CNR Ibimet by leading a CO₂ experiment on an agricultural site located in Follonica (Tuscany). In November 2011 he received a PhD grant at Sassari University (Italy), and started his studies about analysis of surface exchanges measurement between biosphere and atmosphere. In February 2012 he participated to the "International award Brunello di Montalcino - Case Basse Soldera", with a research focused on yeasts-climate interactions. In July 2012 he participated to the International conference "Eurosoil 2012" (Bari - Italy) with a presentation focused on GHG emissions from agriculture. In the year 2013 he spends a formation period (5 months) in the UK, at Aberdeen University (Prof. Pete Smith), increasing and enhancing his basic capacity about modelling flux measurements from crop and natural systems. The positive scientific results enlarge the research activities, in the framework of Italian research projects (PRIN 2011, Carbotrees) and international (FACCE-JPI, 2013; SMARTSOIL, 2011) projects, both of them currently ongoing. In these years his scientific interests extended to remote sensing (e.g. C-fix; Biome-BGC) and its application for biosphere studies. However, the main research lines followed are flux measurements in agro-forestry systems using Eddy Covariance micrometeorology techniques and ecosystem modelling. More specifically about ecosystem modelling, he recently focused his studies on calibration, validation and application of biogeochemical models able to simulate C and N fluxes between soil and atmosphere such as DNDC and Daycent on complex agro-ecosystems such as orchards and vineyards.

Selected publications

- Maselli, F., Chiesi, M., **Brilli, L.**, Moriondo, M. 2012. Simulation of olive fruit yield in Tuscany through the integration of remote sensing and ground data. *Ecological Modelling* 244, 1-12.
- Brilli, L.**, Chiesi, M., Maselli, F., Moriondo, M., Gioli, B., Toscano, P., Zaldei, A., Bindi, M. 2013. Simulation of olive grove Gross Primary Production by the combination of ground and multi-sensor satellite data. *Int. J. Appl. Earth Obs.* Vol 23, 29-36.
- Brilli, L.**, Moriondo, M., Ferrise, R., Dibari, C., Bindi, M. 2014. Climate change and Mediterranean crops: 2003 and 2012, two possible examples of the near future. *Agrochimica*, Vol. LVIII – Special Issue.
- Brilli, L.**, Buscioni, G., Moriondo, M., Bindi, M., Vincenzini, M. 2014. Influence of Interannual Meteorological Variability on Yeast Content and Composition in Sangiovese Grapes. *Am. J. Enol. Vitic.* 65:3 (2014), 375-380, doi: 10.5344/ajev.2014.13116.
- L. Brilli**, R. Ferrise, E. Lugato, M. Moriondo and M. Bindi. 2014. Using mitigation and adaptation strategies to optimize crop yield and greenhouse gas emissions. In: *Sustainable agroecosystems in climate change mitigation* (Maren Oelbermann, editor), Wageningen Academic Publisher, Netherland, 328 pp. ISBN: 978-90-8686-235-1.
- M. Pisante, F. Stagnari, M. Acutis, M. Bindi, **L. Brilli**, V. Di Stefano, M. Carozzi. 2014. Conservation Agriculture and Climate Change. In: *Conservation Agriculture* (Muhammad Farooq & Kadambot H.M. Siddique, editors). Farooq, Muhammad, Siddique, Kadambot (Eds.), Springer 2015, I, 899 p. 40. ISBN 978-3-319-11619-8.